THESE

présentée en vue de l'obtention du diplôme de

DOCTEUR DE L'UNIVERSITE LOUIS PASTEUR DE STRASBOURG

Spécialité: Mécanique des fluides

par

Allelign ZERU

Investigations numériques sur l'inversion des courbes de concentration issues d'un pompage pour la quantification de la pollution de l'eau souterraine

"Numerical investigations on the inversion of pumped concentrations for groundwater pollution quantification"

soutenue le 27 septembre 2004 devant le jury constitué de:

M.	G. SCHÄFER	Directeur de thèse
Mme.	M-G. TANDA	Rapporteur externe
M.	A. K. TYAGI	Rapporteur externe
M.	Y. BERNABE	Rapporteur interne
M.	Ph. ELSASS	Examinateur

Thèse préparée au sein du Groupe d'Animation de la Recherche "IFARE"
de l'Institut Mécanique des Fluides et des Solides (IMFS), UMR 7507 ULP-CNRS

Name and title of members of the jury:

Dr. Yves BERNABE	Professeur Université Louis Pasteur, Strasbourg (France)
Dr. Philippe ELSASS	Directeur Service Géologique Régional Alsace (BRGM)
Dr. Gerhard SCHÄFER	Professeur Université Louis Pasteur, Strasbourg (France) Directeur IFARE de l'Antenne de Strasbourg
Dr. Maria G. TANDA	Professor Department of Civil Engineering (Dipartimento di Ingegneria Civile, dell'Ambiente e Territorio e Architettura) Università di Parma (Italy)
Dr. Avdhesh K. TYAGI	Associate Professor School of Civil & Environmental Engineering Oklahoma State University (USA) President Oklahoma Society of Professional Engineers Director Oklahoma Infrastructure Consortium

Acknowledgements

I would like to gratefully acknowledge the enthusiastic supervision of Prof. Gerhard Schäfer, for his helps, attention and all the intensive discussions I have made with him. He has always had time to look at the details of my scientific works and results and to give invaluable comments, which enormously contributed to the completion of my thesis in a short time.

The successful termination of this thesis was made possible with the financial support from EU R&D Project INCORE, the "Contrat de Plan Etat-Région", and the "Programme Pluriformation (PPF) de l'IFARE. I am grateful for that. I acknowledge Prof. Mathiot and Dr. Zilliox for being the reason for me to pursuit my PhD research at IFARE.

I am pleased to acknowledge the reporters and examiner who managed to get time to read my draft thesis and contributed constructive comments. Thus, I am thankful to Prof. Tanda at the Department of Civil Engineering (University of Parma, Italy), and Dr. Tyagi at the School of Civil & Environmental Engineering (Oklahoma State University, USA) for being testimonies to my research findings. I thank Prof. Yves Bernabé for having accepted to be the president of the jury and for his views and comments. I thank Dr. Phillip Elsass for serving as my examiner and supplying field data related to the site Plaine des Bouchers; and Dr. Gilles Rink in contributing information on field data and for all friendly discussions I made with him at several occasions of project meetings.

I would also like to thank the INCORE project partners who showed their constructive and encouraging comments on my research ideas. I am grateful to Marti (Dr. Bayer) for many useful and friendly discussions I have made with him. Thanks to all who sent me reading materials promptly and selflessly: Dr. Reilly at the USGS, Dr. Bair at Ohio State University, and Dr. Neupauer at University of Virginia. I thank Dr. Kraemer, at the US EPA, and Prof. Haitjema, at Indiana University, for having the occasion to discuss with them on radial flow related topics and for their feedback and encouragement. I always remember and thank Prof. McTernan at the School of Civil & Environmental Engineering (Oklahoma State University) for being a source of inspiration in groundwater pollution modeling, and for the entertaining and joyful discussions I had with him and Scott.

I thank the research team and supporting staff of IFARE who were a direct or indirect help to me throughout this research period. Emilie, thanks for being a last minute help in punching and bundling the draft copies of my thesis.

Many thanks to all of my friends who constantly conveyed their moral support throughout this study period. I thank Haile as a good friend and for supplying relevant information, Awoke for his insistence and moral that I should carryout my PhD research, Frew Kelemu for his encouraging words that I kept in mind and Mulugeta for his wise and immortal advice.

I am grateful to Lise, my wife, and Lea, our daughter , for every elements and moments that we all have shared with and enjoyed together. I also greatly appreciate and thank her family members who have showed me and conveyed their constant moral support. I thank my Sisters and Brothers and, most importantly, I wish to thank my mother, whom I wished she could be there, and my father who has always been everything for me. To them I dedicate this thesis !

Allelign Zeru, 27th September 2004.

Table of Contents

List of Tables

List of Figures

Résumé étendu

Investigations numériques sur l'inversion des courbes de concentration issues d'un pompage pour la quantification de la pollution de l'eau souterraine

1. Introduction

Contexte

L'eau souterraine est la source principale de l'eau domestique et de l'eau industrielle urbaine. Le Bassin du Rhin Supérieur est une des régions d'Europe les plus industrialisées, avec une forte densité de population. Mais confronté à la pression des activités humaines, comme l'industrialisation, il est aussi menacé de pollution. Ce sont pourtant les effluents des zones industrielles, les déversements accidentels et les fuites sur des sites de stockage qui sont à l'origine de la majorité des cas de contamination des aquifères.

Quand une contamination est détectée, il faut en estimer l'étendue et la source de pollution. Pour déterminer l'étendue et le niveau de la pollution, on prend en général un grand nombre d'échantillons en plusieurs points, ce qui nécessite l'installation de plusieurs puits d'observation. Une alternative à cette méthode conventionnelle est la technique d'investigation intégrale, une nouvelle approche qui permet, par inversion de courbes de concentrations mesurées pendant un essai de pompage, de déterminer l'étendue et le niveau de pollution.

L'approche d'investigation intégrale a été testée dans le cadre du projet de recherche européen INCORE « Integrated Concept for Groundwater Remediation », auquel l'Institut de Mécanique des Fluides et des Solides (IMFS) et l'Institut Franco-Allemand de Recherche sur l'Environnement (IFARE) ont été associés en collaboration avec des partenaires locaux et européens, sur des sites industriels pollués par des solvants chlorés dans quatre villes européennes. A Strasbourg, la méthode d'inversion a été appliquée sur le site de la Plaine des Bouchers pour quantifier la concentration moyenne et les flux massiques de perchloroéthylène (PCE) dans la nappe.

Ce travail de thèse a été mené depuis avril 2002 dans le projet INCORE et s'est poursuivi au-delà de juin 2003 afin d'approfondir certains aspects non abordés lors du projet.

Objectifs

Dans un premier temps, l'application de la méthode d'inversion sur le site de la Plaine des Bouchers a été effectuée en supposant que le gradient de concentration dans le panache est négligeable et en considérant l'aquifère du site réel comme un milieu poreux homogène et isotrope. Le travail de cette thèse s'est de ce fait articulé autour des éléments, tels que le gradient de concentration et les hétérogénéités locales, dont on n'avait pas tenu compte auparavant et qui peuvent être sources d'incertitude pour l'utilisation de la méthode d'inversion.

Les recherches menées dans cette thèse se focalisent sur trois objectifs scientifiques liés à la méthode d'inversion pour l'analyse de la pollution de la nappe. Le premier objectif se focalise sur l'influence du gradient de concentration dans un panache sur l'inversion des courbes de concentration. Le second se concentre sur l'effet d'une hétérogénéité locale autour du puits, relatif à la quantification des flux massiques d'un polluant dissous. Le troisième objectif basé sur les résultats issus de la recherche liée aux deux premiers objectifs consiste à appliquer la méthode d'inversion sur le site de la Plaine des Bouchers

Démarche scientifique

Pour atteindre le premier objectif, nous avons utilisé le code de calcul MODFLOW/MT3D pour effectuer une étude numérique de l'écoulement et du transport dans un aquifère hypothétique ayant un coefficient de perméabilité homogène et une zone source de pollution fixe et permanente. Les données de la courbe de concentration issues de la simulation du transport avec MT3D ont été employées pour l'inversion analytique. Puis, la concentration invertie sur la section transversale de contrôle (STC) est comparée avec la concentration observée dans le panache avant pompage. La moyenne de rapport

de gradients de concentration (MRG) est ensuite calculée afin de déterminer l'erreur qui peut être associée à la présence du gradient de concentration. Dans le cas du deuxième objectif, notre démarche a consisté à développer un modèle mathématique appelé VINMOD (**v**olume based **in**verse **mod**el) pour inverser la courbe de concentration en tenant compte de la présence d'hétérogénéité locale autour du puits. La vitesse d'écoulement issue de la simulation de l'écoulement en régime permanent à l'aide de MODFLOW et la position des particules par 'backtracking' à partir de PMPATH sont utilisés pour délimiter les zones de captage du puits et pour définir les tubes de courant. Concernant le troisième objectif, nous avons utilisé les courbes de concentration obtenues sur le site de la Plaine des Bouchers. Le modèle numérique d'écoulement local nous a servi pour la détermination du champ de vitesses ainsi que de la zone de captage du puits IPT2 dans un cas hétérogène. La configuration retenue se rapproche du modèle conceptuel proposé par le BRGM pour la formation géologique de l'aquifère.

Le mémoire est organisé en cinq chapitres. Le premier chapitre, décrit ci-dessus, présente le contexte et les objectifs de cette étude. Les sujets spécifiques liés à la pollution de la nappe phréatique, les risques pour la santé liés à l'exposition aux solvants chlorés, les méthodes d'évaluation ou de quantification de la pollution souterraine sont exposés dans le deuxième chapitre. Dans le troisième chapitre, il s'agit de déterminer l'étendue et le niveau de contamination de la nappe phréatique dans le cas d'un aquifère homogène, en tenant compte du gradient de concentration dans le panache. Le quatrième chapitre porte sur les prévisions concernant l'étendue et le niveau de contamination de la nappe phréatique dans le cas d'un aquifère hétérogène. Le dernier chapitre présente l'application de la méthode d'inversion de la courbe de concentration sur le site de la Plaine des Bouchers à Strasbourg. En conclusion nous présentons les perspectives de cette étude.

2. Analyse bibliographique sur la pollution d'eaux souterraines par les solvants chlorés et les méthodes d'évaluations

La diversité croissante des activités industrielles est une menace pour les réserves d'eaux souterraines de plusieurs zones industrielles. Les rejets industriels, les déversements et fuites accidentels de produits pétroliers sont quelques-unes des nombreuses sources de contamination souterraine. Les solvants chlorés sont des fluides non miscibles à l'eau et appartiennent à la famille de DNAPLs (Dense Non-Aqueous Phase Liquids). Ils sont connus pour être à l'origine de la contamination de nombreux sites industriels. Les solvants chlorés, comme le PCE et le TCE, sont toxiques et peuvent générer de sérieux problèmes de santé pour l'homme par ingestion, inhalation ou adsorption dermique.

Dans plusieurs cas, l'investigation sur la présence d'une contamination de la nappe phréatique commence seulement après un rapport de causalité anormal sur la santé et l'environnement. Une fois la contamination détectée, il est essentiel de déterminer le niveau, l'étendue et la source de pollution. Les méthodes les plus courantes pour évaluer et/ou quantifier la pollution des eaux souterraines incluent l'analyse historique du site, l'inspection visuelle, des méthodes géophysiques, l'extraction d'échantillons et l'interpolation spatiale des concentration relevées, ainsi que l'utilisation de modèles mathématiques de transports.

La méthode d'inversion de la courbe de concentration obtenue par un essai de pompage intégral peut être utilisée pour la quantification de flux massique de polluants dissous dans l'eau, issus d'une zone source connue ou inconnue. Cependant, la solution analytique présentée dans la littérature ne peut pas fournir une information adéquate sur l'état de la pollution de la nappe lorsque le gradient de concentration dans le panache est important et dans le cas où il y a des hétérogénéités locales situées au droit du puits de pompage.

3. Inversion de courbe de concentration en tenant compte du gradient de concentration dans le panache

L'effet de la concentration du gradient sur l'inversion de la courbe de concentration est étudié en utilisant un modèle bidimensionnel pour l'écoulement et le transport d'un cas d'exemple. La moyenne de rapport de gradients de concentration (MGR), qui est le rapport entre le gradient de concentration longitudinal et le gradient de concentration transversal correspondant, est utilisée pour déterminer les incertitudes liées à la présence du gradient de concentration dans le panache. Les deux cas de panache en régime permanent et en régime transitoire sont analysés. Des périodes de transport différentes et les valeurs de la dispersivité sont utilisées pour analyser la MGR et les erreurs correspondantes liées à la présence de gradients de concentration dans le panache.

Les résultats de cette étude concernant l'effet du gradient de concentration dans le panache mettent en relief si l'essai de pompage intégral est effectué proche de la limite avale du panache, alors l'influence du gradient de concentration longitudinal par rapport au gradient transversal sur la concentration calculée par inversion est très significative et l'erreur associée est proportionnellement élevée. Il en résulte une surestimation de la distribution de concentration réelle et du flux massique sur la section transversale de contrôle (STC). Quand il y a une dispersivité longitudinale du milieu poreux plus élevée, la méthode d'inversion de la courbe de concentration peut entraîner une sous-estimation de la distribution de concentration réelle et du flux massique correspondant sur la STC.

Une valeur représentative du flux massique quantifié dans la STC avec des erreurs relativement faibles peut être obtenue dans le cas où la moyenne de rapport de gradients de concentration (MRG) est également minimale et les valeurs de la dispersivité sont relativement plus petites. L'étude numérique a montré qu'une faible MRG, près de zéro, est notamment obtenue dans le cas où la STC serait placée plus près de la source présumée de la pollution. Une MRG inférieure ou égale à 1 est acceptable même si la valeur de l'erreur dépend aussi des valeurs de la dispersivité correspondante. Par contre, une MRG supérieure à 3 peut entraîner une erreur relative de plus de 50 %, ce qui indique que la STC est probablement placée vers la limite avale du panache.

La prise en compte du gradient de concentration peut améliorer les résultats obtenus et réduire les erreurs. Sur site réel, une MRG devrait être déterminée de sorte que le flux massique total puisse être estimé sur la section de contrôle. Il est à noter, cependant, qu'en régime transitoire du panache le flux massique total ne représente pas nécessairement le maximum de flux massique total du panache détecté. Par conséquent, la valeur du flux massique total dépend à la fois de la position de la STC, qui peut ensuite influencer la magnitude de la MRG, et des valeurs de la dispersivité. Plus la MRG est petite, plus la détermination du flux massique total est meilleure, si la valeur de la dispersivité longitudinale n'est pas trop élevée.

4. Inversion de courbe de concentration en tenant compte d'une hétérogénéité locale autour du puits

Afin de traiter l'effet de l'hétérogénéité locale, le modèle mathématique VINMOD basé sur la conservation de la masse a été défini et utilisé pour l'inversion numérique de la courbe de concentration. Cette inversion est basée sur le calcul de volume d'eau pompé à un instant donné en s'appuyant sur les isochrones de l'essai de pompage intégral et les lignes de courants de l'écoulement principal. VINMOD tient compte de la géométrie irrégulière de la zone de captage du puits qui peut être fortement influencée par la présence d'une hétérogénéité locale.

Le volume de la zone de captage est utilisé pour calculer la masse d'eau polluée pouvant être présente dans le sol avant pompage. Cependant, pour calculer la distribution de la concentration sur la STCI, le volume total de la zone de captage est divisé par des tubes de courant d'écoulement principal qui traversent la zone de captage considérée. VINMOD requiert des paramétrages principaux comme les données de courbe de concentration, le champ de vitesse (avant et pendant le pompage), l'épaisseur de l'aquifère, la porosité cinématique du milieu poreux et les surfaces des tubes de courant.

On a remarqué que VINMOD est très sensible à la vitesse d'écoulement de la nappe et aux volumes des tubes de courant dans une zone de captage donnée. En fonction de la

distribution de la perméabilité autour du puits de pompage, le champ d'écoulement hétérogène peut avoir des effets significatifs sur l'inversion. Les résultats obtenus montrent que le flux massique total peut varier par plusieurs ordres de grandeur par rapport au cas homogène et isotrope. Dans cette étude particulière, principalement affectée par l'importance de la vitesse d'écoulement, le flux massique total calculé sur la STC pour le cas hétérogène est plus élevé d'environ 43 % par rapport à celui du cas homogène.

Le changement de la géométrie de la zone de captage du puits, en raison d'une hétérogénéité locale, a entraîné un léger effet sur la moyenne de la concentration obtenue par inversion. Dans ce cas, la moyenne de la concentration sur la STC augmente de 4 % environ par rapport au cas homogène. Ce qui indique que la géométrie de la zone de captage peut légèrement affecter le flux massique total.

L'exactitude du volume des tubes de courants utilisés dans VINMOD peut être affectée par des erreurs liées à la digitalisation (utilisant OS Digitizer) et à la résolution des mailles du modèle numérique. Les erreurs de digitalisation sont en général faibles; elles sont de l'ordre de 2 à 3 %. Par contre, des erreurs liées à la résolution des mailles ont un effet très significatif. Par exemple, une taille de mailles de 5 m × 5 m près du puits de pompage peut provoquer une diminution de volume des tubes de courants d'environ 50 % du volume théorique, ce qui entraîne une sous-estimation du flux massique au niveau de la STC. Ce maillage grossier autour du puits de pompage cause une diminution de la distance parcourue par une particule d'eau, par conséquent, les volumes des tubes de courants sont inférieurs aux volumes théoriques. En augmentant la résolution des mailles à 1 m × 1 m, le résultat du volume quantifié se rapproche de la valeur théorique. Donc, plus la résolution de la maille est haute, plus les volumes des tubes de courants pouvant être obtenus sont meilleurs.

5. Application sur le site industriel de Plaine de Bouchers à Strasbourg

Les courbes de concentration, principalement pour le PCE, obtenues pendant l'essai de pompage intégral du puits IPT2 sur le site de la Plaine des Bouchers, sont utilisées pour l'inversion de la concentration pompée. Par ailleurs, la moyenne de rapport de gradients de concentration (MRG) de 0,87 a été évaluée à partir des isolignes de concentrations mesurées. Cela indique que la position de pompage de la STC utilisée pour l'essai de pompage intégral est bien choisie afin de pouvoir évaluer la pollution des eaux souterraines au moyen de la méthode d'inversion de courbes de concentration. En outre, puisque la teneur en oxygène dissous mesurée est de l'ordre de 2,2 à 4 mg/l, la méthode d'inversion peut être applicable sans tenir compte de l'effet de la biodégradation.

Dans le cas homogène, le flux massique total calculé sur la STC, sans tenir compte de la MRG, on obtient un flux de PCE d'environ de 155 grammes par jour. Puisque la MRG estimée est relativement faible, sa prise en compte dans l'inversion de la courbe de concentration conduit seulement à une petite diminution du flux massique calculé d'environ 5 %. Cependant, il faut noter que le flux massique total réel peut même être plus grand que la valeur présentée ici car la tendance de la courbe de concentration à la fin du pompage reste significative.

D'autre part, afin d'analyser les incertitudes liées à l'effet d'hétérogénéités locales, nous avons utilisé une configuration d'inclusions très perméables se rapprochant du modèle conceptuel proposé par le BRGM pour la formation géologique de l'aquifère. La perméabilité des hétérogénéités locales retenue pour ce test numérique est 10 fois plus grande que la perméabilité du milieu principal. La zone de captage obtenue est très irrégulière. A partir de l'inversion numérique utilisant VINMOD, le flux massique total obtenu est environ 2 fois plus élevé que dans le cas homogène. Cela est principalement provoqué par les vitesses d'écoulement élevées dans la zone de perméabilité modifiée.

Puisque la localisation de l'hétérogénéité autour du puits de pompage est inconnue, les valeurs définitives concernant le flux massique total lié à l'hétérogénéité locale ne

peuvent pas être présentées ici. Cependant, cette étude met en relief l'importance de la distribution réelle des hétérogénéités à proximité du puits de pompage afin de mieux quantifier le flux massique total du panache de PCE.

Par contre, quand une information détaillée sur les hétérogénéités locales est disponible pour un site, le flux massique total réel peut être mieux quantifié. En outre, la méthode d'inversion appliquée suppose ici que le panache détecté est traité comme symétrique par rapport au puits de pompage. Donc, l'incertitude liée à la symétrie pourrait être examinée s'il y avait un autre essai de pompage plus proche de celui existant.

Conclusions et perspectives

La méthode d'inversion de la courbe de concentration peut être utilisée comme une alternative ou une technique complémentaire pour l'évaluation et quantification de pollution d'eaux souterraines. Cette approche est particulièrement appropriée quand il y a peu de mesures ponctuelles et lorsque la source de contamination est inconnue. L'expérience de cette étude montre que la présence du gradient de concentration et l'hétérogénéité autour du puits de pompage peuvent avoir un effet significatif sur la quantification du flux massique total. Une moyenne de rapport de gradients de concentration (MRG) près de zéro peut indiquer une bonne position de la STC en vue d'une quantification du flux massique total. En cas de présence d'hétérogénéités locales, il est recommandé d'utiliser la méthode de l'inversion numérique développée (VINMOD).

Pour l'application de la méthode d'inversion de la courbe de concentration à une échelle plus large, les aspects tels que l'effet de la répartition de la source sur la verticale, la biodégradation des composés dissous, la géométrie de la STC dans le cas hétérogène peuvent être des pistes de recherches possibles dans le futur. En outre, une méthode de localisation de la source par "backtracking", qui peut être intégrée ou inhérente à la méthode d'inversion de courbes de concentration, pourrait fournir un outil complet pour l'analyse de la pollution des eaux souterraines.

Bien que cette étude se soit focalisée sur un puits unique avec un panache symétrique relatif à la position du puits de pompage, l'effet du gradient de concentration ainsi que la présence d'hétérogénéités locales sur l'inversion de la courbe de concentration peuvent être étendus à un système de puits multiple. Les limites techniques de l'inversion de la courbe de concentration pour l'application sur site réel peuvent être les suivantes :

- L'inversion de la courbe de concentration du panache asymétrique requiert une nouvelle solution par le couplage d'une solution inverse obtenue pour un puits unique.
- Dans le cas où plusieurs puits sont utilisés sur site réel, un pompage simultané est conseillé afin de limiter le déplacement du panache contaminé.
- Dans le cas hétérogène, l'installation des puits de pompage peut nécessiter un rapprochement des zones de captage pour mieux quantifier les polluants.
- Dans le cas d'un aquifère avec une conductivité hydraulique très faible, en l'occurrence avec une valeur inférieure a 10^{-5} m/s, l'application de la méthode d'une inversion serait moins appropriée. Pour des aquifères très peu perméables, le puits de pompage doit être configuré de telle sorte qu'un assèchement du puits soit exclus. Dans ce cas, un pompage à très faible débit serait nécessaire, ce qui pourrait nécessiter un temps de pompage élevé et être une méthode coûteuse.
- Dans le cas de panaches comportant un gradient de concentration vertical, il est préférable d'effectuer des mesures de la concentration sur la verticale pour que les valeurs moyennes de concentration représentatives puissent être utilisées comme données de concentration en fonction du temps. En l'occurrence, la distribution de la concentration verticale peut être estimée avec des échantillons à différentes profondeurs.

De plus, une application d'essai de pompage intégral sur le secteur industriel du Dreieckland, région transfrontalière entre la France, l'Allemagne et la Suisse, est prévue dans le cadre d'un projet R&D impliquant un partenariat entre AERM, BRGM, IMFS-IFARE, et ADEME.

Chapter 1

Introduction

1. Introduction

1.1 Background

Groundwater is a major source of water supply for domestic and industrial uses in many urban industrial areas. The Rhine Basin, where the region Alsace is located, is one of the most industrialized areas of Europe with ample reserves of groundwater. However, with ever-growing human activities such as industrialization and agriculture, these immense groundwater reserves are threatened. Effluents from industrial areas as well as accidental spills and leaks are the main sources of groundwater contamination in many industrialized countries. Among others, chlorinated solvents are toxic chemicals that are known to be the most common groundwater contaminants of industrial origin found. For instance, the detection of significant quantity of perchloroethylene (PCE) with a plume width of 200 m and length of several kilometers at the industrial site of "Plaine de Bouchers" in Strasbourg, the regional capital of Alsace, can be cited as an example.. Exposure to these chemicals may cause serious health problems to humans and the natural environment.

In the case when groundwater contamination is detected, it becomes essential to determine the extent, level and source of contamination. Conventionally, among many others, determination of the extent and level of contamination is undertaken by taking as many samples as possible from several points. In general, this requires the installation of several observation wells. As a result, the cost of such operations can be very high, especially when high sampling resolution is required. However, financial resources are, in general, limited. Moreover, drilling of a large number of monitoring wells could also be constrained by geological and land-use factors. Although point measurements provide reliable information at specified locations, the risks and uncertainties from using few monitoring wells could be greater.

The use of spatial interpolation methods based on sparse point measurements can be less reliable in the case when contaminants such as chlorinated solvents are distributed irregularly in the subsurface. Thus, plume lenses with significant level of contamination

can be left unnoticed or undetected. Other methods such as forward mathematical models require knowledge of source parameters. But in many cases, and especially in complex industrial areas, the origin of contamination is not known and determining it could require costly investigations.

Alternatively, in the absence of a sufficient number of onsite measurements, groundwater pollution can be evaluated using a novel approach involving the inversion of the concentration-time series data obtained during pumping tests that last for a few days. In this case, the contaminated site can be screened out by zones of priority and the hot spot zones can eventually be used to determine the extent and level of groundwater contamination.

The method of inversion of pumped concentration helps to determine the total mass flow rate, the mean contaminant concentration, as well as the plume extent or position at a predefined control plane perpendicular to the mean groundwater flow direction called imaginary control plane (ICP). Determining the extent or position of the contaminant plume relative to the ICP position can be achieved by employing multiple pumping positions along the chosen ICP. The method of inversion of pumped concentration can be applied for both cases of known and unknown sources of contamination.

The method of the inversion of pumped concentration has been experimented at some industrial sites in Europe under the framework of the European funded R&D project INCORE (**In**tegrated **Co**ncept for Groundwater **Re**mediation), in which the "Institut de Mécanique des Fluides et des Solides (IMFS)" and the "Institut Franco-Allemand de Recherche sur l'Environnement (IFARE)" have been involved in cooperation with local and European partners. The four sites chosen in Milan, Strasbourg, Stuttgart and Graz are known to be polluted by chlorinated solvents. The method of the inversion of pumped concentration was applied at the industrial site *Plaine de Bouchers* in Strasbourg in order to quantify the mean concentration and the mass flow rate of PCE in the groundwater. However, the method applied here assumed that the concentration gradient

in the longitudinal axis of the plume is negligible and that the aquifer of the site is a homogeneous and isotropic porous medium.

A new study has been carried out since April 2002 with financial support from the INCORE project up to June 2003 and afterwards from the "Contrat de Plan Etat-Région" et "Programme Pluriformation (PPF) - "Institut Franco-Allemand de Recherche sur l'Environnement (IFARE)". The study focuses on some of the elements such as the concentration gradient and local heterogeneity that were not considered previously and could affect the results of the method of inversion of pumped concentration at the site *Plaine des Bouchers*.

1.2 Objectives and scope of the study

The research activities of this study concentrate on three scientific objectives related to the method of inversion of pumped concentration for groundwater pollution analysis.

- The first objective deals with the effect of the concentration gradient on the inverted mean concentration and the corresponding mass flow rate at a predefined ICP. A plume characterized by the presence of a concentration gradient in the longitudinal axis is taken into consideration.
- The second one focuses on the effect of local heterogeneity on the inverted mean concentration and the corresponding mass flow rate.
- The third objective, based on the results obtained through the first and the second objectives, is the application of the inversion of pumped concentration at the site *Plaine des Bouchers*.

Based on the outlined objectives, this study addresses the quantification of groundwater pollution related to a dissolved contaminant plume, such as a chlorinated solvent plume, with the inversion of pumped concentrations. Neither the determination of the contaminant source parameters nor the implementation of the source identification methods are within the scope of this study.

1.3 Methodology

In order to achieve the aforementioned objectives, this study used some flow and transport software, graphical tools. Institutional and personal contacts, and literature reviews pertinent to this study were also helpful. Numerical simulations of flow, transport, and particle tracking were performed using MODFLOW, MT3D, and PMPATH respectively.

A mathematical model called VINMOD (**v**olume based **inv**erse **mod**el) has been developed and used for the numerical inversion of pumped concentration in a heterogeneous media near the pumping well. The concentration-time series data of the site *Plaine des Bouchers*, measured by IFARE and analyzed by the Bureau de Recherches Géologiques et Minières (BRGM), is used for the application of this study. Moreover, the pattern of the hydraulic conductivity blocks used in the vicinity of the pumping well IPT2, at the site *Plaine des Bouchers* is based on a conceptual model proposed by BRGM for the high permeability zones of the underlying geological formation.

PINwin, the analytical inversion code for windows platform, is developed and used for the inversion of pumped concentration in a equivalent homogeneous aquifer model set up. The On-Screen Digitizer (OS Digitizer) is developed and used to calculate the areas bounded by the adjacent streamlines and isochrones that are input to VINMOD. VINMOD and OS Digitizer are written in programming languages Salford Fortran 95 and Visual Basic 6 respectively.

1.4 Organization of this document

In addition to the overall background studies described in this section, the various elements of this study are organized into five chapters. An extended version of the abstract of this study precedes this chapter. The second chapter addresses a review of specific topics related to groundwater pollution, health risks related to exposure to chlorinated solvents, groundwater evaluation or quantification methods. The third chapter deals with the determination of the extent and level of groundwater

contamination for a homogeneous aquifer taking into account the concentration gradient in the plume along the main flow direction. The fourth chapter addresses the prediction of the extent and level of groundwater contamination for a heterogeneous aquifer scenario. The last chapter, Chapter five, presents the application of the method of the inversion of pumped concentration to the site *Plaine des Bouchers*, Strasbourg. The overall conclusions and perspectives of this study is presented next to the last chapter. Other supporting materials used in the course of this study are presented in the appendix section.

Chapter 2

Literature review on groundwater pollution by chlorinated solvents and methods of pollution evaluation

2. Literature review on groundwater pollution by chlorinated solvents and methods of pollution evaluation

This chapter addresses a brief review on the gravity of groundwater pollution and corresponding health risks related to exposure to industrial toxic chemicals such as chlorinated solvents. Some conventional methods of groundwater pollution evaluation are briefly described and an extended summary on the integral investigation method with the corresponding method of the inversion of pumped concentration is presented.

2.1 Introduction

Groundwater is the main source of water supply mainly for domestic, industrial, and agricultural purposes around the world. According to UNESCO's estimation (UNESCO, 2002), more than half of the world's population relies on groundwater resources. In Europe, groundwater provides over 65 % of all water extracted for public water consumption (Holt, 2000) and the estimated groundwater use in France accounts for about 65 % (Pavard, 2001) of the total water being withdrawn. The wider use of groundwater as the main water source compared with surface water source is due to the fact that, unlike surface water sources, groundwater is less exposed to pollutants that may exist in surface waters and its development potential is immense. Under natural condition, deep aquifers, where most of the large-scale production wells for drinking water supplies are situated, are generally much safer and, therefore, require lower treatment cost than surface water sources.

However, due to the ever-growing human activities, particularly due to the expansion of industrialization and urbanization with little consideration to harmful environmental consequences, groundwater sources are getting more and more vulnerable to various forms of contamination. For instance, according to the 1999 estimates of the European Environmental Agency, there are about 1.3-1.5 million potentially contaminated sites in

12 European countries (Prokop et al., 2000; GCR, 2003). In the same report, the estimated figure for potentially contaminated sites in France reaches 700 000 to 800 000 which is the highest figure from all countries included in the study, followed by 110 000 to 120 000 potentially contaminated sites in The Netherlands. However, the number of registered contaminated sites in France as of 1996 is only 896, which is by far smaller than the European Environmental Agency (EEA) estimated figure (Prokop et al., 2000). A report by the General Re Corporation (GRC, 2003) shows that there are as many as 825000 potentially contaminated sites in the United States, which is a little more than the estimated potentially contaminated sites in France. In Canada there are about 30 000 contaminated sites as of 2002 (Regional Analytics Inc., 2002). One can infer that groundwater pollution risk in France is very elevated.

The degradation of the groundwater environment due to harmful human made chemicals can cause significant health and environmental problems for extended periods. This is due to the fact that the very slow movement of groundwater facilitates the retention of contaminants entered the groundwater system. For instance, a contaminant that enters the aquifer may stay up to 1400 years compared to only about 16 days in the case of rivers (Sampat, 2000). Thus, groundwater pollution problems are much more severe than pollution problems that may exist in surface water bodies. As a result, contaminated groundwaters may become unsuitable for domestic or other uses for a long period of time. Moreover, the contaminated groundwater may further pollute other water bodies that can have hydraulic contacts such as rivers, streams, lakes, wetlands, etc.

2.2 Chlorinated solvents

2.2.1 Origins and Types

Among many others, deliberate discharge of industrial wastes, leaking storage tanks, accidental spills and leaks of petroleum products are the most common origins of groundwater contamination in industrial zones. These type of contaminants are toxic to humans and the environment and are mostly non-aqueous phase liquids (NAPLs) (Guillemin and Roux, 1991; Beth and Cherry, 1999). NAPLs because they do not mix

with water and rather form separate layers or pools. NAPLs, which are less dense than water and float on the top of the water table, are called light NAPLs (LNAPLs) whereas those, which are denser than water and tend to sink below the water table, are called dense NAPLs (DNAPLs).

Chlorinated solvents are DNAPLs which are known to be the most common groundwater contaminants of industrial origin found in industrialized countries (Guillemin and Roux, 1991; Beth and Cherry, 1999). For instance, about 28 per cent of the Netherlands's groundwater used for drinking was contaminated by perchloroethylene (chlorinated solvent) with contamination levels above 10 micrograms per liter; in India a survey conducted in the late 1990s in 22 industrial zones showed that the groundwater in all the surveyed zones was contaminated (Sampat, 2000). Similarly, 30 percent of 15 surveyed Japanese cities were found to be contaminated with chlorinated solvents at various levels of contamination. In France out of the registered 896 contaminated sites, 112 sites are known to be contaminated with halogenated hydrocarbons linked to industrial activities (Prokop et al., 2000).

Chlorinated solvents are petrochemical industry products. They are volatile organic compounds (VOCs) which comprise chemicals such as perchloroethylene (PCE), trichloroethylene (TCE), vinyl chloride (VC), 1,1-dichloroethylene (1,1-DCE), cis/trans-1,2-dichloroethylene (cis/trans-1,2-DCE), 1,1,1-trichloroethane (1,1,1-TCA), 1,1-dichloroethane (1,1-DCA), 1,2-dichloroethane (1,2-DCA), etc. The chemicals such as PCE, TCE, and VC are the most important chemicals in terms of health risk concerns (Lee et al., 2002).

2.2.2 Properties of chlorinated solvents

Chlorinated solvents are chemicals with troublesome properties that make them extremely difficult to locate, remove or treat in the subsurface. Table 2.1 shows the physical and chemical properties of chlorinated solvents such as PCE and TCE. The main technical challenges associated with chlorinated solvents are the difficulties related to their detection and remediation owing to their complex distribution, low solubility, slow

diffusion, and the fact that they migrate from contaminated zone to non-contaminated zone during investigation or other form of operations such as drilling of monitoring wells and other Earth works that may cause leaks to the underlying layer.

Table 2.1 Physical and Chemical characteristics of PCE and TCE

Properties	PCE	TCE
Molecular Formula	CCl_2CCl_2	CCl_2=CHCl
Colour	Colourless	Colourless
Melting Point	-22.7°C	-87°C
Boiling Point	121.4°C	86.7°C
Vapor Pressure	24 mm at 30°C	95 mm at 30 °C
Density	1.626 at 20°C	1.46 at 20°C
Odor	Chlorinated Solvent	Chlorinated Solvent
Viscosity	Less than water	Less than water
Solubility in water	1100 mg/L at 20°C	150 mg/L at 20°C

Source: Cheremisinoff, 1990

Being colourless, chlorinated solvents are not suitable for visual examination during site investigation processes. Once released accidentally or intentionally into the subsurface, chlorinated solvents can exist and migrate in multiple phases depending on how they were released and site conditions. Chlorinated solvents can exist in the unsaturated zone as a vapour phase, in the saturated zone as a dissolved phase, or as a liquid phase referred to as non-aqueous phase liquids (NAPLs). Figure 2.1 shows a schematic representation of a typical DNAPL plume that can exist in three phases in the subsurface and its distribution in the different zones of the aquifer media.

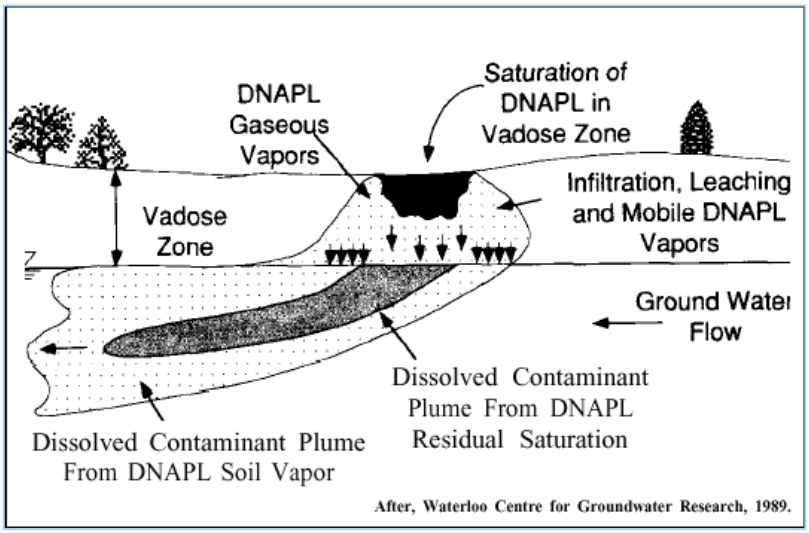

Figure 2.1 Distribution of chlorinated solvents in the aquifer media (source: Kerr, 1992)

2.2.3 Uses of chlorinated solvents

Chlorinated solvents are human made chemicals commonly used as degreasing agents at manufacturing, maintenance and service facilities around the world. For instance, chlorinated solvents are widely used in dry cleaning, wood preservation, asphalt operation, machining, painting, in the maintenance and repair of automobiles, aviation equipment, munitions, and electrical equipment. PCE is one of the most widely used chlorinated solvent chemicals which has been in the market since the early 1900s. According to the International Agency for Research on Cancer (IARC) figure, in 1990 about 135 000 tonnes of TCE and 235 000 tonnes PCE were used in West Europe. In 1991, about 513 000 tonnes of PCE were used for many application in Western Europe, Japan and USA (IARC, 1995). TCE, another CS, has been in the market since the 1920s, mainly used in dry cleaning during the 1930s to 1950s. Presently, about 80-90% of TCE is being used in degreasing around the world.

Even though their uses show a downward trend in Western Europe in particular and around the world in general, the production and use of these chemicals are still enormous.

Table 2.2 shows that the use of TCE and PCE from 1997 to 2002 in Western Europe (EACS, 2002).

Table 2.2 Western European market for chlorinated solvents(*) 1997-2002 (EACS, 2002)

Year	Trichloroethylene (TCE)	Perchloroethylene (PCE)
1997	93	71
1998	85	73
1999	79	74
2000	74	70
2001	63	65
2002	52	61
Yearly Change 1997-2002	-8.8%	-2.8%

(*) in thousands of metric tonnes based on ECSA sales data and Eurostat import figures, excluding intra-company transfers

2.2.4 Potential Health risks

The main health risk associated with chlorinated solvents, mainly PCE and TCE, include kidney and liver damage, central nervous system depression, coma, cardiac arrhythmias. Since chlorinated solvents can exist in liquid, dissolved or vapour form, the exposure mechanisms to these toxic chemicals are mainly by ingestion, inhalation, and dermal adsorption, among which exposure to chlorinated solvents by inhalation is the most frequent. Studies on laboratory animals show that TCE exposures may cause liver, kidney, and lung cancer and similar effects may happen to humans (IARC, 1995; Brown et al., 2003).

Similarly, IARC (1995) case studies from Sweden, Finland and USA show that TCE is potentially carcinogenic, with "elevated" risk of liver and biliary tract cancer, as well as with "modestly elevated" risk of non-Hodgkin's lymphoma. Other case studies on PCE showed the evidence for the associations between PCE and the risk for esophageal and cervical cancer as well as for non-Hodgkin's lymphoma. Table 2.3 shows the International Agency for Research on Cancer (IARC) classifications on the level of carcinogenicity of chlorinated solvents and corresponding health effects.

Table 2.3 Summary of chlorinated solvents and the related health effects (Lee et al., 2002)

Chlorinated solvents	Major target organ[a]		
	IARC[b] cancer group	Carcinogenic effect	Noncarcinogenic effect
Vinyl chloride	1	Liver	Hepatic
Tetrachloroethylene	2A	Liver	Hepatic
Trichloroethylene	2A	Liver/Lung	Hepatic/renal
1,1-Dichloroethylene	3	-	Hepatic
1,1,1-Trichloroethane	3	-	Hepatic
Cis-1,2-Dichloroethylene	NA	-	Hepatic/blood
1,1-Dichloroethane	-	-	Renal

[a]Toxicity values derived from animal bioassays based on which target organ is primarily affected.
[b]International Agency for the Research on Cancer (IARC) classification: 1= carcinogenic, 2A= probably carcinogenic, 3= not classifiable as to carcinogenicity to humans.

As a result, some countries have set threshold values as a part of the drinking water quality standards. Some examples of threshold values of some chlorinated solvents are presented in the below (Table 2.4).

Table 2.4 Threshold values of chlorinated solvents in drinking water (MCL (µg/l))

Product (CS)	US[a]	EU	France [c]
PCE	5	10 (IARC[b])	10 (PCE+TCE)
TCE	5	10 (IARC[b])	
Vinyl chloride	5	0.5 (Fehr et al., 2003)	0.5

[a] USEPA, 2002.
[b] Written communication, IARC.
[c] Décret n°2001-1220 du 20 décembre 2001.

2.2.5 Control measures

Investigating the presence of groundwater contamination usually begins, however, after users have been exposed to potential health risks, for example, after reports of abnormal casualties. In the case when contamination of groundwater by chlorinated solvents is detected, it becomes essential to estimate the level, extent, and source of contamination

so that appropriate control measures can be taken so as to reduce future health and environmental risks.

The most common control measures for groundwater contamination can be classified into three categories: contaminant mass removal, containment of contamination, and remediation measures. Methods of contaminant mass removal include source excavation, free product pumping, pump and treat, air sparging, surfactant flooding, etc. Containment of contamination can be achieved by installing low permeability walls or by hydraulic containment through use of pump and treat, solidification or stabilization of sources. Methods of treatment for controlling further contamination include bioremediation or biodegradation, ozone sparging, permeable treatment walls, etc. In industrial complexes, where most chlorinated solvents originate, Bardos (2001) presents recommended control measures with respect to source removal or plume management measures (Table 2.5).

Table 2.5 Recommended remediation strategy based on cases of contaminated sites

Site type	Advised remediation strategy
Underground tanks	Monitor If possible source removal
Gas Plant	Source removal and treatment
Industry near river	MNA
Petroleum filling	Injection of air up-gradient Funnel and gate down-gradient
Industrial Complex	Source removal MNA for plume management

(*source* : Bardos, 2001)

It should be noted however that, the cost of the control measures of contaminated sites is in general very high. For instance, in Western European countries, the total cleanup cost for known and suspected contaminated sites lies in the range of 88.5-163.5 billion euros (GCR, 2003). In France, between 2.3 million euros in 1992 to a maximum of 15.3 million

euros in 1995 was assigned by the 'French Organization of Enterprises for the Environment' (EPE) for cleaning contaminated sites (Prokop et al., 2000).

As most of the cleanup techniques or methods may last for several decades, the total cleanup cost would certainly be counted in terms of billions. However, the cost of not cleaning the contaminated sites is much higher than the cost of control measures. In this context, not recovered contaminated sites may not only lead to possible health disaster but also results negative economic consequences in the long term. Similarly, the use of highly sophisticated control measures might not necessarily be optimal. For instance, Hardisty (2001) shows that control measures by removing sources of contamination result in relatively maximum economic returns than any other measures such as containment of contamination, complete site cleanup, etc (Figure 2.2).

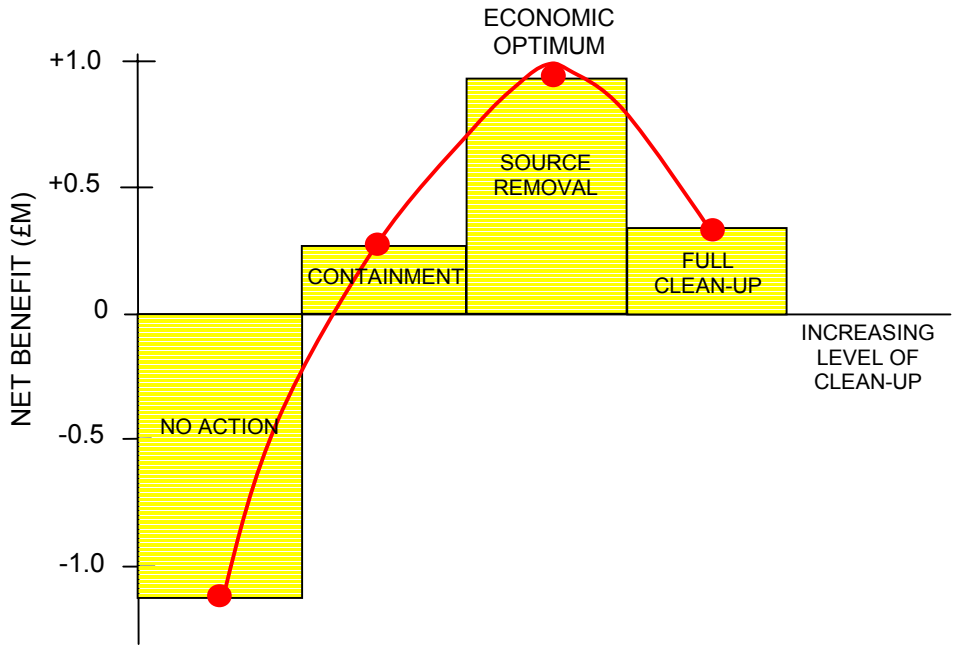

Figure 2.2 Cost and Benefit Analysis for Contaminated Site Cleanup Strategy (*source*: Hardisty, 2001; Cummings, 2002)

Obviously, when sources of contamination by chlorinated solvents are known, source removal measures could be a more appropriate action than any other plume control measures. But, in many cases, sources of contamination especially from complex industrial sites are not known. In this case, the determination of the level and extent of the contaminant plume can help decide whether source identification and removal is necessary.

2.3 Evaluation methods of groundwater pollution by dissolved chlorinated solvents

As discussed earlier, before a decision for source removal or remediation is made, one has to determine the level and extent of groundwater contamination by chlorinated solvents in dissolved form. Some of the methods presented here for evaluation or quantification of groundwater pollution are classified into two categories: 1) conventional methods and 2) the method of inversion of pumped concentration, a novel approach. For comprehensive descriptions of each method, readers may consult the respective references.

2.3.1 Conventional methods

The most common methods for groundwater pollution evaluation include site history analysis, visual inspections, use of transport models, geophysical methods, field sampling and interpolation, use of ANN, fuzzy logic models, etc.

Site history analysis:

A site history investigation may be applied once the contamination is detected in a monitoring or production well. Such steps are mainly applicable in urban areas where there can be several suspected sources of contamination and when one needs to identify the sources of contamination. Site history investigations mainly provide qualitative information that can serve as a basis for a more detailed analysis of contamination. It is mostly used for identifying suspected sources of contamination and the types or compositions of contaminants delivered to the subsurface. The reliability of site history

investigation depends on several factors such as the availability of documentation on various land-use activities in space and time, the composition of the detected chemicals, the underlying hydro-geological systems, the sources of information.

Visual inspections:

Visual inspection of potentially contaminated site can be made through a field visit to the site under consideration, evaluation of aerial photographs or satellite images if any. Visit to the suspected site may aid to identify certain indices directing to a possible contamination. Information on vegetal type and distributions, soil cover, local and regional terrain configurations, etc, may provide a clue for possible contamination of the site. Visual inspections may provide qualitative information and can only prepare to a next step for a more detailed analysis of contamination.

Geophysical Methods:

Geophysical methods are indirect methods of field investigations that help map contaminant pools and preferential groundwater flow paths in the subsurface using methods, for instance, ranging from soil vapor measurements to radar and electromagnetic surveys (Osienskya and Donaldsonb, 1995; Olivar et al. 1995). Soil vapor measurements are used to measure light volatile organic compounds such as LNAPLs that can be found closer to the ground surface. Electromagnetic surveys are used to measure the electrical conductivity of the soil and rock matrix. Most organic compounds are known to have lower electrical conductivity than that of water and, therefore, the presence and location of contaminants can be determined based on a decrease in the electrical conductivity measurements. Figure 2.3 shows an example of 3-D electromagnetic survey for detecting high concentrations of a dissolved DNAPL plume (>100 mg/l).

The method of ground penetrating radar is similar to electromagnetic surveys but it uses a much higher frequency than the electromagnetic method and measures the reflection of the electromagnetic waves caused by the conductivity and dielectric properties of the

features below the ground surface. In this case, the extent of contamination can be determined based on the variation of these properties relative to the same properties of water.

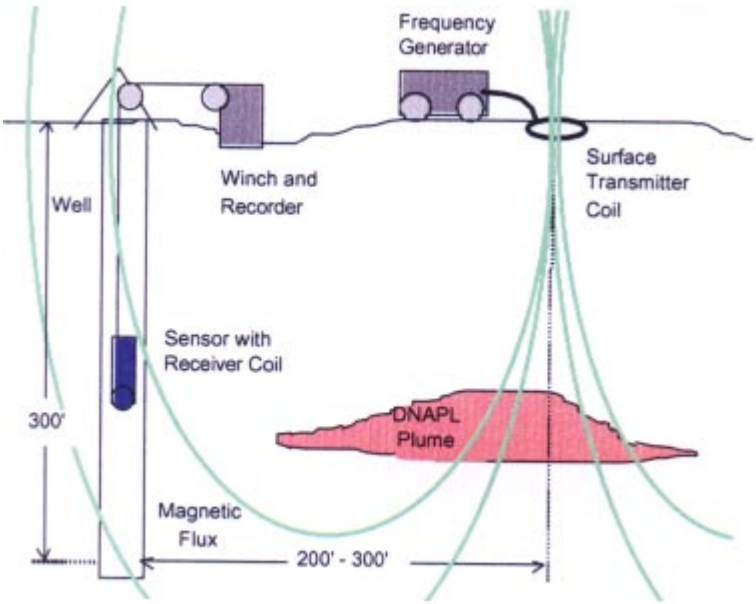

Figure 2.3 3-D resistivity transmitter and receiver system (*source*: NAVFAC, 1999)

For better determination of the extent and/or source of pollution, the geophysical methods need to be supplemented with field measurements through systematic installation of monitoring wells within the mapped plume

Onsite sampling and spatial interpolation:

In order to determine the actual level of contamination at some specified points, direct sampling, such as short time well purging, or passive sampling methods that uses dialysis cells as a passive collection devices, such as with the DMLS^{TM} sampler (Tunks et al., 2001), can be employed at different spatial locations. In either case, the reliability of the result depends on the resolution of data points, the design of the monitoring well as well as other factors which may influence the accuracy of the measured values. For instance, in the case of a very heterogeneous aquifer, it is necessary to collect as many samples as possible from several points, which in general requires the installation of several

monitoring wells. Several point measurements with higher resolution help minimizing the chances of missing some plume lenses, but the costs of installing a dense array of measurement wells can certainly be very high. On the other hand, using only a few measurement points do not provide adequate information on the state of groundwater pollution. In this case, interpolation methods from known data values can be employed.

Interpolation methods are in general used to estimate missing values from known values in a spatial data grid. The reliability of the results depends on the density or spatial distribution of the known data points as well as on the interpolation techniques used. The denser the spatial distribution of the known data points the better the interpolation results. Interpolation from sparse data points are less reliable in the case when contaminants are distributed non-uniformly in heterogeneous aquifer materials. The most common spatial interpolation techniques are linear interpolation, inverse distance weighted, and kriging.

Linear interpolation is the simplest method. It approximates the variation of the concentration between two points by a linear trend. Spatial interpolation with inverse distance weighting method is based on the separation distance and the corresponding concentration of spatially distributed data points. In this case, it is assumed that the interpolated data is highly influenced by the value of the nearby points than anywhere further from the point under consideration.

Kriging is a method used to estimate unknown values based on the statistical correlation of distributed values. For instance, points that are closer to each other are statistically more correlated than points which are sparsely distributed. Kriging uses a plot of the semivariances as a function of the separation distance called semivariogram so as to measure the degree of correlation of distributed values. The most commonly used semivariogrram models for fitting with experimental semivariograms are linear, pure nugget, spherical and exponential.

Mathematical models for contaminant transport:

In the case when sources of contamination are known and time of delivery information is obtained during site history investigations, forward mathematical models for contaminant transport can be used to determine the extent and level of contamination down-gradient of the sources. The partial differential equation for the transport of dissolved contaminants from some known source of contamination is given as (Zheng and Wang, 1999):

$$\frac{\partial(\theta C^k)}{\partial t} = \frac{\partial}{\partial x_i}\left(\theta D_{ij}\frac{\partial C^k}{\partial x_j}\right) - \frac{\partial}{\partial x_i}\left(\theta v_i C^k\right) + q_s C_s^k + \sum R_n \tag{2.1}$$

Where θ [-] is the porosity of the subsurface medium, C^k [ML^{-3}] is the dissolved concentration of specie k, t [T] is the time, $x_{i,j}$ [L] is the distance along the respective Cartesian coordinate axis, D_{ij} [L^2T^{-1}] is the hydrodynamic dispersion coefficient, v_i [LT^{-1}] is the seepage or linear pore water velocity, q_s [T^{-1}] is the volumetric flow rate per unit volume of aquifer representing fluid sources (positive) and sinks (negative), C_s^k [ML^{-3}] is concentration of the source or sink flux for species k, and R [$ML^{-3}\ T^{-1}$] is the chemical reaction term.

The mathematical model for the contaminant transport requires groundwater flow velocity field. The partial differential equation describing the movement of groundwater of constant density is given as (McDonald and Harbaugh, 1988):

$$Ss\frac{\partial h}{\partial t} = \frac{\partial}{\partial x}\left(Kxx\frac{\partial h}{\partial x}\right) + \frac{\partial}{\partial y}\left(Kyy\frac{\partial h}{\partial y}\right) + \frac{\partial}{\partial z}\left(Kzz\frac{\partial h}{\partial z}\right) - W \tag{2.2}$$

Where Kxx [LT^{-1}], Kyy [LT^{-1}], and Kzz [LT^{-1}] are hydraulic conductivity values along the x, y, and z co-ordinate axes respectively; h [L] is the potentiometric or hydraulic head; W [T^{-1}] is the source/sink term; Ss [L^{-1}] is the specific storage of the porous medium; and t [T] is the time.

Depending on the complexity of the subsurface system and availability of data the mathematical models for contaminant transport described above can be approximated analytically or numerically. When the system geometry is simple and the input parameters are constant, analytical models are simple to use and can provide quick results. There are a number of analytical models for solving one-, two-, and three-dimensional problems (Wilson and Miller,1978; Mironenko and Pachepsky, 1984; Domenico, 1987; Dillon, 1989; Wexler, 1989; Lerner and Papatolios, 1993; Basha and El Habel, 1993). For instance, Wilson and Miller (1978) provided an analytical solution for contaminant transport in a homogeneous, isotropic aquifer with a source term of continuous mass injection as follows:

$$c(x,y,t) = \frac{\overline{C_0}}{4\sqrt{\pi\alpha_T}} \exp\left(\frac{x - r\gamma}{2\alpha_L}\right) \frac{1}{\sqrt{r\gamma}} erfc\left(\frac{r - ut\,\gamma/R}{2\sqrt{\alpha_L ut}}\right);$$

$$\text{with } r = \sqrt{x^2 + (\alpha_L/\alpha_T)y^2}\ ;\ \gamma = \sqrt{1 + 4\alpha_L \lambda R/u}\ ;\ r/(2\alpha_L) > 1 \tag{2.3}$$

where $\overline{C_0}$ [ML^{-3}] is initial mean concentration of the source, u [LT^{-1}] is the mean groundwater flow velocity, α_L [L] and α_T [L] are the respective longitudinal and transverse dispersivities, λ [L^{-1}] is the decay coefficient, R [-] is the retardation factor, x and y are the spatial coordinates relative to the source location, and t [T] is the elapsed time between the source introduction and sampling time.

However, in the case when flow and transport parameters change in space and time and the aquifer geometry is complex, analytical solutions may not be sufficiently accurate. In this case, numerical models can be employed to handle the complex system geometry as well as the variable system parameters. The most commonly used numerical solution methods are finite element and finite difference methods.

Finite difference methods define the model space in a rectangular grid, from which parameters such as hydraulic conductivity, layer thickness, etc, are specified for each grid cell. In general, finite difference methods are relatively easier to use but less suitable to define irregular model boundaries. Numerical groundwater flow and transport models such as MODFLOW (McDonald and Harbaugh, 1988) and MT3D (Zheng, 1990) respectively are based on numerical solutions with finite difference method.

The mathematical models presented above can best be used for determining the extent and level of groundwater evaluation if the source concentration and time of delivery are known. In the case when source parameters are unknown, implementation or application of transport models could be limited and require intensive simulations using random source parameters, which could in general be computationally very costly.

Artificial Neural Network modeling:

Artificial Neural Networks (ANN) have been applied recently for groundwater flow and contaminant transport simulation. Using ANN with respect to groundwater problems has several advantages in that it can help to supplement or partially replace numerical models as well as find optimal solutions for remediation design. A typical ANN structure consists of an input layer, hidden layer, and output layer in which both layers are connected by one or more nodes (neurons) as shown in Figure 2.4. In this case, information enters from one node to the next node (neurone) pre-multiplied by a weight that models the synaptic efficiency (Hebbian learning). Thus, a three-layer feed forward ANN with the type shown in Figure 2.4 can be used as a universal function approximator and as a powerful tool to solve problems related to groundwater flow and contaminant

transport, which otherwise require a large number of simulations (Morshed and Kaluarachchi, 1998).

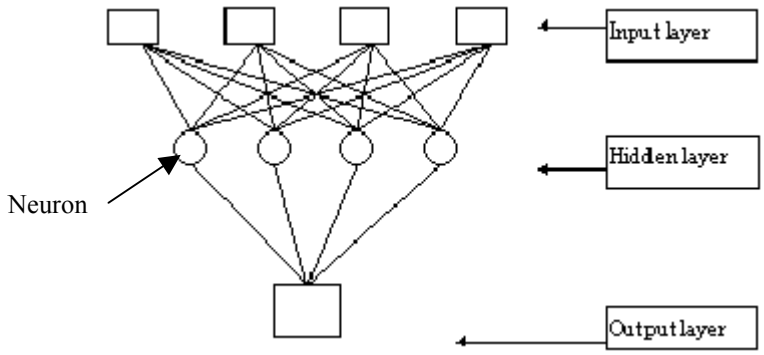

Figure 2.4 Architecture of artificial neural network

The ANN functions with on the input-output response based on the historical data used to train it. Unlike traditional flow and transport models, ANN does not require knowledge of any of the physical processes that govern the flow and transport in the groundwater system. Thus, once the ANN is trained, using for instance the output of a numerical model, it can then be applied to predict the behavior of another site with similar conditions. The ANN models are used mainly for a system that can be difficult to describe mathematically (Morshed and Kaluarachchi, 1998).

Structure of an ANN may be classified into 3 groups depending on the arrangement of neurons and the connection patterns of the layers: 1) feed-forward (error back propagation networks), 2) feedback (recurrent neural networks and adaptive resonance memories), and 3) self-organizing (Kohonen networks). In terms of their learning features ANN may be roughly categorized into two types: 1) *supervised* learning algorithms, where networks learn to fit known inputs to known outputs, and 2) *unsupervised* learning algorithms, where no desired output to a set of input is defined.

Fuzzy logic modeling:

Fuzzy logic is a superset of conventional (Boolean) logic that has been extended to handle the concept of partial truth-truth values between "completely true" and "completely false". Fuzzy logic is used when a system is difficult to model exactly (but an inexact model is available), when the system is controlled by a human operator or expert, or when ambiguity or vagueness is common. In many cases, under field condition, exact parameter values are unknown and subjected to human judgement with values provided in intervals or qualitatively. Fuzzy logic deals with parameter uncertainties related to vague definition of values rather than using probability theories like stochastic modeling. For instance, the solution to the governing equation for contaminant transport can be constrained by vague definition of aquifer parameters. In this context, fuzzy logic modeling can be applied so as to reduce subjective uncertainties through use of fuzzy set mathematics (Dou et al., 1997). This method follows some rules to determine whether the defined value belongs to a level of presumption, α-level, for a given interval of parameter values. Figure 2.5 shows a schematic description of fuzzy set approach related with the fuzzy set mathematics.

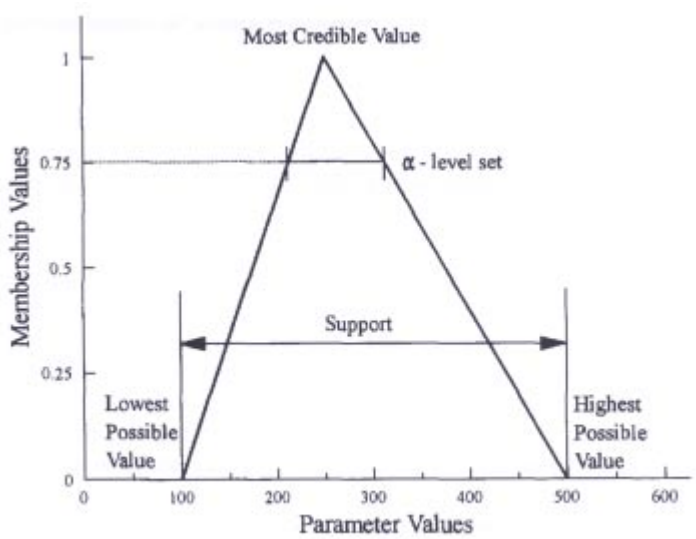

Figure 2.5 Schematic representation of fuzzy set theory with fuzzy number, its support and an α-level set (*source*: Dou et al., 1997)

Detailed descriptions of fuzzy set mathematics and applications to solute transport modeling is presented by Dou et al. (1997). Related applications of fuzzy modeling in groundwater problems can be found in, for instance, Mohamed and Karl Côté (1999), Freissinet et al. (1998).

2.3.2 Inversion of pumped concentration

Quantification of the level and extent of groundwater pollution can also be made using mathematical inversion of pumped concentration in the course of the integral investigation process. The integral investigation method is a new approach for groundwater pollution analysis in urban industrial zones (INCORE, 2003). Figure 2.7a shows a land-use pattern of variable pollution distribution that can be addressed with the integral investigation method. The integral investigation method operates with a series of site screening cycles ranging from the integral pumping tests to the quantification of groundwater pollution using the method of inversion of pumped concentration.

The screening procedures help to identify the area of maximum interest for further analysis. It follows a step-by-step three cycle procedure (Figure 2.6b). The first cycle (Cycle I) begins the evaluation of groundwater pollution at the largest scale, i.e. by investigating the whole industrial zone. The first cycle deals mainly with plume screening so as to identify zones of higher contamination. The part of the investigated zone with contamination level above some predefined limit is considered in the next evaluation cycle (Cycle II). Further investigation on the extent, level and source of contamination is dealt with during the second screening stage. Cycle II involves the decision whether the contaminated site or source of contamination needs remediation action or not.

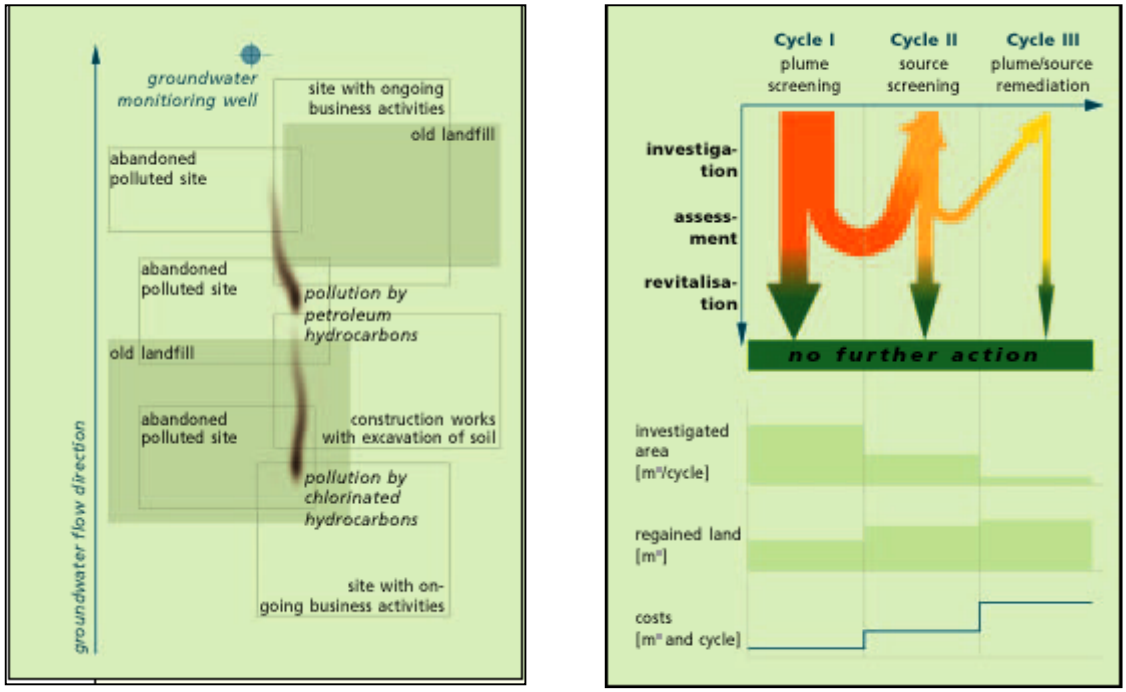

(a) (b)

Figure 2.6 Schematic representation for the integral investigation approach : a) example of polluted industrial zone configuration, b) Cyclic approach of the integral investigation method (*source*: INCORE, 2003).

Cost evaluation of the integral investigation relative to conventional methods such as point measurements shows that the former is more economical for application at regional scale (Kirchholtes et al., 2003). Table 2.6 shows cost comparison for integral investigation methods and conventional methods such as point measurements based on specific case studies.

Table 2.6 Cost comparison for integral investigation approach and conventional approach (Kirchholtes et al., 2003)

Cycle I Costs (€)	Cycle II Costs (€)	Number of single sites	Average costs per site (€): Conventional approach	Total costs (€): Conventional approach	Total costs (€): Integral investigation approach
Stuttgart (regional scale)					
750,000	150,000	80	20,000	1,600,000	900,000
Milan (local scale)					
135,000	27,000	5	20,000	100,000	162,000
Strasbourg (regional scale)					
124,000	25,000	10	20,000	200,000	149,000

The method of inversion of pumped concentration involves the inversion of concentration-time series data obtained from the radially captured contaminated groundwater during the integral pumping tests. Integral pumping tests refer to conventional pumping tests with simultaneous recording of the concentration from single or multiple pumping wells at a predefined imaginary control plane (ICP) as shown in Figure 2.7. The zonal concentration data for each isochrone (Figure 2.7b) is then used to determine the inverted concentration distribution as a function of the transverse distance (Figure 2.7c) at the ICP.

The knowledge about the inverted concentration distribution at the ICP allows to calculate the mean concentration crossing the ICP. In addition, the concentration-time series curves from multiple pumping tests help provide information on the most probable position of the plume with respect to the transversal direction. For instance, the concentration-time series curve from the second well P2 shows elevated values compared to the other two wells, P1 and P3. Since the concentration-time series data from P3 is very small compared to P1, one can infer from concentration-time series values of P2 and P1 that the major part of the plume passes between pumping well P2 and pumping well P1.

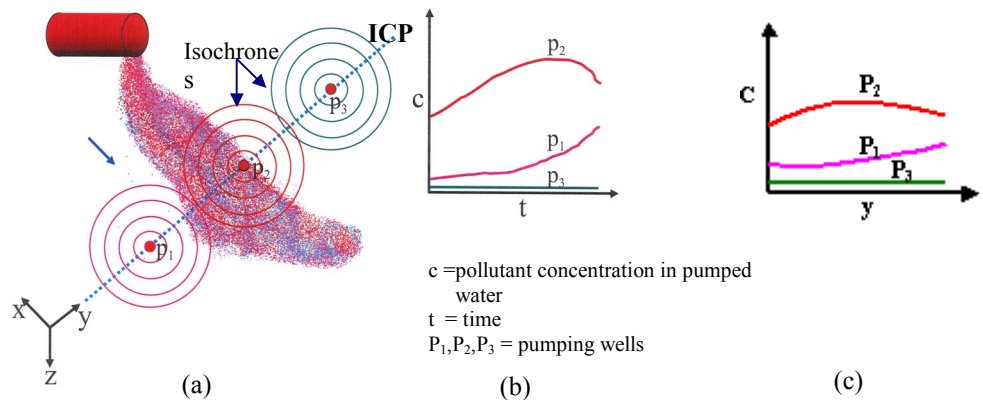

Figure 2.7 Schematic representation of integral pumping test for the inversion of pumped concentration (after Bockelmann et al., 2001)

The applicability of the method for known or unknown sources of contamination and in the situation when there are very few measurements makes it advantageous over the conventional methods for groundwater pollution evaluation. A recursive analytical solution for the inversion of pumped concentration is provided by Schwarz et al. (1998) as:

$$C_{inv_j} = \frac{\pi Cp_j - 2\sum_{k=1}^{j-1} C_{inv_k}\left[\arccos\left(\frac{r(t_{k-1})}{r(t_i)}\right) - \arccos\left(\frac{r(t_k)}{r(t_j)}\right)\right]}{2\arccos\left(\frac{r(t_{j-1})}{r(t_j)}\right)} \tag{2.5}$$

where C_{inv} [ML^{-3}] is the inverted concentration along the transverse direction y where the ICP is positioned, C_p [ML^{-3}] is the pumped concentration, r [L] is the radius of influence, t [T] is the pumping time in the concentration-time series, and j is the index (j=1,2,3....n) in the concentration-time series of n data points. The radius of influence, for radially symmetric flow field, can be determined as:

$$r_j = \sqrt{\frac{Qt_j}{\pi b \phi}} \tag{2.6}$$

where r_j [L] radius of influence, Q [L^3T^{-1}] is the pumping rate, t [T] is the time since the start of pumping, ϕ [-] is the porosity, and b [L] is the thickness of the aquifer, and j is the index in the concentration-time series of n data points (j=1,2,3...n). Some of the main assumptions to the solution of Equation 2.5 include: 1) the flow towards the pumping well is radial and the aquifer is confined, homogeneous and isotropic with constant thickness (Figure 2.8), 2) the contaminant transport is governed by pure advection and, therefore, the contaminant plume can be represented by piston type flow stripped with streamlines of the natural groundwater flow, 3) the concentration in a given streamtube is constant.

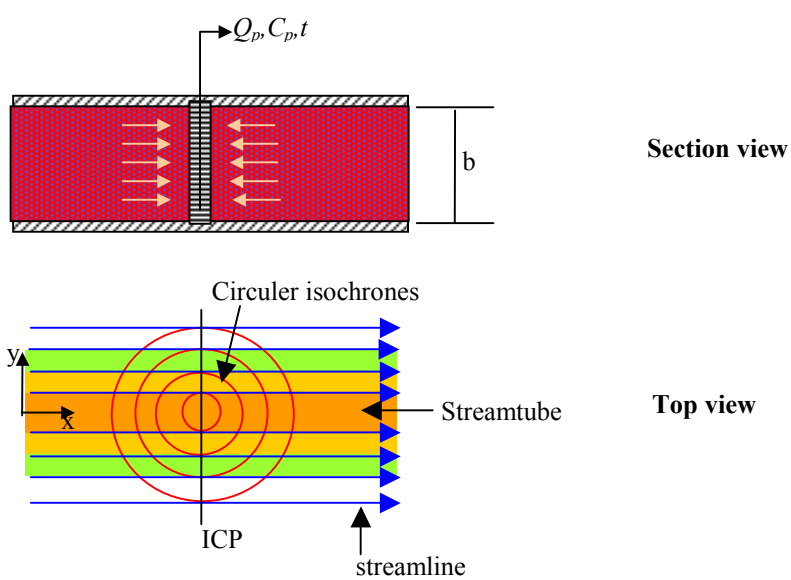

Figure 2.8 Schematic representation of a well capture zone from a hypothetical single layered confined homogeneous aquifer with a fully penetrating pumping well having a constant discharge of Q_p.

In order to derive Equation 2.5, the circular isochrones that can be obtained during pumping are superimposed with the plume, which is stripped with streamlines, before

pumping (Figure 2.9). It should be noted here that the natural flow gradient is neglected so that the isochrones can be simplified by circles.

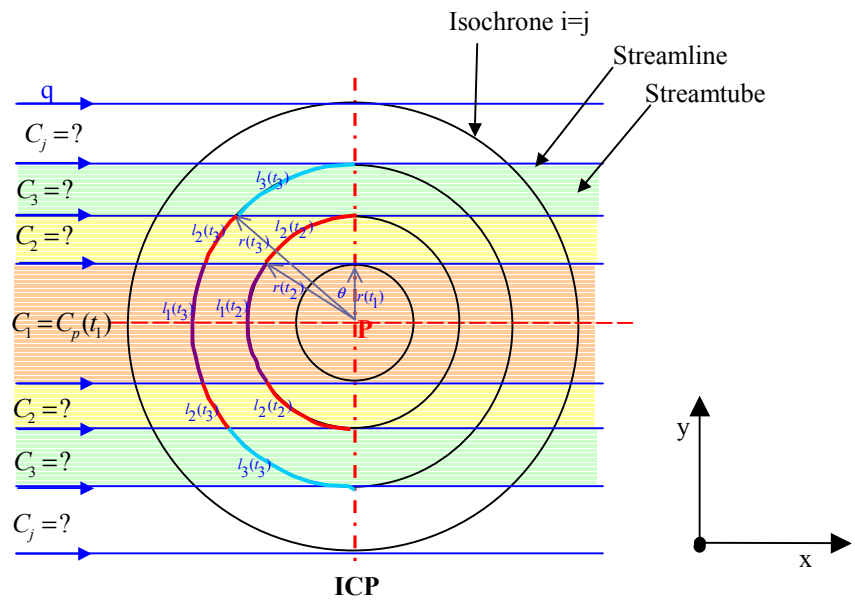

Figure 2.9 Schematic representation of isochrones and streamtubes for mathematical representation of the analytical inversion of pumped concentration

At the initial time t_1, the concentration in the middle streamtube is assumed to be equal to the pumped concentration. In this case, the first isochrone is assumed to represent the pumped concentration at time t_1. For the pumping time $t_{i>1}$, with i as the time index in the concentration-time series data, the pumped concentration in the corresponding time is assumed to be equal to the length weighted mean of the concentration values in the streamtubes crossing the well capture zone at the same time. Since the isochrones are circular and the plume is symmetrical, half of the circle can be used to derive the solution. A part of a given isochrone that crosses a streamtube is assumed to represent the concentration of that streamtube. Thus, the pumped concentration at a given time is assumed to be equal to the arc length weighted of the concentrations of the streamtubes

encompassed by the isochrone. In the schematic representation shown above (see Figure 2.9), the arc length $\ell_j(t_i)$, with j as the streamtube index, that intersect the streamtubes under consideration are used in the weighting. For instance, at time t_2, the pumped concentration can be expressed as:

$$C_p(t_2) = \frac{\ell_1(t_2)C_1 + \ell_2(t_2)C_2\big|_{left} + \ell_2(t_2)C_2\big|_{right}}{\ell_1(t_2) + 2\ell_2(t_2)} \tag{2.7}$$

However, taking the pumping well **P** as a reference, the concentration in the mirror image streamtubes of a symmetrical plume are assumed to be equal. Thus, Equation 2.7 can be rewritten as:

$$C_p(t_2) = \frac{\ell_1(t_2)C_1 + 2\ell_2(t_2)C_2}{\ell_1(t_2) + 2\ell_2(t_2)} \tag{2.8}$$

Rearranging Equation 2.8, the unknown concentration C_2 in the second streamtubes can be defined as:

$$C_{j=2} = \frac{C_p(t_2)\left[\ell_1(t_2) + 2\ell_2(t_2)\right] - \ell_1(t_2)C_1}{2\ell_2(t_2)} \tag{2.9}$$

Given a circle with radius r, the arc length ℓ from a subtending radian angle θ can be defined as :

$$\ell = r\theta$$

Taking two consecutive circular isochrones with the respective radii r_1 and r_2, the radian angle θ can be defined from trigonometry as:

$$\theta = \arccos\left(\frac{r_1}{r_2}\right)$$

Therefore, from Figure 2.9 and Equation 2.9, the arc lengths ℓ_1 and ℓ_2 can be calculated as:

$$\ell_1(t_2) = \pi r(t_2) - 2\ell_2(t_2)$$

with

$$\ell_2(t_2) = r(t_2)\arccos\left(\frac{r(t_1)}{r(t_2)}\right) \tag{2.10}$$

Thus, substituting Equation 2.10 in Equation 2.9, the concentration C_2 in the second streamtubes can be obtained as:

$$C_{j=2} = \frac{\pi C_p(t_2) - 2C_1\left[\pi/2 - \arccos\left(\frac{r(t_1)}{r(t_2)}\right)\right]}{2\arccos\left(\frac{r(t_1)}{r(t_2)}\right)} \tag{2.11}$$

In order to calculate the concentration C_3 in the third streamtubes, the pumped concentration at time t_3 can similarly be expressed as:

$$C_p(t_3) = \frac{\ell_1(t_3)C_1 + \ell_2(t_3)C_2\big|_{left} + \ell_2(t_3)C_2\big|_{right} + \ell_3(t_3)C_3\big|_{left} + \ell_3(t_3)C_3\big|_{right}}{\ell_1(t_3) + 2\ell_2(t_3) + 2\ell_3(t_3)} \tag{2.12}$$

Equating the concentration in the mirror image streamtubes, Equation 2.12 can be expressed as:

$$C_p(t_3) = \frac{\ell_1(t_3)C_1 + 2\ell_2(t_3)C_2 + 2\ell_3(t_3)C_3}{\ell_1(t_3) + 2\ell_2(t_3) + 2\ell_3(t_3)} \tag{2.13}$$

The arc length crossing the five streamtubes, i.e. for the third isochrone at time t_3, is equal to $\pi r(t_3)$. Therefore, the individual arch lengths ℓ_1, ℓ_2, and ℓ_3 can be obtained as:

$$\begin{aligned}
&\ell_1(t_3) = \pi r(t_3) - 2\left[\ell_3(t_3) + \ell_2(t_3)\right] \\
&\textit{with} \\
&\ell_3(t_3) = r(t_3)\arccos\left(\frac{r(t_2)}{r(t_3)}\right) \\
&\ell_2(t_3) = r(t_3)\arccos\left(\frac{r(t_1)}{r(t_3)}\right) - r(t_3)\arccos\left(\frac{r(t_2)}{r(t_3)}\right)
\end{aligned} \tag{2.14}$$

Rearranging Equation 2.13 and substituting Equation 2.14, the concentration in the third streamtube $C_{j=3}$ can be obtained as:

$$C_{j=3} = \frac{\pi C_p(t_3) - 2\left[C_2\left(\arccos\left(\frac{r(t_1)}{r(t_3)}\right) - \arccos\left(\frac{r(t_2)}{r(t_3)}\right)\right) + C_1\left(\pi/2 - \arccos\left(\frac{r(t_1)}{r(t_3)}\right)\right)\right]}{2\arccos\left(\frac{r(t_2)}{r(t_3)}\right)}$$

(2.15)

Please note that at the outer streamtubes just beside to a streamtube with known concentration, the streamtube index j is always equal to the pumping time index i. For instance, at the third streamtube presented in this example, the streamtube index j is 3 at the third time with time index i=3. For a contaminant plume stripped with several streamtubes, Equation 2.15 can be extended and generalized into Equation 2.16, which is exactly the same as Equation 2.5.

$$C_j = \frac{\pi C_p(j) - 2\sum_{k=1}^{j-1} C_k\left[\arccos\left(\frac{r(t_{k-1})}{r(t_j)}\right) - \arccos\left(\frac{r(t_k)}{r(t_j)}\right)\right]}{2\arccos\left(\frac{r(t_{j-1})}{r(t_j)}\right)}$$

(2.16)

The total mass flow rate that may pass through the ICP, for a plume with constant concentration strip, can then be calculated from the sum of individual mass flow rate in each plume stripe as:

$$m_j = \left(C_{inv} q\right)_j$$

(2.17)

where m [MT^{-1}] is the mass flow rate, C_{inv} [ML^{-3}] is the inverted concentration, j is the index in the concentration-time series of n data points (j=1,2,3,…, n), and q [L^3T^{-1}] is the

flow rate for a stream tube corresponding with the index *j*. Thus, for axi-symmetrical flow, the total mass flow rate M [MT^{-1}] at the ICP can be given as:

$$M = 2\sum_{j=1}^{n}\left(C_{inv}q\right)_j \tag{2.18}$$

However, in reality, with a plume shape that can be represented as in Figure 2.10, it is more likely that there would be a change of concentration between the source point and the point of detection somewhere down gradient to the source (Zeru and Schäfer, 2002, 2003a, 2003c, 2004).

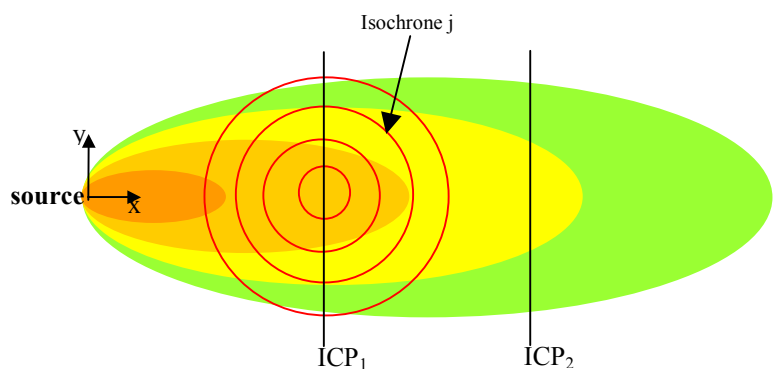

Figure 2.10 Schematic representation of a plume with longitudinal concentration gradient

In other words, the source concentration is not the same as the concentration measured somewhere downstream to the source. For instance, the concentration distribution values at the ICP_1 are not the same as that of ICP_2. Moreover, the concentration distribution that can be calculated at a given ICP can be affected by the presence of heterogeneous materials. Therefore, the inverse model presented above may not provide adequate information on the state of groundwater pollution in the case when there are local heterogeneities and the concentration gradient in the plume is not negligible. Detailed analyses of the inversion of pumped concentration taking into account the effect of

concentration gradient in the plume and local heterogeneities are presented in the following chapters.

2.4 Summary

The ever growing and increasing diversities of industrial activities have been a threat to the underlying groundwater reserves in many industrial areas. Industrial waste discharges, accidental spills and leaks of petroleum products are some of the many sources of industrial zone groundwater contamination. Chlorinated solvents are non-aqueous phase liquids (DNAPLs) that are known to be the cause of groundwater contamination in many industrial areas. Chlorinated solvents such as PCE and TCE are toxic products that can cause serious health problems to humans through one or more of means of exposures such as ingestion, inhalation and dermal adsorption.

In many cases, the investigation for the presence of groundwater contamination begins after reports of abnormal casualties on human health and the environment. Once contamination has been detected, it becomes essential to determine the level, extent and source of contamination. The most common methods for the evaluation and/or quantification of pollution include site history analysis, visual inspection, geophysical methods, onsite sampling and spatial interpolation methods, and use of contaminant transport models, artificial neural network (ANN) and fuzzy logic models. The method of the inversion of pumped concentration, as part of the integral investigation process, can be used for groundwater pollution quantification of known and unknown sources. However, the analytical inverse solution presented in this section may not provide adequate information on the state of groundwater pollution in the case when there are local heterogeneities and the concentration gradient in the plume is not negligible.

Chapter 3

Inversion of pumped concentration taking into account concentration gradient in the plume

3. Inversion of pumped concentration taking into account concentration gradient in the plume

This chapter addresses the analysis of groundwater pollution with the method of inversion of pumped concentration by taking into account the effect of concentration gradient in the longitudinal axis of a contaminant plume. The uncertainties related to the presence of a concentration gradient is briefly highlighted and detailed analysis on the longitudinal concentration gradient relative to the corresponding transversal concentration gradient, using the gradient ratio (GR), is presented using a 2D analytical model for contaminant transport. Moreover, a comparative study between the inverted concentration distribution results and the corresponding numerical simulation results (assuming the numerical model represents a real aquifer) is presented in order to estimate the discrepancies between the inverted concentration distribution and the real concentration distribution. The inverted concentrations can either overestimate or underestimate the real concentration values. An empirical relationship between the calculated errors and the corresponding gradient ratio GR values are presented for a range of dispersivity values. The total mass flow rate that can be calculated from the inverted concentration distribution is thus reformulated and presented so as to determine the state of groundwater pollution by taking into account the presence of concentration gradient in the longitudinal axis of a contaminant plume.

3.1 Introduction

In the absence of enough point measurements or monitoring wells, the state of groundwater pollution can be evaluated from the pumped concentration. Several studies have been conducted and mathematical models have been developed for use and applications of radial flow to a pumping well (Kamra et al., 2002; Kaleris et al., 1995; Rock and Kupfersberger, 2002; Fleming et al. 2002; Peng et al. 2002). The applications of most of these studies have focused mainly on capture zone delineation, aquifer

parameter determination, groundwater pathline and travel time studies, point concentration profile studies, etc.

With a recent approach, however, delineation and quantification of contamination can be made by the method of inverting pumped groundwater quality data obtained during conventional pumping tests (Schwarz et al., 1998). The application of radial flow for groundwater pollution analysis from zonal concentration profile, i.e. with the inversion of concentration-time series data, has been experimented at some industrial sites in Europe within the framework of the European R&D project INCORE (Integrated Concept fore Groundwater Remediation) (Holder et al., 1998; Bockelmann et al., 2001; Schäfer et al., 2001; Bockelmann et al., 2003). However, the concentration gradient in the longitudinal axis of the plume was neglected. This study presents the analyses of the method of inversion by taking into account the concentration gradient in the longitudinal axis of a contaminant plume.

3.2 Uncertainties on the concentration gradient in the plume

The basic assumptions used in the analytical inversion (see section 2.3.2) are that 1) the concentration gradient along the longitudinal axis of a contaminant plume is zero and 2) the flow to the pumping well is radial. The concentration within a given stream tube is assumed to be constant regardless of the magnitude of the distance between the source point and a detection point down gradient to the suspected source. Thus, theoretically, constant concentration in the longitudinal direction within each stream tube means a zero longitudinal concentration gradient within the plume.

However, in reality, with a plume shape that can be represented as shown in Figure 3.1, it is more likely that there would be a change of concentration between the source point and the point of detection somewhere down gradient (Zeru and Schäfer, 2002, 2003a, 2004). For instance, the concentration values at ICP_1 are not the same as those of ICP_2.

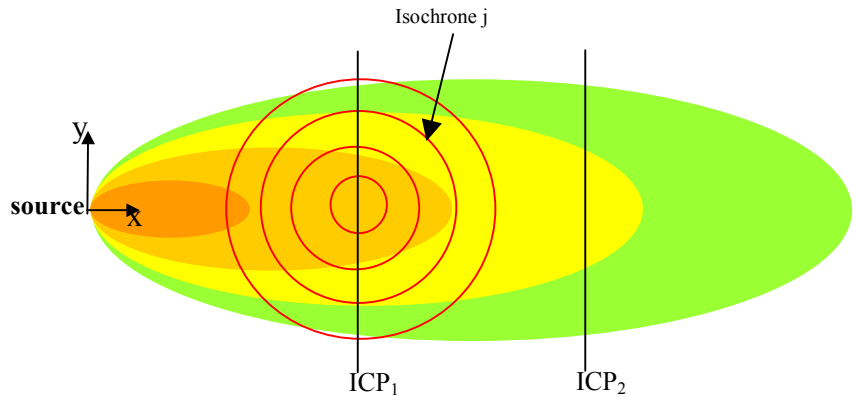

Figure 3.1 Schematic representation of a plume with longitudinal concentration gradient

3.2.1 Analysis of concentration gradient

In order to verify the hypothesis related to the effect of concentration gradient on the inversion of pumped concentration, a two-dimensional transport model is taken into consideration. For a simple hydrogeological problem with scarce data, the analytical model can provide a reasonably good and economical estimation. Several studies with analytical solutions have been conducted with various range of applications in contaminant mass transport problems and analytical models have been developed for 1D, 2-D or 3D analysis of contaminant transport (Wilson and Miller,1978; Domenico, 1987; Dillon, 1989; Wexler, 1989; Basha and El Habel, 1993). Many of the analytical models can provide reasonably good estimations for the analysis of contaminant transport under homogeneous, isotropic condition. Wilson and Miller (1978) provided an analytical solution (Equation 3.1) for contaminant transport in a homogeneous, isotropic condition with a source term of continuous mass injection (Kinzelbach 1987).

$$c(x,y,t) = \frac{\overline{C_0}}{4\sqrt{\pi\alpha_T}} \exp\left(\frac{x - r\gamma}{2\alpha_L}\right) \frac{1}{\sqrt{r\gamma}} erfc\left(\frac{r - ut\gamma/R}{2\sqrt{\alpha_L ut}}\right);$$

$$\text{with } r = \sqrt{x^2 + (\alpha_L/\alpha_T)y^2}\ ;\ \gamma = \sqrt{1 + 4\alpha_L \lambda R/u}\ ;\ r/(2\alpha_L) > 1 \tag{3.1}$$

where $\overline{C_0}$ [ML^{-3}] is initial mean concentration of the source, u [LT^{-1}] is the mean groundwater flow velocity, α_L [L] and α_T [L] are the respective longitudinal and transverse dispersivities, λ [T^{-1}] is the decay coefficient for the dissolved phase, R [-] is the retardation factor, x and y are the spatial coordinates relative to the source location, and t [T] is the elapsed time between the source introduction and sampling time.

With the absence of decay and retardation (λ=0; R=1), Equation 3.1 can be expressed as:

$$c(x,y,t) = \frac{\overline{C_0}}{4\sqrt{\pi\alpha_T}} \exp\left(\frac{x - r\gamma}{2\alpha_L}\right) \frac{1}{\sqrt{r}} erfc\left(\frac{r - ut}{2\sqrt{\alpha_L ut}}\right)$$

$$\text{with } \overline{C_0} = \frac{\dot{M}}{n_e bu} \tag{3.2}$$

where $\dot{M}$ [MT^{-1}] is the mass flow rate at the source, b [L] is the aquifer thickness, and n_e [-] is the porosity.

Some preliminary studies (Zeru and Schäfer, 2002, 2003a) suggested that the effect of the longitudinal concentration gradient on the inversion of pumped concentration can be expressed through a gradient ratio terms that can be correlated with the corresponding mass flow rate uncertainties. The gradient ratio GR is a non-dimensional term expressed in terms of the ratio of the longitudinal concentration gradient to the corresponding transverse concentration gradient. Preliminary evaluation shows that higher gradient ratio corresponds to significant uncertainties. This study looks into this problem in a more detailed way. The goal is to identify the important parameters which can have a significant effect on the gradient ratio GR. For a comprehensive evaluation, both the stationary and non-stationary plume conditions are taken into consideration. Thus, for a non-stationary case, the gradient ratio GR can be derived (Equation 3.3) by differentiating Equation 3.2 with respect to both x and y.

$$GR \equiv \frac{\partial c/\partial x}{\partial c/\partial y} = \frac{A+B}{D-C} \tag{3.3}$$

with

$$A = \left[\frac{r}{2\alpha_L} - \frac{x}{2\alpha_L} - \frac{x}{2r}\right] erfc\left(\frac{r-ut}{2\sqrt{ut\alpha_L}}\right)$$

$$B = \frac{x}{\sqrt{\pi}}\left(\frac{r-ut}{ut\alpha_L}\right)\exp\left(-\left(\frac{r-ut}{2\sqrt{ut\alpha_L}}\right)^2\right)$$

$$C = \frac{\alpha_L}{\alpha_T}\left(\frac{y}{2r} + \frac{y}{2\alpha_L}\right) erfc\left(\frac{r-ut}{2\sqrt{ut\alpha_L}}\right)$$

$$D = \frac{2y\alpha_L}{\pi\alpha_T}\left(\frac{r-ut}{ut\alpha_L}\right)\exp\left(-\left(\frac{r-ut}{2\sqrt{ut\alpha_L}}\right)^2\right)$$

The gradient ratio GR for a non-stationary plume is a function of the reference coordinate, the Peclet numbers, and the interval of time since the beginning of injection at the source, assuming the aquifer is homogeneous and isotropic. From dimensionless analysis, the gradient ratio GR as a function of these terms can be expressed as :

$$GR = f\left(\frac{x}{y}, Pe_x, Pe_y, \frac{\alpha_L}{\alpha_T}, \frac{ut}{x}\right) \text{ ; with } Pe_x = \frac{x}{\alpha_L} \text{ and } Pe_y = \frac{y}{\alpha_L} \tag{3.4}$$

where Pe_x and Pe_y are the respective Peclet numbers in the longitudinal and transversal directions, x and y are the respective longitudinal and transversal coordinates, and α_L [L] is the longitudinal dispersivity. Figure 3.2 shows the state of the gradient ratio GR for a given coordinate (x,y) at the transversal section of a 2D plume, with x equal to the

separation distance between the source and the transversal section. In general, keeping all other geometrical and transport parameters constant, higher gradient ratio GR can be expected at earlier transport period ($ut/x = 1.25$). However, as the transport period increases, the plume tends to stabilize. For instance, the last two curves for larger transport period ($ut/x = 2$ and $ut/x = 4$) show nearly overlapping trend, indicating that the plume reached stationary condition.

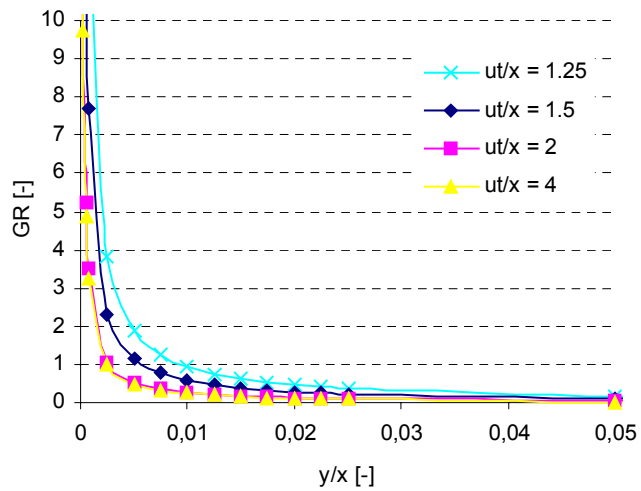

Figure 3.2 Gradient ratio GR versus dimensionless distance, transversal distance referenced from the pumping well at the origin divided by the separation distance x, as a function of dimensionless transport time (x=400 m, α_L=10 m, α_T=1 m, $y_{\min}$=0, $y_{\max}$=15 m, u=1 m/day).

As indicated earlier, once the plume reaches stationary condition, the transport period is not a significant parameter for evaluating the state of gradient ratio GR. For a infinitely long transport period, i.e. $t \to \infty$, Equation 3.2 has an exponential form and, from Kinzelbach (1987), can be expressed as:

$$c(x,y) \approx \frac{\overline{C_0}}{2\sqrt{\pi r \alpha_T}} \exp\left(\frac{x-r}{2\alpha_L}\right)$$

$$\text{with } r = \sqrt{x^2 + (\alpha_L/\alpha_T)y^2} \tag{3.5}$$

where the definition of the parameters and variables are as presented earlier in Equation 3.2. Thus, in a similar manner, the gradient ratio GR for a stationary plume can then be derived from Equation 3.5 and be expressed as:

$$GR = \frac{\frac{x}{2\alpha_L} + \frac{x}{2r} - \frac{r}{2\alpha_L}}{\frac{\alpha_L}{\alpha_T}\left[\frac{y}{r} + \frac{y}{2\alpha_L}\right]} \tag{3.6}$$

The parameters that are relevant to evaluate the state of the gradient ratio GR for a stationary plume can be expressed as:

$$GR = f\left(\frac{x}{y}, Pe_x, Pe_y, \frac{\alpha_L}{\alpha_T}\right); \text{ with } Pe_x = \frac{x}{\alpha_L} \text{ and } Pe_y = \frac{y}{\alpha_L} \tag{3.7}$$

Thus, the gradient ratio GR for a stationary plume is a function of the reference coordinates, the Peclet numbers, and the magnitude of the dispersivity ratio for a homogeneous and isotropic aquifer. At a given location within a 2D plume, the gradient ratio GR depends on the dispersivity terms. The figure below (Figure 3.3) shows the gradient ratio GR for a given point (x,y) on the transversal section of a 2D plume, with x the separation distance between the source and the transversal section, and a constant dispersivity ratio of 10 per cent. Since the interest here is the effect of the longitudinal concentration gradient in, the Peclet values with respect to the longitudinal axis are used for this presentation.

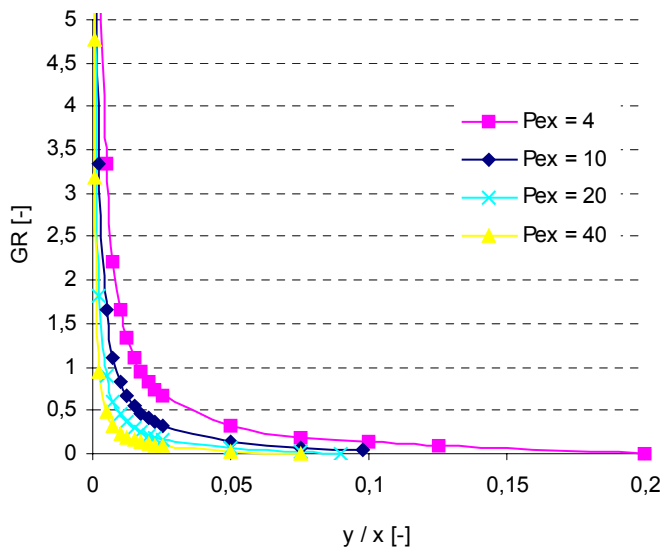

Figure 3.3 Gradient ratio GR versus dimensionless distance, transversal distance referenced from the pumping well at the origin divided by the separation distance x, as a function of the Peclet number Pe (x=400 m, α_L=10 m, 20 m, 40 m, and 100 m, α_T/α_L=0.1, $y_{\min}$=0, $y_{\max}$=15 m)

It can be noticed that higher gradient ratios GR correspond to lower Peclet numbers. It is also noticed that a higher gradient ratio GR can be expected for the points near the longitudinal axis of the plume.

3.2.2 Determination of gradient ratio GR

As mentioned in the preceding section, the gradient ratio GR is defined as the ratio of the longitudinal concentration gradient to the corresponding transversal concentration gradient. A representative gradient ratio GR can be estimated and expressed in two ways: 1) zonal averaged gradient ratio; and 2) directional gradient ratio. The zonal averaged gradient ratio, from the capture zones as indicated schematically in Figure 3.4, can be estimated from the average of the individual concentration gradient calculated at each node of the grid within the well capture zone (Equation 3.8).

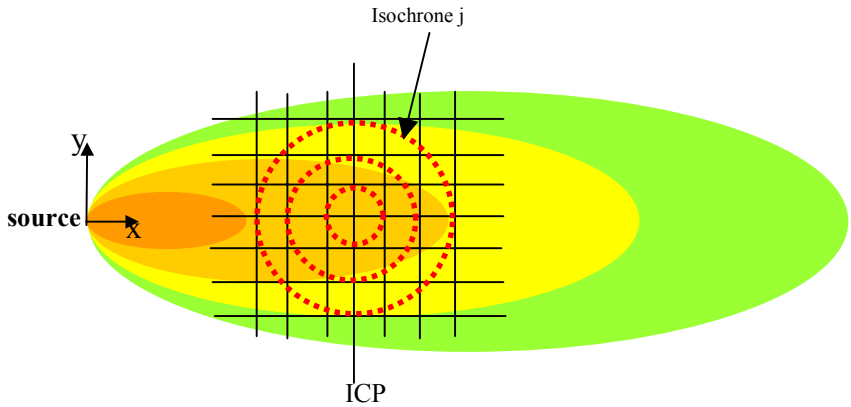

Figure 3.4 Schematic representation for zonal averaged gradient ratio estimation.

$$ZA = \frac{\sum_{i=1}^{N} \left| GR_{i,j} \right|}{N} \tag{3.8}$$

where ZA [-] is zonal averaged gradient ratio, $GR_{i,j}$ [-] is the gradient ratio GR at node i,j, and N is the number of nodes within the capture zone.

On the other hand, the directional averaged gradient ratio can be estimated from the ratio of the mean concentration gradient in the longitudinal axis of the plume to the mean of the concentration gradient in the transversal axis of the plume (Equation 3.9) as shown in Figure 3.5, where the origin of the axes is taken at the pumping well position. It has been shown in the preceding figures (Figure 3.2 and 3.3) that higher gradient ratio GR values occur at or closer to the longitudinal axis of the plume.

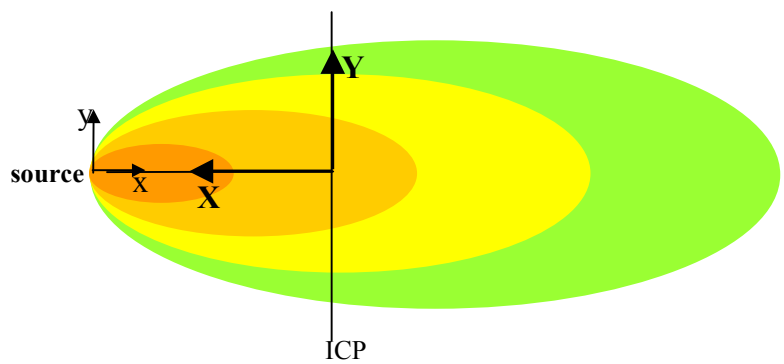

Figure 3.5 Schematic representation of directional averaged gradient ratio estimation

The mean of the concentration gradient in the longitudinal direction can be calculated by taking the concentration gradient at each node where each isochrone intersects the longitudinal axis of the plume. Similarly, the mean of the concentration gradient in the transversal direction can be calculated by taking the concentration gradient at each node where each isochrone intersects the transversal axis that passes through the ICP. Though several averaging methods exist to calculate the mean values, the distance ratio weighted mean (DRW) was employed (Equation 3.10) in order to give more weights for the concentration gradients around the vicinity of the well.

$$DA = \frac{MG_X}{MG_Y} \tag{3.9}$$

with:

$$MG_X = \frac{\sum_{i=1}^{n} \left| G_{X_i} \frac{1}{X^p{}_i} \right|}{\sum_{i=1}^{n} \left| \frac{1}{X^p{}_i} \right|} \text{ ; and } MG_Y = \frac{\sum_{j=1}^{m} \left| G_{Y_j} \frac{1}{Y^p{}_j} \right|}{\sum_{j=1}^{m} \left| \frac{1}{Y^p{}_j} \right|} \tag{3.10}$$

where DA [-] is directional averaged gradient ratio estimate, MG [-] is the mean concentration gradient, X [L] is the longitudinal direction with the reference point at the

pumping well, G [-] is the concentration gradient at a given point, Y [L] is the transversal direction at the ICP with the reference point at the pumping well, i and j are the indices for the longitudinal and transversal direction respectively, p [-] is a positive integer indicating the power, m and n are the number of data points in the transversal and longitudinal direction respectively. The absolute value used for the mean gradient in the longitudinal direction is caused by the change of the x-origin. In this case the x-origin is at the pumping well instead of the source point. The higher the power p the more the weights given to the concentration gradient in the vicinity of the well.

Depending on the choice of averaging method, the result of the gradient ratio GR estimate may vary. However, both the zonal averaged and directional estimation of gradient ratio GR show similar trend with parameters such as dispersivities in the case of a stationary plume (Figure 3.6) and the magnitude of transport period as in the case of non-stationary plume (Figure 3.7). It can be noticed that the directional averaged (DA) gradient ratio is smaller than the zonal averaged (ZA) gradient ratio. This is because, unlike the zonal averaged gradient ratio, the directional averaged gradient ratio takes into account only the mean gradient ratio values in the longitudinal and transversal direction regardless of the length of the well capture radius.

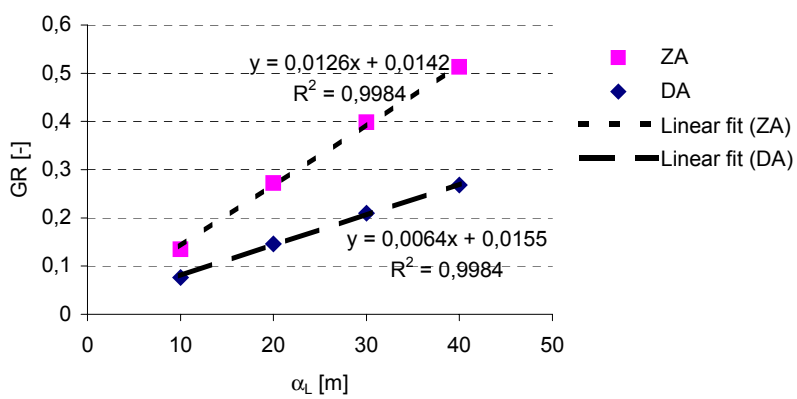

Figure 3.6 Comparison of zonal averaged (ZA) with directional averaged (DA) gradient ratio GR estimation for stationary plume (α_L = longitudinal dispersivity).

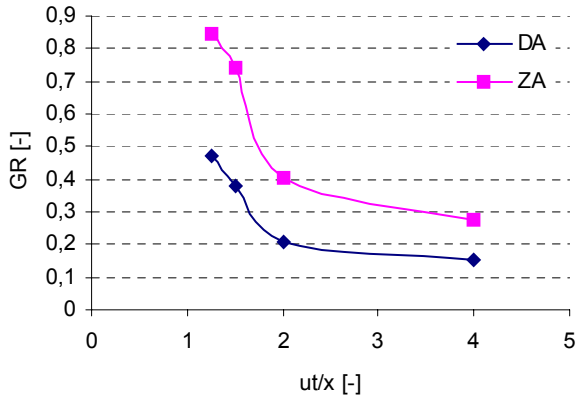

Figure 3.7 Comparison of zonal averaged (ZA) with directional averaged (DA) gradient ratio GR estimation for non-stationary plume (α_L =20 m)

From a practical point of view, estimating the gradient ratio GR with ZA could be difficult as a dense grid of measurement points within the well capture zone may not always be available. Thus, instead, the directional averaged gradient ratio GR can be used for practical application. In general, for field applications, a rough estimate of the gradient ratio with DA can be made if a minimum of two points of concentration measurements can be made, one in the transverse direction and the other in the longitudinal direction (Figure 3.8). Here, the main direction of groundwater flow is assumed to be in the x direction and the ICP position is along the y axis.

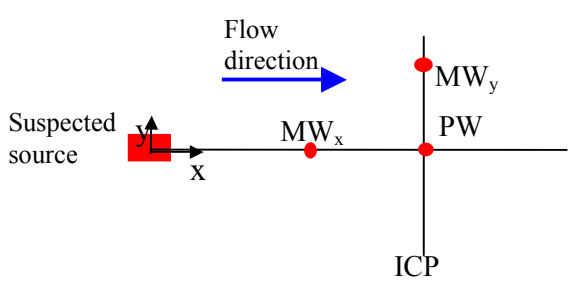

Figure 3.8 Example for rough estimation of directional averaged gradient ratio GR at a real site (MW_y = monitoring well in the transverse direction at the ICP, MW_x = monitoring well in the longitudinal direction upstream to the pumping well, and PW = the pumping well).

It should be noticed that this rough assumption is applicable in the case when there are no enough point measurements. Gradient ratio value can be improved if there are a few more measurements both in the longitudinal and transversal direction relative to the pumping position. For a contaminant plume with unknown source and without additional point measurements in the longitudinal and transverse direction, finding an ICP-Pump position by trial and error where a gradient ratio is closer to zero may be difficult in practice. Nevertheless, results can be improved or errors can be minimized by considering the relatively closest ICP-Pump position from the suspected source.

3.3 Evaluation of the effect of concentration gradient

3.3.1 Numerical model setup

In order to study the hypothesis related to the effect of concentration gradient on the determination of the level and extent of groundwater pollution, a numerical flow and transport model is set up in the ideal case of a single layer, isotropic, homogeneous, confined aquifer. Both the groundwater flow and contaminant transport model was built using the numerical codes MODFLOW (McDonald and Harbaugh, 1988; Harbaugh and M.G. McDonald,1996) and MT3D (Zheng, 1990), interfaced in Processing Modflow (Chiang and Kinzelbach, 1998). In contrast to the solution for the analytical inversion discussed earlier, the numerical simulation tests take into account various dispersivity scenarios and transport periods so as to study the significance of the concentration gradient on the inversion of pumped concentration for groundwater pollution analysis.

The detail of the numerical model set up is presented in Table 3.1. A total of 32 simulations were made from four dispersivity values with eight different transport periods each. A known source with a fixed concentration of 12.5 µg/l was considered and positioned at about 150 meters upgradient of the ICP position. Both the steady state and transient flow regimes are considered. For the transient period, a single pump was set to extract contaminated groundwater at the rate of 250 cubic meters per hour for three consecutive days, a pumping time long enough to get nearly circular capture zones.

Table 3.1 Main variables or parameters used in the numerical model

Variable or parameter	Value
Model area	500 m × 500 m
Grid size	5 m × 5 m
Layer thickness	35 m
Hydraulic conductivity	0.001 m/s
Hydraulic gradient	0.002
Porosity	0.17
Source concentration	12.5 µg/l
Source-to-pump distance	150 m
Longitudinal dispersivity:	α_L =5 m (Test1)
	α_L =10 m (Test2)
	α_L =20 m (Test3)
	α_L =30 m (Test4)
Dispersivity ratio (α_T/α_L)	0.1
Pumping rate	250 m^3/h
Stress period 1 (T) (Steady state period)	60, 90, 120, 150, 180, 365, 730, 1095 days (for each test)
Stress period II (Transient period)	3 days (for each steady state flow period)

In most practical cases, neither the source of contamination nor the position of the plume are known. However, for better understanding of the effect of the relevant parameters on the state of gradient ratio GR and thereby the longitudinal concentration gradient, an ideal source-to-pump position for single pumping test is defined along the longitudinal plume axis so that the concentration distribution in the transversal direction is symmetrical.

Moreover, although the inverted pumped concentration depends on the position of the ICP relative to the plume position (Zeru and Schäfer, 2003a, 2003b), the position of the ICP, 150 meters from the predefined source as shown in Figure 3.9, is not varied in this study. Thus, the ICP lies at the transversal axis that passes through the pumping well position. The concentration gradient both in the longitudinal and transversal directions with respect to the ICP-Pump position can then be evaluated.

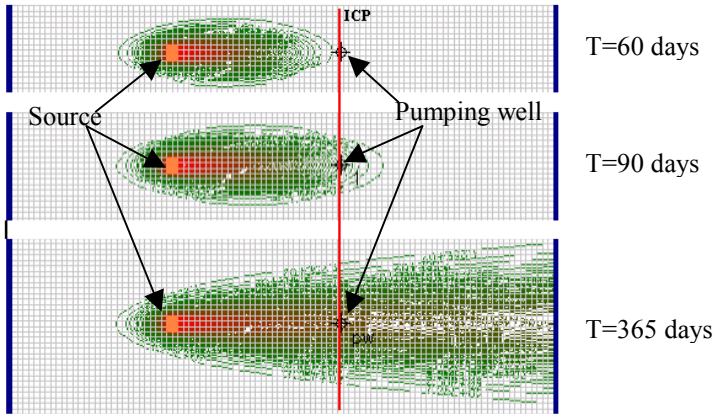

Figure 3.9 Example evolution of the plume from the source through the fixed ICP-Pump position for the transport period of 60 days, 90 days, and 365 days.

From the fixed type ICP set up, by varying the plume coverage, the change of longitudinal gradient relative to the corresponding transversal concentration gradient can then be evaluated. Thus, it is necessary to look in detail the trend of concentration distribution both in the longitudinal and transverse direction for each ICP-Plume set up.

At the end of the transient period simulation, for each steady state flow period, the concentration-time series data obtained from MT3D simulation output is used as an input data for the inversion of pumped concentration. An example of the concentration-time series data curves, from MT3D simulation output, is shown in Figure 3.10. Though simulations have been performed for four types of dispersivities as discussed earlier, for the purpose of demonstration and as the curves for the CTD show similar trend, the concentration-time series data for the dispersivity value of 10 meters is chosen here for presentation. As can be noticed, the concentration-time series curves for the larger transport periods of 365, 730, and 1095 days are nearly coincident, which indicates that the plume has reached steady state transport condition.

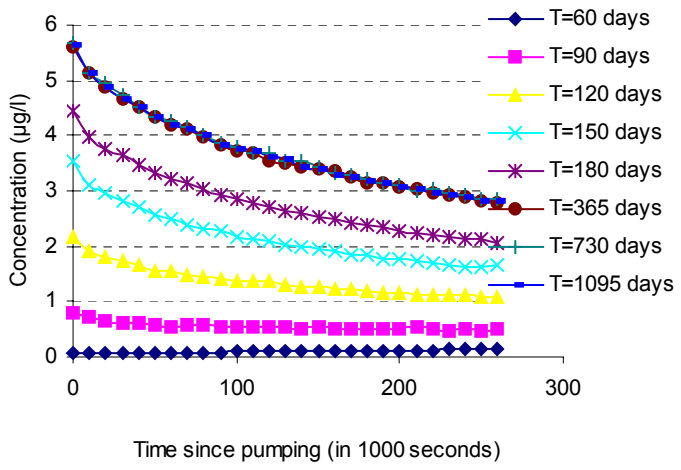

Figure 3.10 Example of concentration-time series data at the pumping well just after eight transport periods (α_L=10 m.)

Thus all the concentration-time series data are used for the analytical inversion so as to determine the concentration distribution in the transverse direction. The concentration-time series data was taken from MT3D simulation outputs at the observation well for the second stress period of three days. The observation well is located at the same position as the pumping well.

3.3.2 Inverted versus "real" concentration distributions at the ICP

The intention here is to evaluate how the inverted concentrations respond to various dispersivities and transport period scenarios and whether the inverted pumped concentrations are consistent with the "real" concentration distribution. One has to bear in mind that the "real" concentration distribution mentioned throughout this paper refers to that of the MT3D simulated concentration distribution observed across the plume width at the ICP for the period before pumping was performed. The inverse code PINwin, developed in the course of this study (Appendix A1), is used for the analytical inversion. Figures 13a-13d show the inverted concentration distribution compared with the "real" concentration distribution observed across the transverse direction at the ICP for various transport periods and dispersivity values. It is noticed that, in all cases of dispersivity

values considered here, the inverted concentration distribution at earlier transport periods overestimates significantly the "real" concentration distribution as in the case of, for instance, the 60 days transport period (Figures 3.11-3.14). In fact, from the numerical simulation, the plume has not well reached the ICP-Pump position and, therefore, the "real" concentration distribution values at the ICP are very small. In this case, the overestimation from the inverted concentration distribution is attributed to the part of the plume captured upstream of the ICP-Pump position. As the transport period increases, as the plume reaches the closer to the ICP-Pump position, the inverted concentration distribution curve tends to converge towards the "real" concentration distribution. Relatively best fit has been observed once the plume reached steady state transport condition, for instance, after 365 days of transport period (Figures 3.11 and 3.12).

However, for larger longitudinal dispersivity values, the inverted concentration distribution curve drops below the "real" concentration distribution curve (Figure 3.14). For instance, the inverted concentration distribution with the longitudinal dispersivity of 30 meters underestimates the "real" concentration distribution at the ICP. This is due to the fact that the pumped concentration itself, which is the main input data for the analytical inversion, is affected by the presence of dispersion. However, in order to meet the assumption of the analytical solution, the value of dispersion in the numerical simulation is artificially modified to zero only during the transient flow period. As it can be seen in Figure 3.15a, the pumped concentration values at zero longitudinal dispersivity are greater than that of the pumped concentration values with a longitudinal dispersivity of 30 meters. The longitudinal dispersivity of 30 meters is used here for both the transient and steady-state periods. The analytical inversion is then employed and the result is compared with the numerically simulated ("real") concentration distribution at zero longitudinal dispersivity. The resulting concentration distribution curves from the analytical inversion and numerical simulation at zero longitudinal dispersivity show similar trend (Figure 3.15b). However, in reality, the aquifer material can be highly dispersive and cannot be neglected during pumping. In that case, the analytical inversion leads to underestimation of the "real" concentration distribution.

Test 1

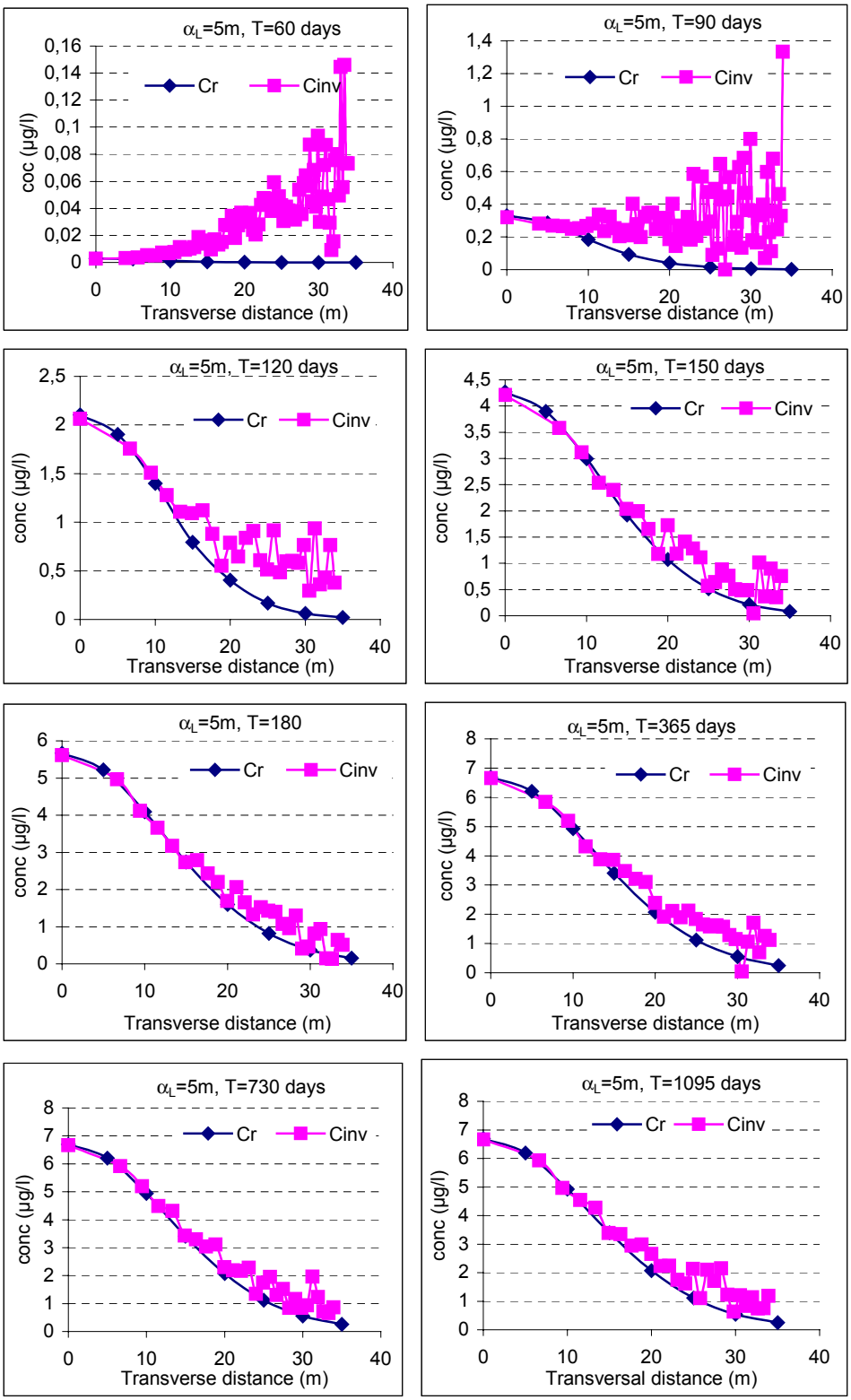

Figure 3.11 Comparison of inverted concentration distribution versus measured concentration distribution (C_{inv} = inverted concentration; C_r= "real" concentration).

Test 2

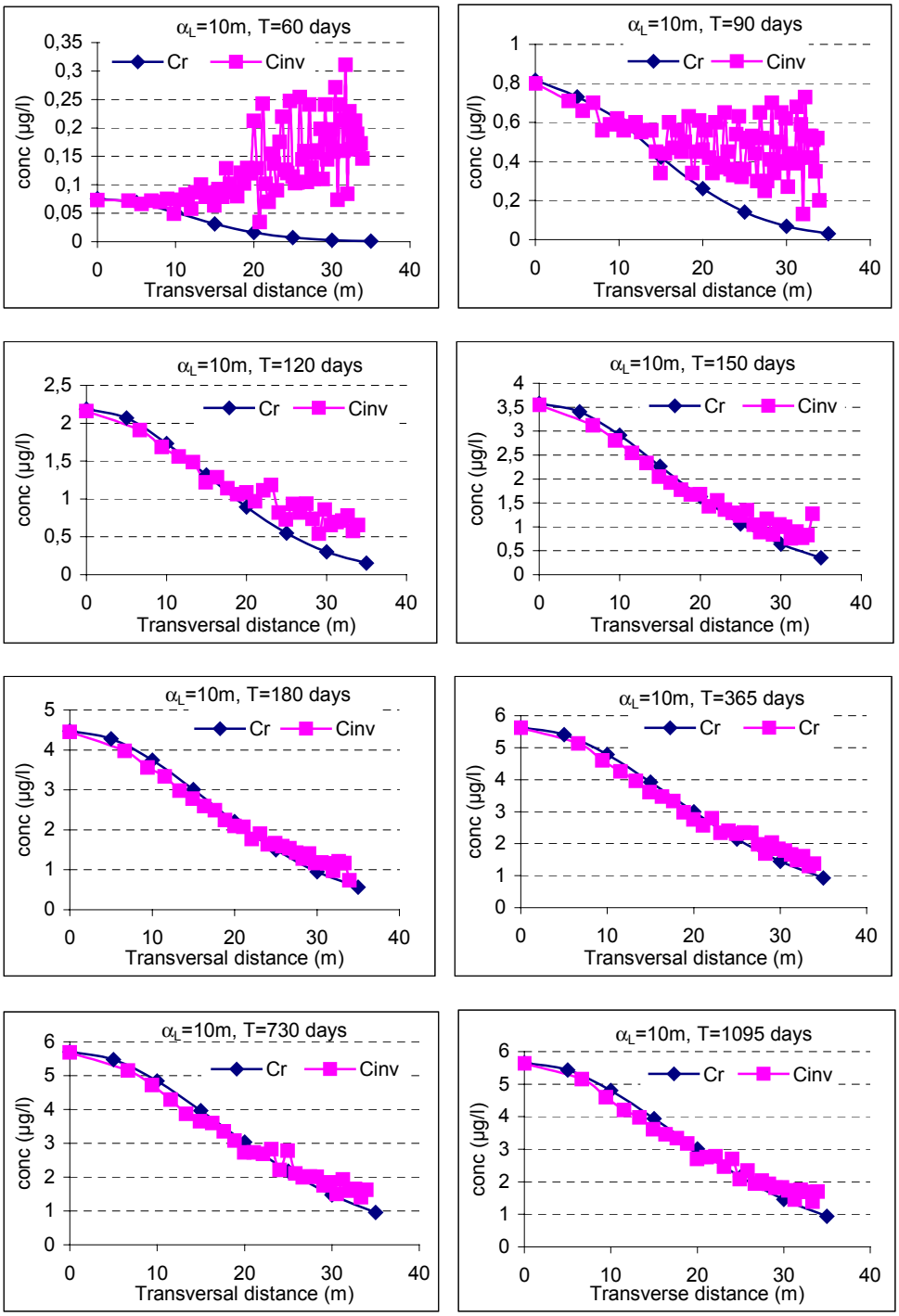

Figure 3.12 Comparison of inverted concentration distribution versus measured concentration distribution (C_{inv} = inverted concentration; C_r= "real" concentration).

Test 3

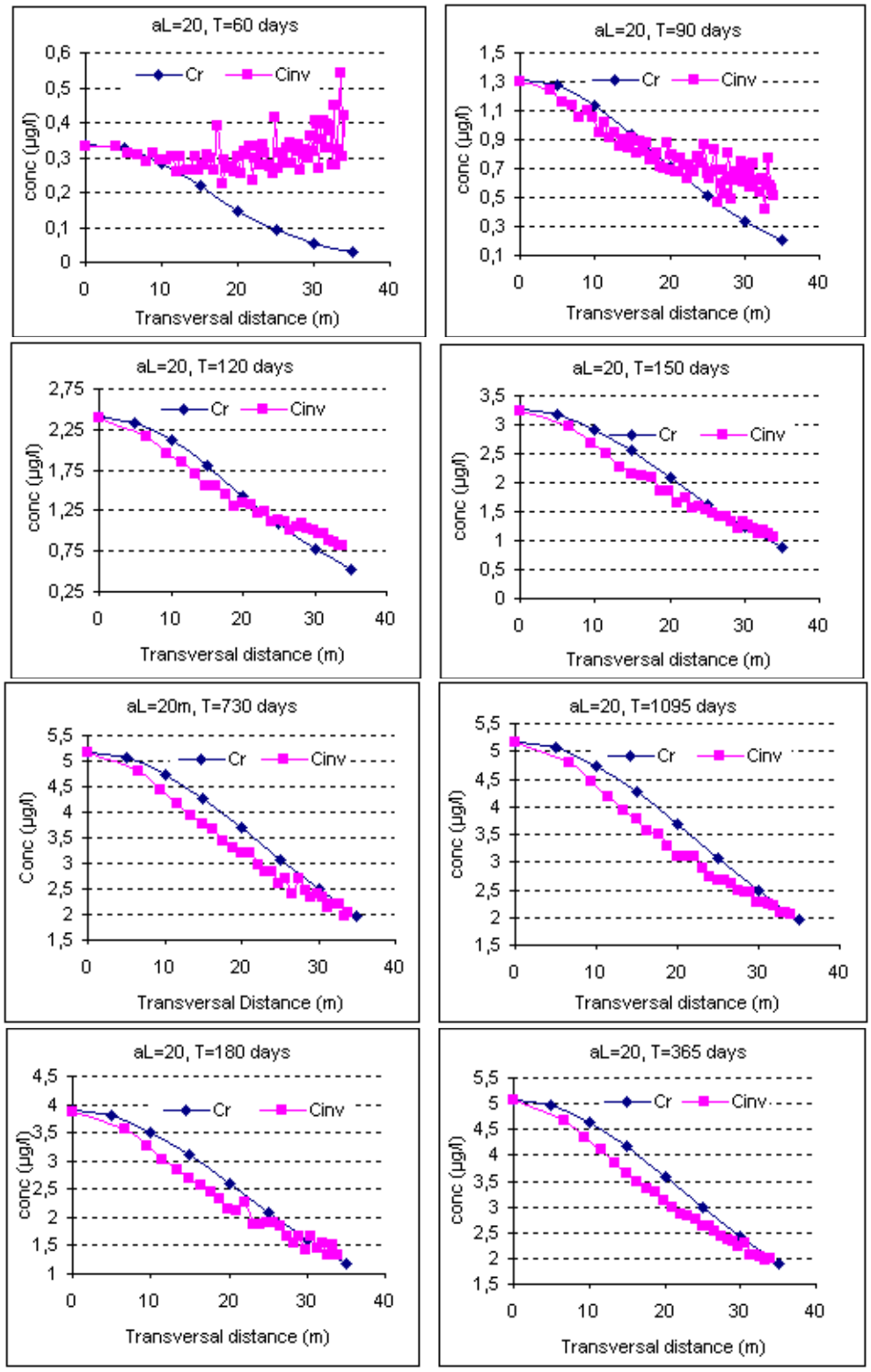

Figure 3.13 Comparison of inverted concentration distribution versus measured concentration distribution (C_{inv} = inverted concentration; C_r= "real" concentration)

Test 4

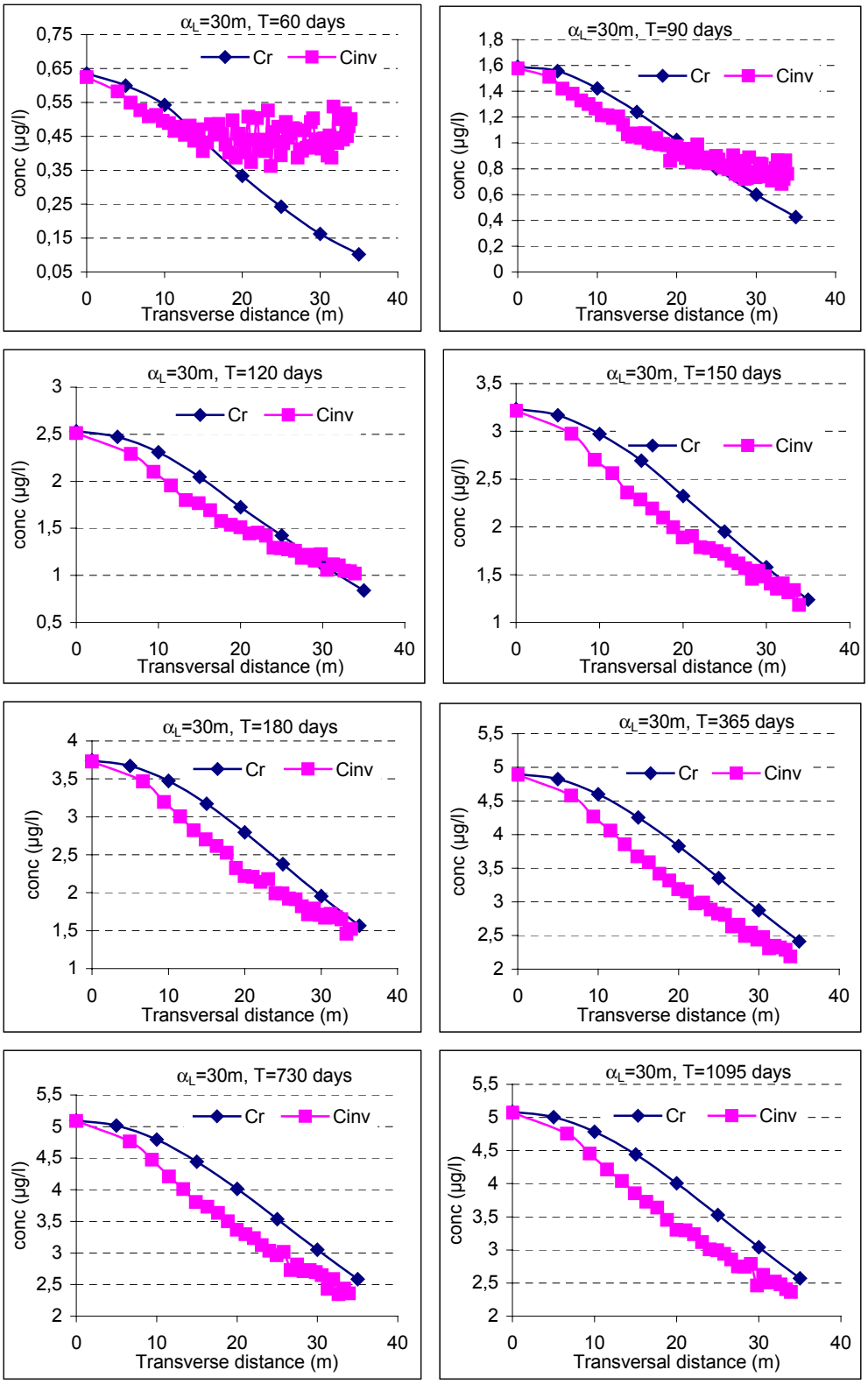

Figure 3.14 Comparison of inverted concentration distribution versus measured concentration distribution (C_{inv} = inverted concentration; C_r= "real" concentration).

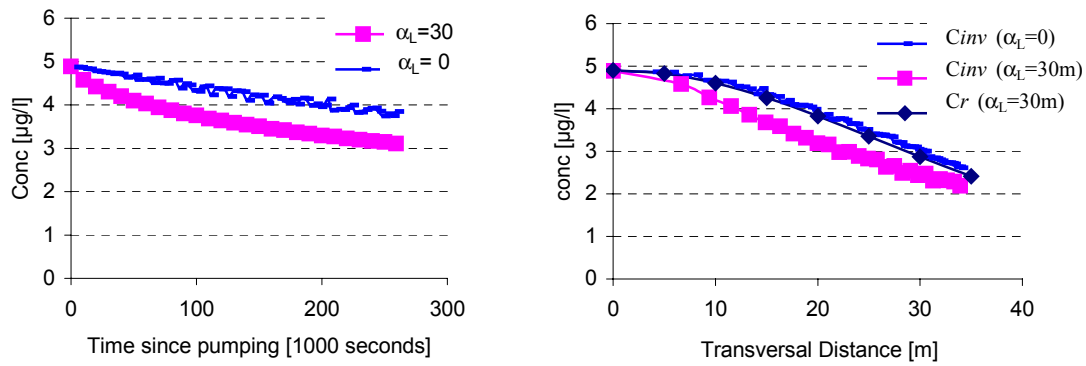

(a) (b)

Figure 3.15 Effect of dispersivity on: a) pumped concentration; b) inverted concentration (C_{inv}= inverted concentration, C_r="real" concentration, transport period, T = 365 days).

It should be noted here that all the α_L values shown are used only in the numerical simulation. The inverted concentration C_{inv} (α_L) is used only to identify the results of the analytical inversion with respect to the magnitude of dispersion used in the numerical simulation. Figure 3.16 shows the effect of dispersion on the "real" concentration distribution at the longitudinal and transversal directions respectively for the four dispersivity values considered for this study. In the longitudinal direction (Figure 3.16a), the higher the dispersivity the lower the concentration distribution values from the source point to the pumping well position.

On the other hand, the concentration distribution in the transverse direction under relatively higher transverse dispersivity (Figure 3.16b), however, shows a mixed trend with a drop in the concentration distribution near the pumping well and then tends to pass over those distribution curves with relatively lower dispersivity values. For instance, with 30 meters longitudinal dispersivity and 3 meters of transversal dispersivity, the transverse concentration distribution drops with in the vicinity of the pumping well but, at farther distance, it turns up to override those with longitudinal dispersivity of less than 30 meters. Because dispersion in radial transport is typically very significant in the vicinity of the well, higher dilution can be involved during early stage of pumping.

Even though the inverted concentration distribution with higher dispersivity may take advantage from elevated distribution values at farther distance, the magnitude of the longitudinal concentration distribution relative to the corresponding transverse concentration distribution remains an important parameter.

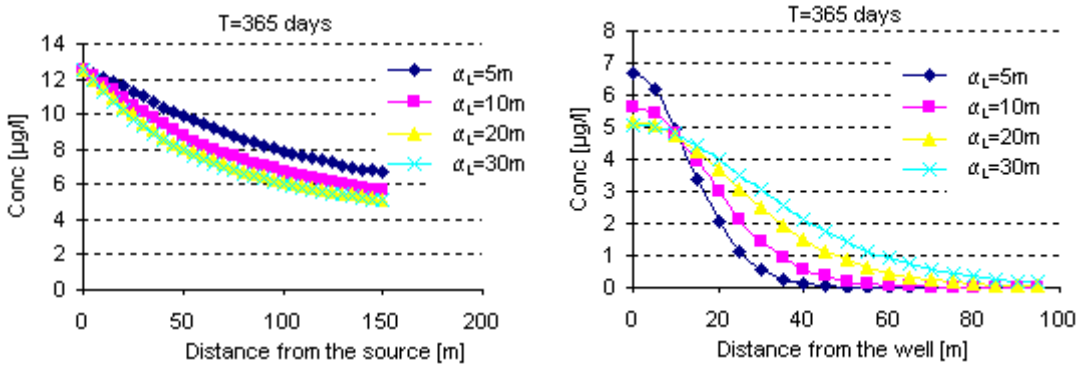

(a) (b)

Figure 3.16 Concentration distribution trend in the longitudinal and transverse direction from a transport period of 365 days: a) concentration distribution in the longitudinal direction; b) concentration distribution in the transversal direction.

3.3.3 Evaluation of concentration gradient

As discussed in the preceding section, the effect of concentration gradient on the inverted concentration distribution can be analyzed by evaluating in detail the relationships between the concentration gradients in the longitudinal and transversal directions for various transport periods. The concentration gradients in the transverse and longitudinal direction can be evaluated from the corresponding concentration distributions that are obtained from the result of the numerical simulation (see Figure 3.16).

As can be noticed visually in Figure 3.17a, the slope of the longitudinal concentration is steeper for shorter transport period. For instance, the plume with the transport period of 60 days shows a concentration distribution with a steeper gradient than the plume with the transport period of 365 or more days. In the longitudinal direction, the slope of the transverse concentration distribution is steeper for the plume with longer transport

periods (Figure 3.17b). In other words, the slope of the concentration distribution in the longitudinal direction relative to the corresponding slope in the transversal direction, expressed in terms of gradient ratio GR, is greater for shorter transport periods than the gradient ratio for longer transport periods.

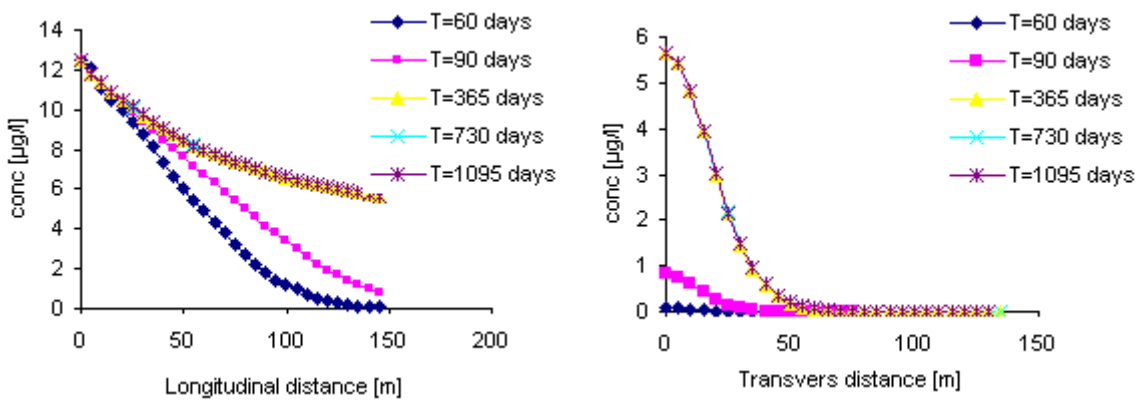

(a) (b)

Figure 3.17 Evaluation of the concentration distribution trend from Test 2 : a) in the longitudinal direction, along the source-pump axis; b) in the transverse direction, along the fixed ICP located 150 meters from the source.

Having noticed the slope of the concentration distribution both in the longitudinal and transversal directions, it is essential to quantify the mean concentration gradient ratio from the mean of the concentration gradient in the respective directions. Thus, the directional averaged (DA) estimate of the gradient ratio GR (see Equation 3.9) is used for the determination of the mean gradient ratio (MGR). For a power p =1, the distance ratio weighted mean (DRW) of Equation 3.10 is then expressed as:

$$MG_x = \frac{\sum_{i=1}^{n} \left| G_{x_i} \frac{1}{X_i} \right|}{\sum_{i=1}^{n} \left| \frac{1}{X_i} \right|} \quad \text{; and} \quad MG_y = \frac{\sum_{j=1}^{m} \left| G_{y_j} \frac{1}{Y_j} \right|}{\sum_{j=1}^{m} \left| \frac{1}{Y_j} \right|} \tag{3.11}$$

where *MG* [-] is the mean concentration gradient, *X* [L] is the distance in the longitudinal direction with the reference point at the pumping well, *G* [-] is the concentration gradient at a given point with the indices x and y indicating the respective direction, *Y* [L] is the transversal direction at the ICP with the reference point at the pumping well, *i* and *j* are the indices for the data points in the longitudinal and transversal directions respectively.

The calculated mean gradient ratio for various transport periods as a function of the dispersivity values is shown in Figure 3.18. It is noticed that, given a fixed ICP-pump position relative to the source, contaminant plumes with shorter transport period result very high mean gradient ratio (MGR). The plumes at shorter transport periods such as 60 days or 90 days do not reach or traverse the ICP and, therefore, the well pumps only the very tail of the plums. Thus, the concentration-time series data obtained under this situation do not provide representative concentrations for determining total mass flow rate. This indicates that the effect of the longitudinal concentration gradient for non stationary plume is very significant.

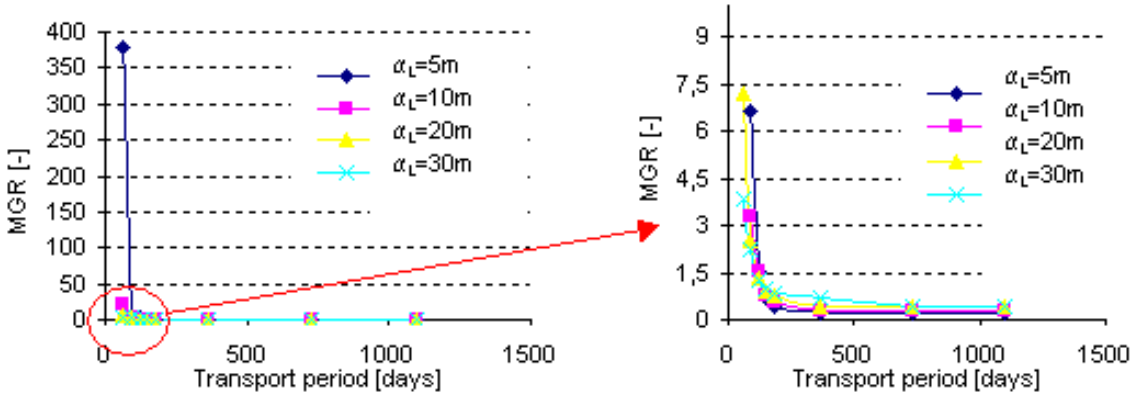

Figure 3.18 Mean gradient ratio (MGR) calculated from the mean of the "real" concentration distribution at the fixed ICP

The mean gradient ratio, in general, decreases with increasing transport period for all the dispersivity values. Though significantly weaker, the relatively higher mean gradient ratio values observed for the plume with larger dispersivity can be influenced by the relatively elevated values of the transversal concentration distribution (see Figure 3.16b).

3.3.4 Gradient adjusted determination of mass flow rate

As was noticed previously from the comparison of the inverted concentration distribution with the "real" concentration distribution, the method of the inversion provides overestimated values for the plume with shorter transport period. In the case of longer transport period, particularly with higher dispersivity values, the method of inversion rather underestimates the "real" concentration distribution. The deviations, overestimation or underestimation, can be expressed in terms of error ε as shown in Equation 16. The magnitude of the error can be determined from the relative difference of the inverted concentration distribution with respect to the "real" concentration distribution.

$$\varepsilon = \frac{\int_{j=1}^{m_1} \left(C_{inv}\Delta y\right)_j - \int_{j=1}^{m_2} \left(C_r\Delta y\right)_j}{\int_{j=1}^{m_2} \left(C_r\Delta y\right)_j} \tag{3.12}$$

where C_{inv} [ML^{-3}] the inverted concentration, C_r [ML^{-3}] is the "real" concentration, Δy [L] is the width of the stream tube j, and m_1 and m_2 are the number of data points for the inverted and "real" concentration distributions the respectively in the transverse direction at the ICP.

The calculated errors for the transport periods and dispersivity values are shown in Figure 3.19. Similar to the calculated mean gradient ratio (MGR) in the previous section, higher error values correspond to the plume with shorter transport period. As the transport period increases, the magnitude of the error correspondingly decreases. However, in the case of higher dispersivity values, the error values are rather negative. For instance, the calculated error for higher longitudinal dispersivity values such as for 20 and 30 meters are related to the drop in the concentration distribution values. As discussed earlier, this

is due to the underestimation caused by the dilution of pumped concentration as a result of higher dispersivity values.

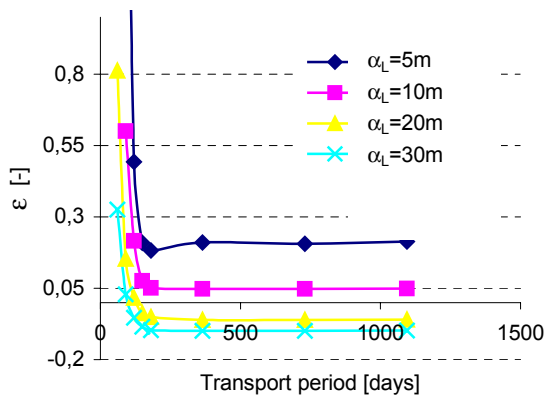

Figure 3.19 Calculated error ε or deviation of the inverted concentration distribution from the "real" concentration distribution.

As can be noticed from the trend of the mean gradient ratio (Figure 3.18) and the calculated error $\boldsymbol{\varepsilon}$ graphs (Figure 3.19), the higher the gradient ratio the more the deviations or errors that can be expected from the inversion of pumped concentration.

However, for a given mean gradient ratio, the magnitude of the calculated error depends on the dispersivity values as it can be seen in Figure 3.20a. Higher errors can be expected for the plume with lower dispersivity values. The negative error values, as in the case of the plume with larger dispersivity values, indicate that the inverted concentration distribution values are smaller than the "real" concentration distribution values due to the dilution of the pumped concentration. The disparities of the calculated error versus the mean gradient ratio curves can be brought together by lumping the mean gradient ratios with the corresponding dispersivity values (Figure 3.20b). The lumped gradient ratio (LGR) can be defined as in Equation 3.13.

$$LGR = MGR\left(\frac{R}{\alpha_L}\right) \tag{3.13}$$

where LGR [-] is the lumped gradient ratio, MGR [-] is the mean gradient ratio, R [L] is the maximum well capture radius, and α_L [L] is the longitudinal dispersivity.

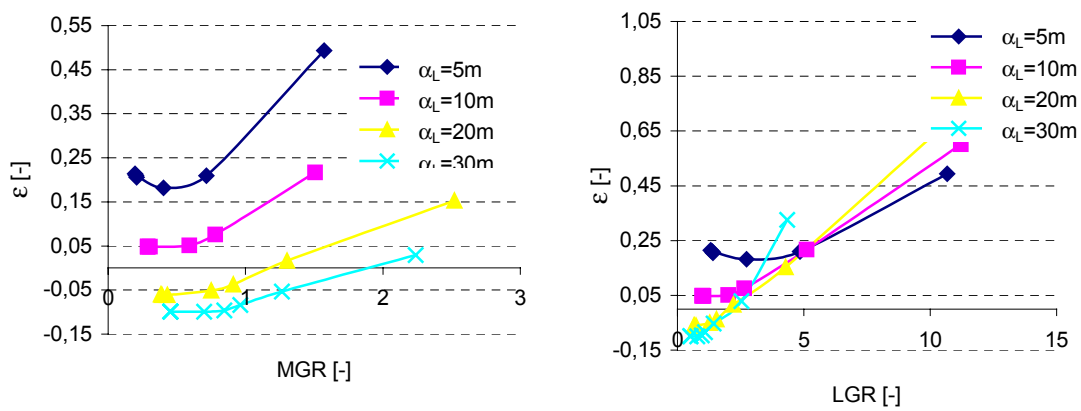

Figure 3.20 a) Calculated error ε versus mean gradient ratio (MGR); b) calculated error ε versus lumped gradient ratio (LGR).

Since the graphical relationship of the calculated error versus the lumped gradient ratio (LGR) does not provide a continuous function, some functional relationships of the calculated error and the mean gradient ratio (MGR) can be estimated from individual functions for each dispersivity values. For instance, in the case of this study, the error versus gradient ratio curve for a dispersivity value of 10 meters can be empirically expressed as:

$$\varepsilon = 2.49e^{0.96(MGR)} \tag{3.14}$$

where *MGR* [-] is the site specific mean gradient ratio which can be calculated from the ratio of the mean longitudinal concentration gradient to the mean transverse concentration gradient. However, as it can be noticed from Figure 20, the calculated error versus the mean gradient ratio curves for each dispersivity value show almost similar functional trend. Thus, from Equation 3.14, dispersivity proportionate error function can be approximated as:

$$\varepsilon = \left(\frac{\alpha_L^*}{\alpha_L} \right) 2.49 e^{0.96(MGR)} \text{; with } 0 < \alpha_L < 15 \tag{3.15}$$

where α_L^* [L] is the reference longitudinal dispersivity of 10 meters, α_L [L] is the longitudinal dispersivity in meters, and *MGR* [-] is the mean gradient ratio estimated from the "real" concentration distribution. Therefore, taking into account the error function of Equation 3.15, for non-negative error values, the total mass flow rate of Equation 2.8 (see section 2.2.4) can be adjusted as:

$$M_e = M(1 - \varepsilon) \tag{3.16}$$

Substituting Equation 3.15 into Equation 3.16, the total mass flow rate for gradient imposed concentration in the plume can be expressed as:

$$M_e = 2 \left[\frac{\alpha_L - \alpha_L^* (2.49 e^{0.96(MGR)})}{\alpha_L} \right] \sum_{j=1}^{n} (C_{inv} q)_j \tag{3.17}$$

where M_e [MT^{-1}] is the total mass flow rate adjusted for gradient imposed concentration in the plume, C_{inv} [ML^{-3}] is the inverted concentration, and q [L^3T^{-1}] is the flow rate for a stream tube corresponding to the data point j, and n is the total number of data points in the concentration-time series.

Though the adjusted mass flow rate, M_e, indicates the extent and level of groundwater pollution during each transport period, the maximum mass flow rate can only be determined at the maximum width of the plume. For instance, taking the plume with the longitudinal dispersivity of 10 meters, the total mass flow rate for the transport period of 365 days, i.e. in stationary plume case, is about six times greater than of the non-stationary plume with transport period of 60 days. In general, a representative of the total mass flow rate can be can be obtained from the plume that has reached or traversed the ICP. In this case, the mean gradient ratio is weaker and therefore the associated error is smaller. For the plume which is still located upstream of the ICP, the mean gradient ratio is larger and, therefore, one has to find a closer ICP-Pump position for better determination of the total mass flow rate.

3.4 Summary

The method involving the inversion of the pumped groundwater quality data, in this case the concentration-time series data, can be used as an alternative and/or complementary method for groundwater pollution evaluation. This approach is particularly important when there are not enough point measurements and source of contamination is unknown.

The result of this study show that if concentration-time series measurements are taken around the very tail of the plume, the effect of the longitudinal concentration gradient relative to the transverse gradient, expressed in terms of the gradient ratio GR, is significant and the associated error is proportionally high. On the other hand, for an ICP positioned relatively closer to the suspected source, the method of inversion can provide reasonable estimate of the concentration distribution and the corresponding mass flow

rate at the ICP with a minimum error. It is assumed that the reach of the capture zone is smaller than the distance to the source.

Determination of the extent and level of groundwater contamination by taking into account the concentration gradient in the plume can improve results and minimize errors. In this case, a rough estimate of a site specific mean gradient ratio (MGR) should be determined so that adjusted mass flow rate can be estimated at the ICP position. It should be noted, however, that the adjusted mass flow rate does not necessarily represent the "actual" mass flow from the detected plume. The relatively maximum value for the total mass flow rate depends on the ICP-Pump position which in turn determines the magnitude of the mean gradient ratio as well as the dispersivity values. The results of study show that the method of inversion of pumped concentration for groundwater pollution analysis can provide reasonable estimates, i.e. with relatively lower errors, in the case when the mean gradient ratio is correspondingly minimum and the dispersivity values are relatively low.

For a contaminant plume with unknown source and without additional point measurements in the longitudinal and transverse direction, positioning the ICP-Pump by trial and error where a gradient ratio is close to zero may be practically difficult. Nevertheless, results can be improved or errors can be minimized by considering the relatively closest ICP-Pump position from the suspected source.

In the case of a contaminant plume under higher dispersivity condition, the method of the inversion of pumped concentration can result in an underestimation of the actual concentration distribution. Underestimating the actual concentration implies higher risk from the environmental and health issues stand point. Thus, for highly dispersive aquifers materials with dispersivity values greater than 15 meters and assuming a dispersivity ratio of 10 per cent, special care should be taken while making a decision from using the method of the inversion of pumped concentration.

The application of the method for inversion of pumped concentration is limited to ideal aquifers, i.e. homogenous-isotropic with uniform layer thickness. The method can in general be applied in field conditions if the aquifer is assumed to have uniform permeability and the layer containing the major part of the contamination is identified. Future work will look into the effect of local aquifer heterogeneity for the evaluation of groundwater pollution with the method of the inversion of pumped concentration.

Chapter 4

Inversion of pumped concentration taking into account local heterogeneities

4. Inversion of pumped concentration taking into account local heterogeneities

In the case of homogeneous-isotropic media with radially dominated flow field, the method of inversion of pumped concentration can be performed analytically. However, in many cases, the real geo-hydrological systems are complex and, therefore, the aquifer media must be characterized by heterogeneous media. In this case, the method of inversion of pumped concentration must be approached numerically. Thus, this chapter addresses the development and implementation of a ***v****olume based* ***in****verse* ***mod****el (VINMOD) for the numerical inversion of pumped concentration by taking into account heterogeneity within the entire well capture zone. VINMOD calculates the mean concentration and the corresponding mass flow rate of the "undisturbed" plume for groundwater pollution quantification taking the imaginary control plane (ICP) as a reference.*

4.1 Introduction

For a homogeneous-isotropic aquifer configuration, Schwarz et al. (1998) presented an analytical solution for the inversion of pumped concentration, with the assumption of a zero concentration gradient in the longitudinal axis of the plume. Field applications and related studies on the method were reported (Holder et al., 1998; Bockelmann and Teusch, 2001; Schäfer et al., 2001; Bockelmann et al., 2003). The inversion of pumped concentration in the case of non-zero concentration gradient in the longitudinal axis of the plume was later presented by Zeru and Schäfer (2003a, 2004) (see also Chapter 3).

However, in many cases, the real geo-hydrological systems are complex and, therefore, the aquifer media must be characterized by heterogeneous media. In this case, depending on the local permeability values, the well capture zone geometry may vary and differ from that of a circular capture zone as presented by some authors (Franzetti and Guadagnini, 1996; Riva et al., 1999). Thus, the total mass flow to be calculated from the

inversion of pumped concentration in homogeneous and isotropic conditions can correspondingly differ from that of the heterogeneous formation (Elder, 2002). Moreover, the contaminants may not be evenly distributed in the aquifer and, therefore, contaminant lenses can be present, as a result of the heterogeneous nature of the aquifer. In this case, the method of inversion of pumped concentration must be approached numerically.

This study addresses the analysis of groundwater pollution with the method of inversion of pumped concentration by taking into account the effect of local heterogeneity in the well capture zone. In this case, the volume of the stream tubes is used to determine the contaminant mass.

4.2 Effect of heterogeneity on capture zone geometry

Under homogeneous-isotropic aquifer condition, the geometry of the well capture zone can be simplified and represented by a circular surface (Bennett et al., 1990). For instance, Figure 4.1a shows a schematic representation of a circular well capture zone for transient flow fields where the influence of the natural groundwater flow is neglected. However, in the case of heterogeneous aquifer formations, depending on the local permeability values, the well capture zone geometry varies and differs from that of a circular capture zone (Figure 4.1b).

During pumping, the water particles flowing towards the pumping well can travel different distances in a given time interval. Therefore, delineating the points of the origin of these particles reaching the pumping well at the same time forms an irregular capture zone. Detailed and comprehensive studies on traveltime related capture zones are presented, for instance, in Bair et al. (1990) and Bair et al. (1991).

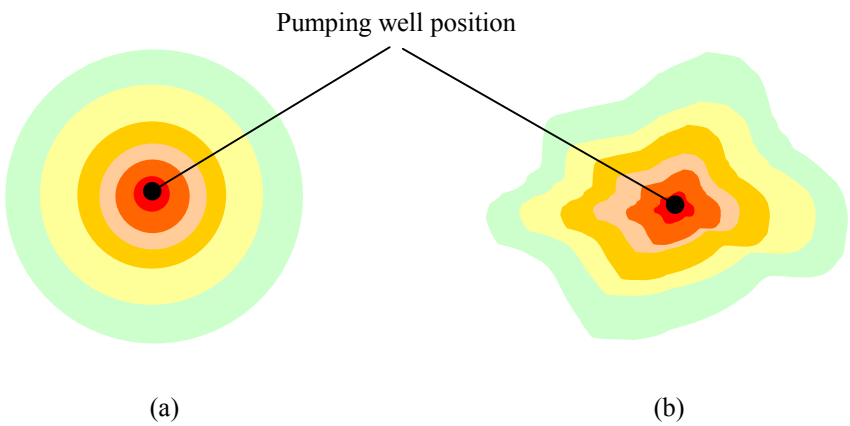

Figure 4.1 Schematic 2D representations of hypothetical capture zones for a radial flow to the pumping well, given the same travel-time: a) homogeneous aquifer, b) heterogeneous aquifer.

Similarly, in steady-state flow condition, the streamlines representing the natural groundwater flow in a homogenous aquifer are generally represented by straight lines. Whereas, in the presence of heterogeneity, water particles follow preferential paths having relatively higher permeability. As a result, the streamlines of groundwater flow in a heterogeneous aquifer can diverge or converge. Figure 4.2 shows a superimposition of the streamlines of the steady-state flows in the aquifer and the isochrones plotted using the transient flow field.

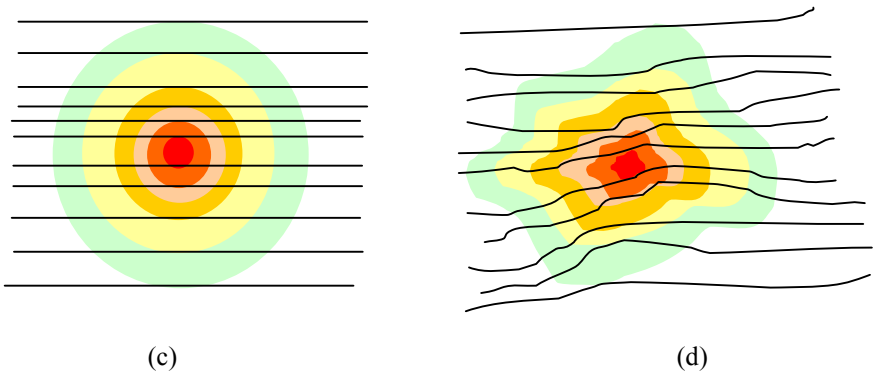

Figure 4.2 Schematic 2D representations of capture zones for a radial flow from similar pumping time series: a) for homogeneous aquifer, b) for heterogeneous aquifer.

As noted in the preceding chapters (see chapter 2 and chapter 3), the quantification of groundwater pollution with the inversion of pumped concentration depends mainly on the zonal concentration data, i.e. the concentration-time series data from a given constant well discharge, the groundwater flow velocity, and the aquifer geometry. Therefore, the change in the well capture zone geometry as well as that of the flow velocity field as a result of the presence of local heterogeneity can affect the result of the inversion of pumped concentration.

4.3 Development of inversion model for heterogeneous media

4.3.1 Conceptual model

In order to implement the concept of the inversion of pumped concentration from a heterogeneous media, a fully penetrating pumping well with a constant discharge of Q_p is assumed to withdraw contaminated groundwater from a hypothetical heterogeneous aquifer with natural groundwater flow (Figure 4.3). With the presence of heterogeneous aquifer material in the vicinity of the pumping well, the corresponding well capture zone is irregular in shape. In this case, the contaminant mass M_p that can be calculated from the pumped water depends on the contaminant concentration C_p in the pumped water, the well discharge Q_p, and the duration of the pumping period t. For a given pumping time or pumping time interval, the contaminant mass M_p in the pumped water corresponds to the contaminant mass in the capture zone that can be attained in the same time interval.

For a dissolved contaminant concentration present in the saturated aquifer zone, the contaminant mass that could reside in the groundwater just before pumping M_g is assumed to be equal to the sum of the aqueous phase contaminant mass M_a and the sorbed concentration mass M_s for the corresponding capture zone. However, neglecting sorption, the pumped concentration mass M_p is assumed to be equal to the mass of the aqueous phase concentration M_a.

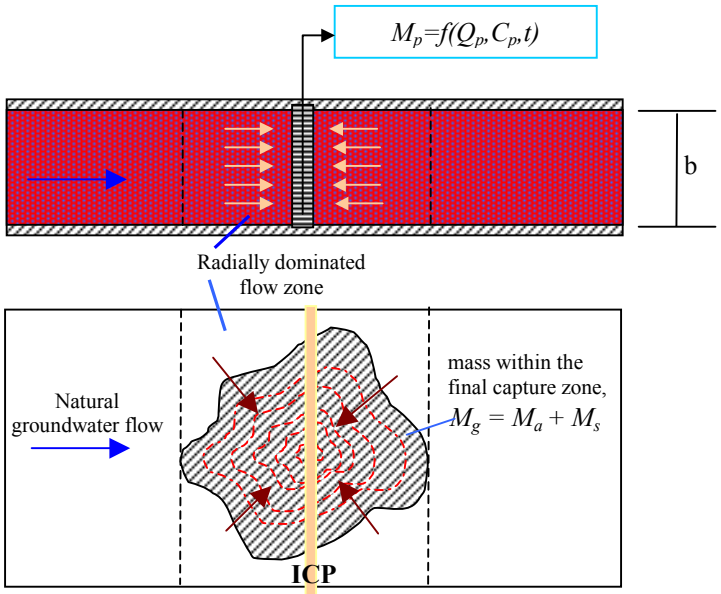

Figure 4.3 Schematic representation of a well capture zone from a hypothetical single layered confined heterogeneous aquifer with a fully penetrating pumping well having a constant discharge of Q_p.

The pumped concentration however is attributed to the undisturbed contaminant plume partitioned with streamlines of the natural groundwater flow that form streamtubes. Thus, the intention here is to estimate the natural concentration distribution that would have been present at the ICP if pumping were not performed. In order to determine the total contaminant mass flow rate at the ICP, the concentration distribution at the transversal axis of the undisturbed plume along the ICP has to be determined. In this case, the total mass flow rate M that can pass through a predefined ICP depends on the concentration C, the groundwater flow velocity q, the width of the plume W at the ICP, the porosity of the subsurface material ϕ, and the layer thickness of the aquifer b.

Figure 4.4 shows a schematic representation for the contaminant mass flow rate that can be determined at the ICP. Since the concentration distribution at the ICP is initially unknown, the average zonal concentration between two isochrones, which is the pumped concentration as a function of time, is used for the inversion.

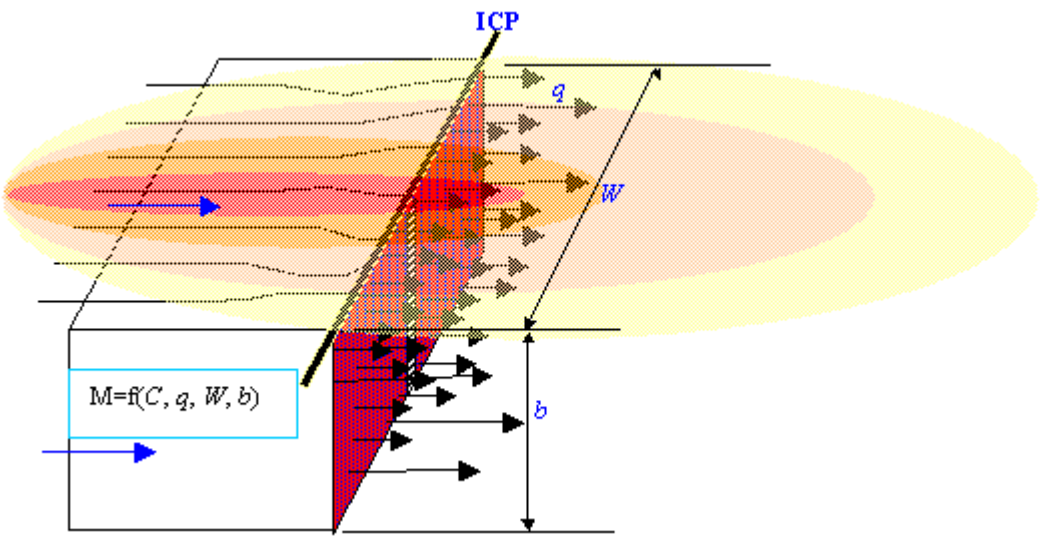

Figure 4.4 Schematic representation for the contaminant mass flow rate at the ICP from undisturbed contaminant plume.

4.3.2 Mathematical model

In order to obtain the concentration distribution of the undisturbed plume, the following assumptions are made: (1) the part of the plume with the highest concentration is assumed to reach the capture zone at the ICP and, therefore, a symmetrical plume relative to the pumping well position can be considered, as represented schematically in Figure 4.5, (2) since the well capture zone from a few days of pumping could be small enough compared to the aquifer domain, the variation of layer thickness around the pumping well is assumed to be negligible and, therefore, a constant layer thickness can be considered, (3) neglecting sorbed mass, the well pumps the total dissolved contaminant mass residing within a given capture zone corresponding to a given pumping time interval t, (4) the pumping well is screened throughout the layer thickness and the contaminant concentrations are assumed to be mixed uniformly. In this case, the pumped concentration is assumed to represent the depth averaged concentrations, (5) the pumped concentration from the corresponding capture zone for a given time interval in the concentration-time series data represents the mean concentration of the change of the capture zone for that time interval, (6) for a section of a contaminant plume as shown in

Figure 4.5, i.e. for a relatively short distance from the pumping well, the concentration within a given stream-tube of a contaminant plume is assumed to be constant.

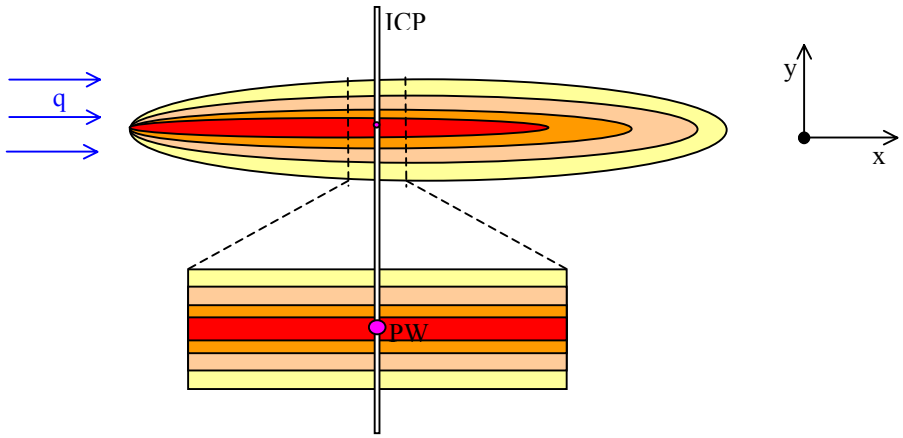

Figure 4.5 Schematic representation of symmetrical plume relative to the pumping well (PW) position.

As mentioned earlier, for a dissolved contaminant present in the saturated zone, the total contaminant mass in a given capture zone can be expressed as:

$$M_g = M_a + M_s \tag{4.1}$$

Where M_g [M] is the total mass of dissolved contaminant in a defined capture zone, M_a [M] is the aqueous phase contaminant mass, and M_s [M] is the sorbed contaminant mass. Neglecting the sorbed mass, the total contaminant mass in the saturated subsurface is equal to the aqueous phase contaminant mass. From the third assumption, the contaminant mass in the subsurface is, therefore, equal to the pumped contaminant mass as:

$$M_g = M_p \tag{4.2}$$

Where M_p [M] is the pumped contaminant mass. The total contaminant mass in the ground in a given volume of the capture zone at the end of the pumping period can be expressed as:

$$M_g = \phi \int_{v(T)} c(t) dv \tag{4.3}$$

where $v(T_p)$ [L^3] is the total volume of the soil within a capture zone at the end of the pumping time T [T], $c(t)$ is the mean concentration for the isochrone corresponding to time t, and ϕ [-] is the porosity. For the total pumping period, with a constant layer thickness and a capture zone as shown in Figure 4.6, Equation 4.3 can be rewritten as:

$$M_g(T) = \phi b \int_{A_c(T)} c(t) dA_c \tag{4.4}$$

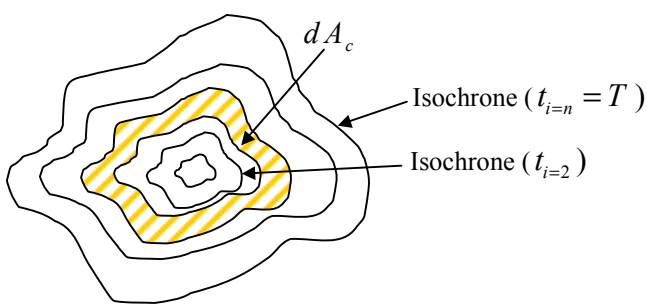

Figure 4.6 Schematic representation of consecutive capture zones (dA_c = the surface area of the capture zone increased for the time interval dt).

Where dA_c [L^2] is the area of the capture zone for the time interval dt as shown in Figure 4.7, b [L] is the constant aquifer thickness. By superimposing the streamlines that bound each streamtube of the natural groundwater flow (Figure 4.7a) and the well capture zones that are plotted from the transient flow field (Figure 4.7c-4.7d), the areas of the stream

that are common to both the capture zones and the corresponding streamtubes can be obtained. Thus, the value of the concentration in a given streamtube, after superimposition, is in fact attributed to the concentration of the undisturbed plume (Figure 4.7a). That is, as the pumping period increases, the outer capture zone intercepts the concentration of the undisturbed plume. As noted from the sixth assumption that the concentration within a given streamtube of the plume is constant.

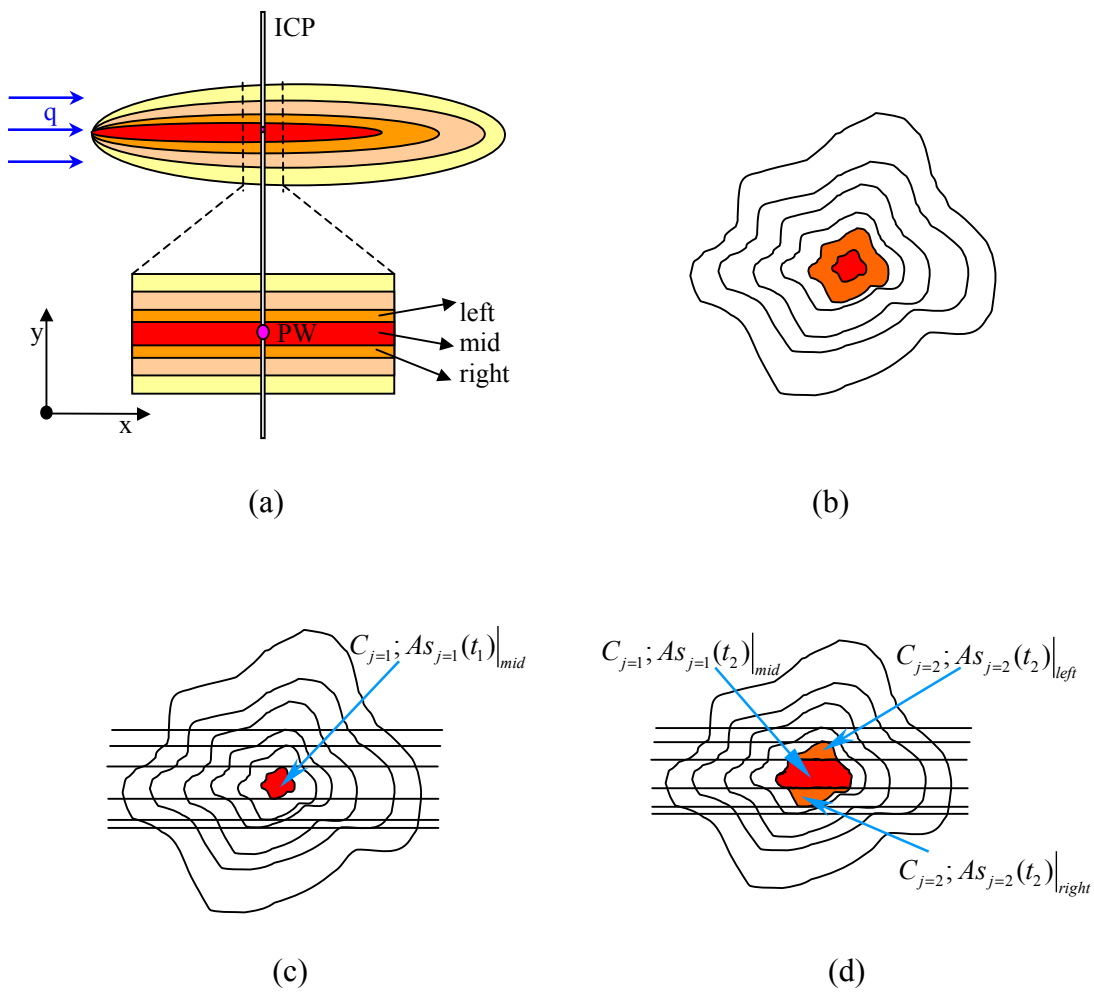

Figure 4.7 Example of superimposition of the streamlines in a contaminant plume and the well capture zones: a) Contaminant plume representation with streamlines that form streamtubes, b) zonal concentration that can be obtained from pumping on a contaminant plume, c) superimposed stream area that is common to the first capture zone and the middle streamtube, and the corresponding concentration, d) superimposed stream areas that are common to the second capture zone and the corresponding streamtubes, and the corresponding concentration distribution.

Thus, the concentration from the middle stream area corresponds to the concentration of the first capture zone and the concentration from the immediate neighboring stream areas, on the left and right side of the middle stream area, corresponds to the concentration of the concentration of the left and the right streamtubes respectively. Similarly, the concentration of any of the outer stream areas on the respective sides corresponds to the concentration of the respective streamtubes until the end of the concentration-time series data.

As an example, taking the first two isochrones for the superimposed capture zones and streamtubes (Figure 4.6d), the sum of the contaminant mass (see Equation 4.4) at time t_2 can be expressed as:

$$M_g(t_2) = \phi b \left[\int_{As(t)} c_s(t) dA \Big|_{left} + \int_{As(t)} c_s(t) dA \Big|_{mid} + \int_{As(t)} c_s(t) dA \Big|_{right} \right] \tag{4.5}$$

where c_s [ML^{-3}] is the concentration in a given streamtube that is considered as constant throughout the streamtube length as noted in the assumption six of the previous section, As [L^2] is the superimposed stream area within the capture zone under consideration, the indices *left, mid* and *right* indicate the position of the streamtubes in the plume relative to the pumping well location, assuming the groundwater flow direction is in the x-direction. Taking the volume of the pumped water for the defined pumping period with two isochrones (see Figure 4.7b), the pumped contaminant mass M_p can be expressed as:

$$M_p = Q_p \int_t c_p(t) dt \tag{4.6}$$

where Q_p [L^{3}T^{-1}] is the pumping rate which is assumed to be constant throughout the entire length of the pumping period, c_p [ML^{-3}] is the concentration in the pumped water at

the elapsed time t. Figure 4.8 shows an example for the pumped concentration as a function of time. It should be noted here that a pumped concentration at a given time in the concentration time series with n data points represents the average zonal concentration between two isochrones. Thus, for instance, $c_p(t_1)$ corresponds to the first capture zone associated to the first time interval and $c_p(t_2)$ corresponds to the zone between the first and the second capture zones, associated to the second time interval.

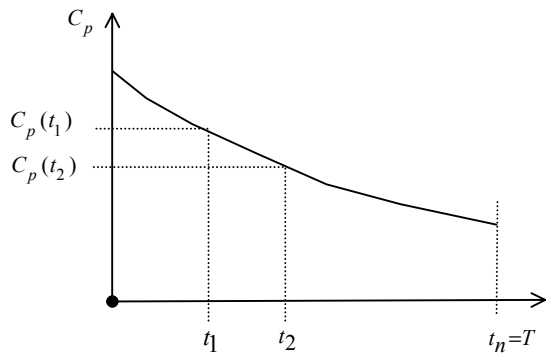

Figure 4.8 Example of pumped concentration as a function of the elapsed time.

Therefore, from Equation 4.5 and Equation 4.6, Equation 4.2 can then be rewritten as:

$$\int_{As(t)} c_s(t)dA\Big|_{left} + \int_{As(t)} c_s(t)dA\Big|_{mid} + \int_{As(t)} c_s(t)dA\Big|_{right} = \frac{Q_p}{\phi b}\int_t c_p(t)dt \tag{4.7}$$

For a symmetrical plume, the concentrations for mirror image streamtubes relative to the pumping well position are equal. In this case, the concentrations in the left and right streamtubes are equal but are also unknown. However, the value of the concentration in the middle streamtube is assumed to be equal to the pumped concentration recorded during the first time interval, i.e., corresponding to the first well capture zone. Since the pumped concentration is known, the concentration in the middle streamtube is thus

known. Rearranging the known and unknown terms of Equation 4.7, the inverted concentration at the ICP for the given example with two isochrones and three streamtubes can be expressed as:

$$C_s(t)_{inv} = \frac{1}{As(t)\big|_{left} + As(t)\big|_{right}} \left[\frac{Q_p}{\phi b} \int_t c_p(t)dt - \int_{As(t)} c_s(t)dAs \Bigg|_{mid} \right] \tag{4.8}$$

Where the index *inv* represents the inverted flux concentration for the time interval under consideration in the concentration-time series data. For the case with more than three streamtubes, Equation 4.8 can simply be recursively extended. Thus, the generalized formulation for the volume based inversion of pumped concentration for a symmetrical plume can be given as:

$$C_{inv_j} = \frac{Q_p \sum_{k=1}^{j} C_{p_k} \Delta t_k - b\phi \sum_{k=1}^{j-1} C_{inv_k} (As_k\big|_{left} + As_k\big|_{right})}{(As_j\big|_{left} + As_j\big|_{right}) b\phi} \tag{4.9}$$

where C_{inv_j} [ML^{-3}] is the inverted concentration for the streamtube j, j is the streamtube index (j=1,2,..,n), and the indices *left* and *right* represent the mirror image streamtubes. However, for a symmetrical plume with respect to the pumping well position, the mirror image streamtubes are assumed to have the same concentration. Hence, the total mass flow rate passing through the ICP, for a plume with constant concentration streamtube, can be calculated from the sum of individual mass flow rate of each streamtube as:

$$m_j = \left(C_{inv} q\right)_j \tag{4.10}$$

where m [MT^{-1}] is the mass flow rate, C_{inv} [ML^{-3}] is the inverted flux concentration, and q [L^3T^{-1}] is the flow rate for a streamtube corresponding with the index j. However, unlike the homogeneous aquifer configuration, the groundwater flow velocity profile at the ICP in a heterogeneous aquifer can vary from one streamtube to the other. Thus, the total mass flow rate M [MT^{-1}] at the ICP given in the previous chapter (Chapter 2, Section 2.3.2) can be adapted to heterogeneous velocity profile as:

$$M = \sum_{j=1}^{n} \left(C_{inv} q \right)_j \Bigg|_{left} + \sum_{j=1}^{n} \left(C_{inv} q \right)_j \Bigg|_{right} \tag{4.11}$$

4.3.3 Numerical implementation

A computer code, hereafter called "**v**olume based **in**verse **mod**el" (VINMOD), is developed based on the solutions provided in the previous section (see Equation 4.9 and Equation 4.11) for the numerical inversion of pumped concentration and quantification of the total mass flow rate at a predefined ICP. The total mass flow rate and the inverted concentration distribution that can be calculated with VINMOD, represent the mass flow rate and the natural concentration distribution of the undisturbed contaminant plume.

VINMOD requires principal input parameters such as the concentration-time series data, groundwater flow velocity field, aquifer thickness, porosity of the aquifer material, and areas of streamtubes. Figure 4.9 shows the flowchart for the numerical inversion model VINMOD. The dashed lines indicate input parameters that can be used in the case when simplified model configuration such as for homogeneous aquifer with radially dominant flow is used.

The concentration-time series data are measured during the integral pumping test, i.e., pumping test with simultaneous recording of the contaminant concentration in the pumped water as a function of the time. The velocity field can be obtained from the

calculated head of the groundwater flow field by, for instance, MODFLOW (McDonald and Harbaugh, 1988).

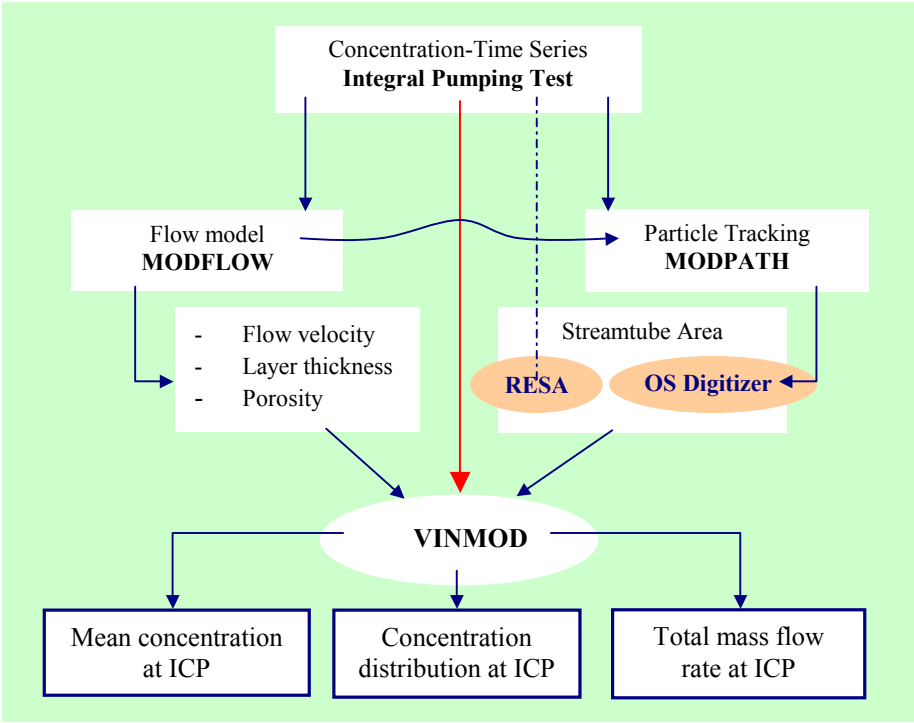

Figure 4.9 Simplified flow chart for the numerical inversion model VINMOD

A particle tracking code such as MODPATH (Pollock, 1989, 1994) can be used to calculate the pore velocity based on the calculated head. In this case, the mean pore velocity is calculated at the center of each grid cell assuming that the directional velocity components vary linearly within a grid cell. Figure 4.10 shows the schematic representation of the groundwater flow velocity profile at the ICP in a finite difference scheme. In this particular example, the groundwater flows in the x-direction and, therefore, only the x-component of the flow velocity is shown. However, in the case when the mean flow is diagonal, the resultant velocity of the x- and y components needs to be used. For the natural groundwater flow under homogeneous condition, the velocity profile at the ICP is assumed to be constant.

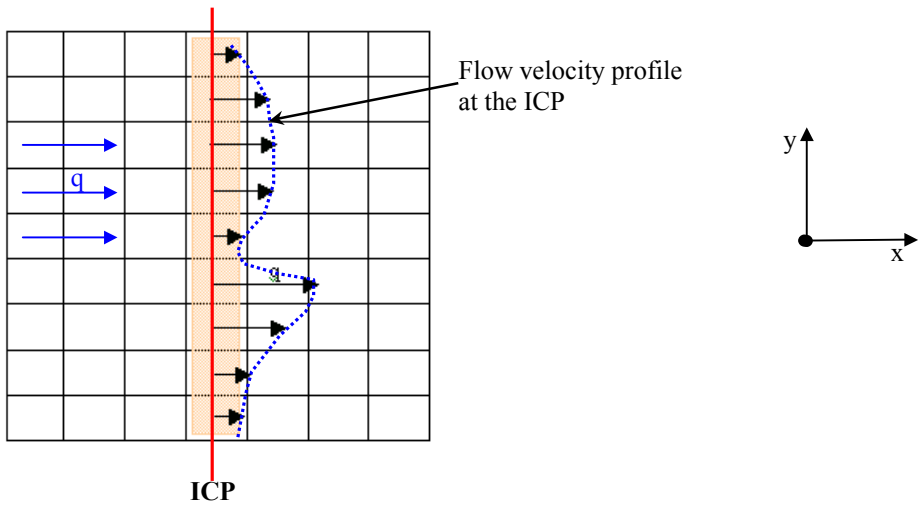

Figure 4.10 Schematic representation of groundwater flow velocity profile at the ICP in a finite difference grid domain.

In addition, the velocity field that can be obtained during the transient flow period can be used to determine the well capture zones for the eventual determination of streamtube areas. Well capture zones can be obtained by means of backward particle tracking. Particle tracking involves the tracking of water particles paths from their points of origin to some destinations or, inversely, from some destination points to their points of origin.

The tracking of particle paths from known point of origin to some destination point is called forward particle tracking. Whereas the tracking of particles from the destination point to the point of origin is called backward particle tracking or backtracking. In a finite difference numerical model, such as with MODPATH (Pollock, 1989) or PMPATH (Chiang and Kinzelbach, 1998), the pathlines of water particles can be computed based on the velocity vectors of the groundwater flow field that can be obtained from the intercell flow rates. Thus, with forward particle tracking, a particle follows the prevailing velocity vector in the normal flow direction. To employ a backward tracking, the forward velocity vector can simply be reversed by multiplying the velocity term by -1. In this particular study, a semi-analytical particle tracking scheme (Pollock, 1989) is used to calculate particle paths and positions. The semi-analytical particle tracking scheme uses

simple linear interpolation to compute the principal velocity components at any point within a model cell. The position of the particle can then be determined using the velocity and particle travel time information. The length of the particle traveltime depends on the permeability of the aquifer along the particle path. In a heterogeneous aquifer, the particles that arrive the pumping well at the same time can have different origins and, therefore, the well capture zone can be defined by irregular isochrones.

A on-screen digitizer (OS Digitizer) is developed and used for digitizing and calculating the streamtube areas within the irregular capture zone. Figure 4.11a shows the OS Digitizer interface for digitizing and calculating a given streamtube areas in a capture zone. OS Digitizer calculates a given area of a streamtube based on a polygon method. A brief description of the polygon method and the digitizing procedures is given in Appendix A2.

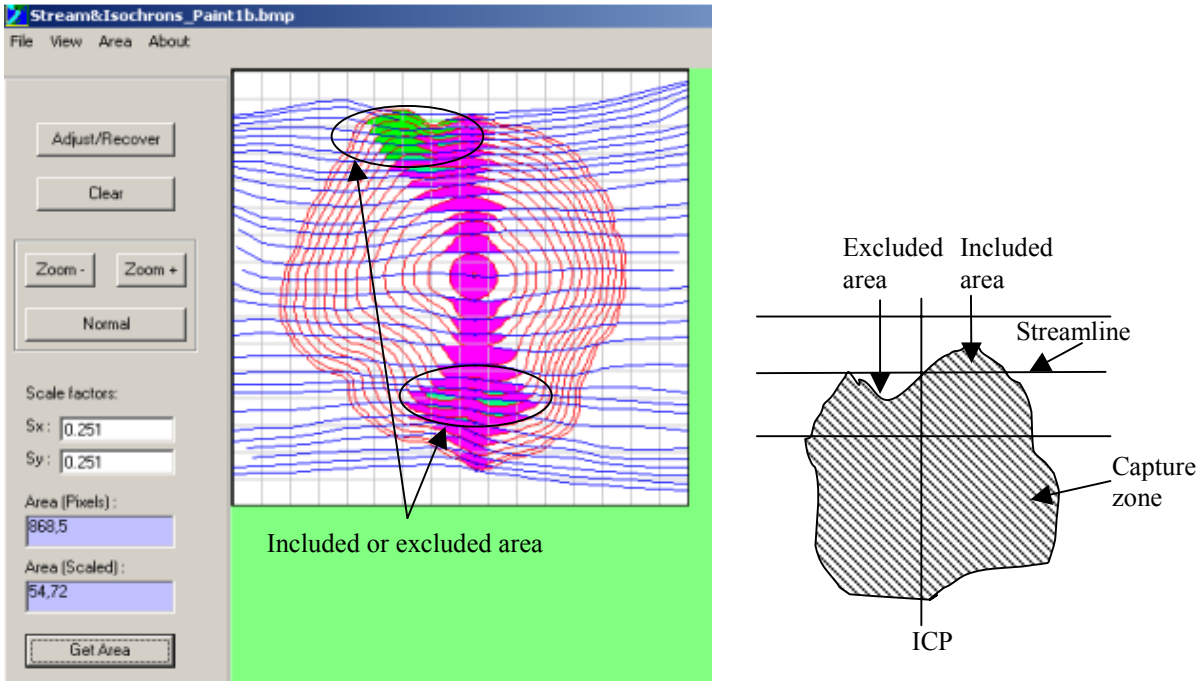

(a) (b)

Figure 4.11 a) OS Digitizer interface for digitizing and calculating streamtube areas, b) demonstration on inclusion and exclusion of a part of a streamtube area for a given capture zone.

Due to the irregular shapes of the streamlines and capture zones in a heterogeneous aquifer, a streamline crossing the ICP might not be tangent to the corresponding capture zone. Thus, some streamtube areas can cross a streamline common to them. Thus, in order to conserve the contaminant mass that can be pumped in a given capture zone, inclusion or exclusion of a part of a given streamtube area must be applied as shown in Figure 4.11b. Inclusion is required if a capture zone enters the adjacent streamtube whereas exclusion is required if the adjacent streamline passes outside of the capture zone under consideration.

It should be noted here that, for capture zones obtained by particle backtracking, the accuracy of the streamtube area can be affected by errors associated with digitization and the grid resolution of the numerical model itself. Digitization errors by using OS Digitizer are in general less significant and are, on the average, in the range of 2 - 3 %. However, errors associated with the grid resolution of the numerical model can affect significantly the size of the well capture zone which in turn results in faulty values on the streamtube area that can be calculated. For instance, Figure 4.12 shows the superimposition of two capture zones obtained by changing the grid resolution in the vicinity of the pumping well.

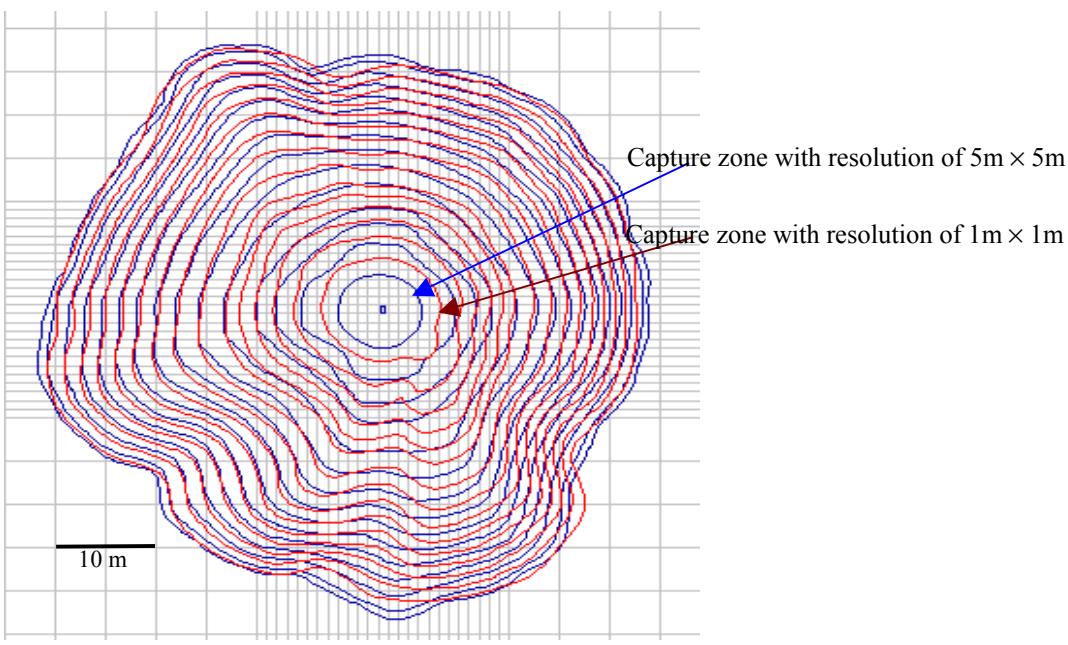

Figure 4.12 Effect of grid resolution on the size of the well capture zone

In this particular example, the grid resolution with 5m by 5m results a distortion of the capture area by about 50 per cent from the theoretical area, which in fact results in underestimation of the actual total mass flow rate at the ICP. By increasing the grid resolution to 1m by 1m, the result of the digitized capture area is improved.

For the coarser grid cells, the diminution of the capture area around the pumping well relative to the theoretical area is caused by the distortion of the particle travel distance. This problem can be attributed to the method of the backward tracking itself and the linearly interpolated pore velocity at the center of the grid cell. In backward tracking from a pumping well, particles start from the face of the constant head cell and not from inside the constant head cells. In addition, the mean pore velocity calculated at the center of the grid cell can affect the value of the particle travel distance (Pollock, 1994). Frederick (2001) demonstrated a nested grid rediscretization method of the grid cell where the pumping well is located so as to improve the particle travel distance and capture area. The higher the grid resolution the better is the streamtube area that can be obtained.

In the case when the well capture zones are circular and the streamlines are represented by straight lines, the streamtube areas needed for VINMOD can be approximated from the rectangular equivalent streamtube areas (RESA) as shown in Figure 4.13. For instance, given a streamtube index j and the time index i in the concentration-time series data with n data points, the length L of rectangle in a given streamtube under consideration can be given as:

$$L_{i,j} = 2X_{i,j} \tag{4.12}$$

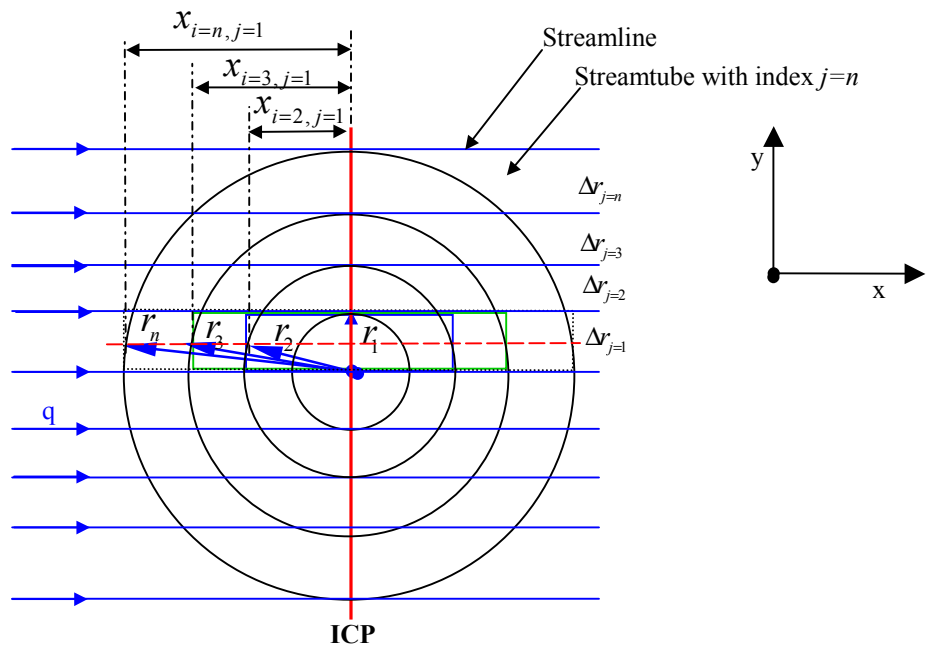

Figure 4.13 Schematic representation of circular capture zones for determining the rectangular equivalent streamtube area (RESA).

Taking the quadrant of the circle, half of the length X of a streamtube with index j corresponding with the time interval index *i* in the concentration-time series data can then be approximated from Pythagoras theorem as:

$$X_{i,j} = \left[r_i^2 - (r_j - 0.5\Delta r_j)^2 \right]^{1/2} \quad ; \; r_j \le r_i \tag{4.13}$$

Where r_j [L] is the radius of the capture zone corresponding with a streamtube with index j along the ICP, r_i [L] is the radius of the latest capture zone corresponding to the latest pumping time, i and j are time and streamtube indices respectively with $i = j$, $j+1$, …, n and $j=1, 2, \ldots, n$ and. Thus, the area of each streamtube j at a given time i, $As_{i,j}$, in the concentration-time series with n data points can be approximated from the

equivalent rectangular area having a width the same as the streamtube width Δr_j and the mean length of the streamtube $L_{i,j}$ as follows:

$$A_{s_{i,j}} = L_{i,j} \Delta r_j \tag{4.14}$$

With $i = j$, taking half of the capture circle, the area of the sector for the outer stream can be approximated in the way that the total mass within a given capture zone can be conserved.

$$As_{i=j} = 0.5\pi r_j^2 - \sum_{k=1}^{j-1} As_{k,j} \tag{4.15}$$

Under homogeneous condition with radially dominant flow, the rectangular equivalent streamtube area (RESA) method determines the streamtube areas reasonably well. Thus, for a simplified model with radially quasi circular capture zone, the use of RESA in VINMOD can save the digitizing time that would otherwise be spent by using OS Digitizer.

Figure 4.14 shows a schematic presentation of VINMOD compatibility and applicability in terms of the profile of the concentration-time series data and the expected well capture zone geometry. In this case, VINMOD can be applied in four cases classified by type as Type I, Type II, Type III, and Type IV depending on the concentration-time series data profile and the corresponding capture zone geometry. With some knowledge about the underlying aquifer material, the applicability and compatibility of VINMOD for homogeneous or heterogeneous aquifer settings can be evaluated from the concentration-time series profile. Although the four types presented here can be handled by VINMOD, Type III and Type IV may cause additional oscillation effect on the inverted concentration distribution.

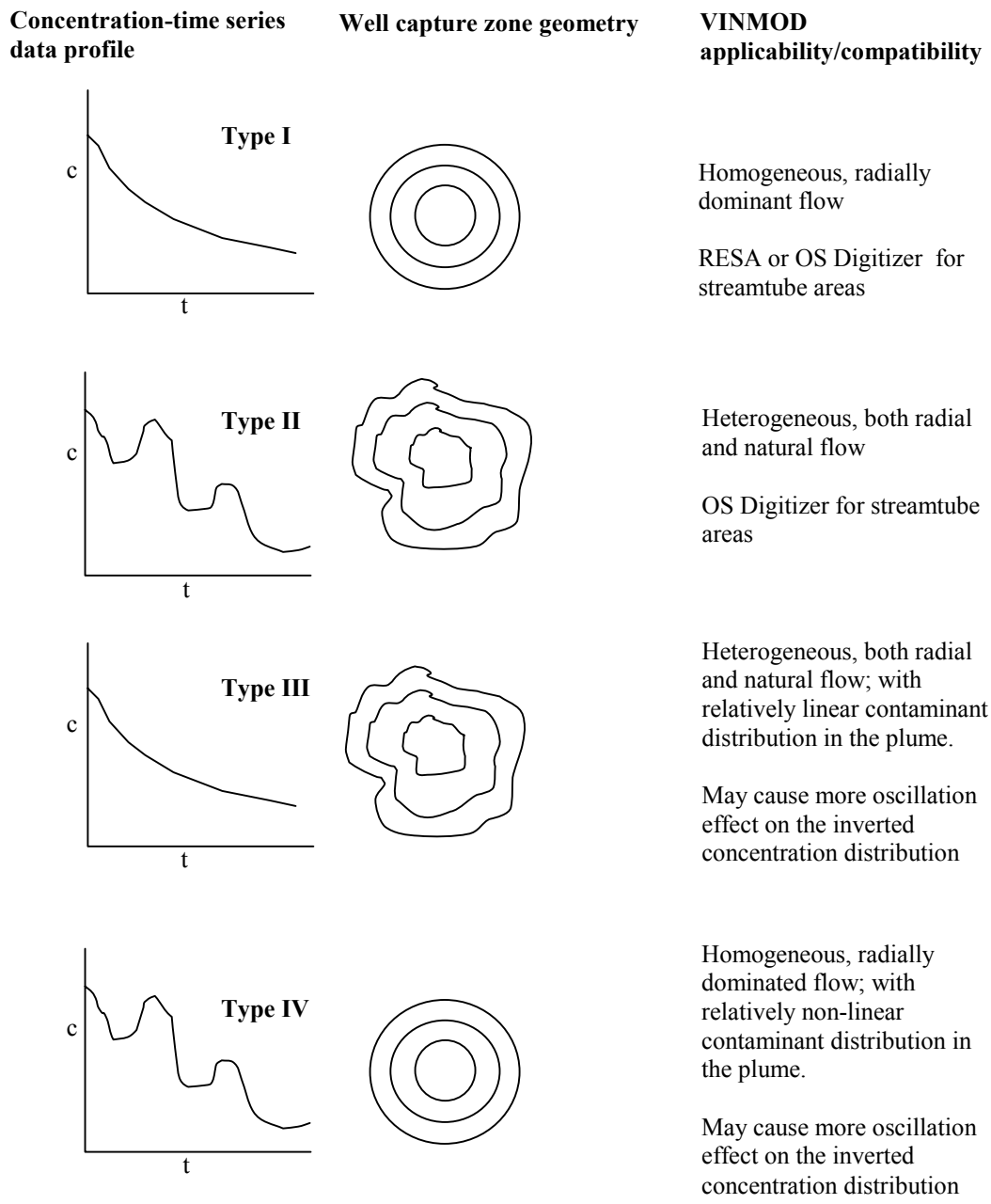

Figure 4.14 Schematic representation of VINMOD compatibility and applicability in terms of the concentration-time series profile and the type of well capture geometry.

4.4 Model verification

4.4.1 Model verification on homogeneous aquifer scenario

The reliability of VINMOD is tested by comparing the volume based inverted concentration distribution at the ICP with that of the analytical inversion interfaced with PINwin (Appendix A1) under homogeneous condition. In addition, the MT3D simulated concentration distribution referred hereon as "real" concentration distribution at the same ICP is used for further comparison. A stationary plume relative to the pumping well is used for the test. In this case, the concentration gradient in the plume is neglected. Thus, a single layered numerical flow and transport model is set up with an ideal representation of a homogeneous- confined aquifer in order to get the flow field, particles positions for the eventual delineation of well capture zones, and the equivalent pumped concentrations. Both the groundwater flow, contaminant transport, and particle tracking models such as the numerical codes MODFLOW (McDonald and Harbaugh, 1988; Harbaugh and M.G. McDonald,1996), MT3D (Zheng, 1990), and PMPATH (Chiang and Kinzelbach, 1998) respectively are used for flow and transport simulation as well as for capture zone delineation. The detail of the numerical model parameters are presented in Table 4.1.

Table 4.1 Main variables or parameters used in the numerical model

Variable or parameter	Value
Model area	500 m × 500 m
Grid size	5 m × 5 m (1 m × 1 m around the well)
Layer thickness	35 m
Hydraulic conductivity	0.001 m/s
Hydraulic gradient	0.002
Porosity	0.17
Hydraulic conductivity	K = 0.001 m/s
Longitudinal dispersivity:	α_L =10 m
Dispersivity ratio (α_T/α_L)	0.1
Source concentration	12.5 µg/l
Source-to-pump distance	150 m
Pumping rate	250 m^3/h
Stress period 1 (T) (Steady state period)	1095 days (3 years)
Stress period II (Transient period)	3 days

In this case, a known source with a fixed concentration of 12.5 µg/l was injected and positioned at about 150 meters upgradient of the ICP position. Both the steady state and transient flow regimes are considered. For the transient period, a single pumping well was set to pump contaminated groundwater at the rate of 250 cubic meters per hour for three consecutive days. The corresponding concentration-time series data observed from MT3D simulation output is in turn used for the inversion of pumped concentration with VINMOD and PINwin. Figure 4.15 shows the concentration-time series data obtained from the MT3D simulation results for the homogeneous model configurations under consideration.

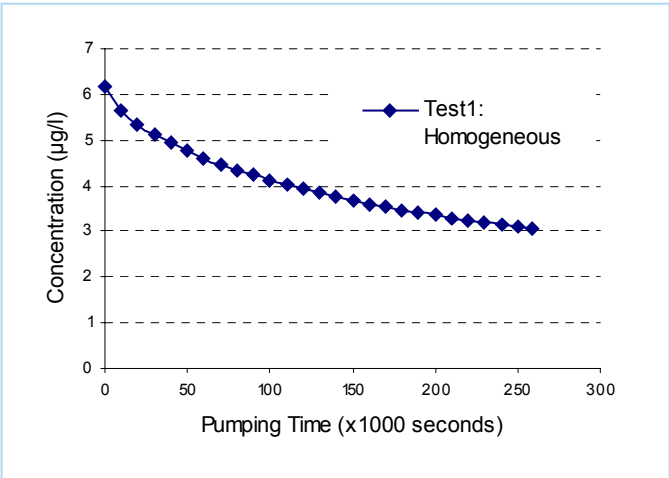

Figure 4.15 Concentration-time series data from MT3D simulation output under homogeneous condition.

The well capture zones corresponding to the concentration-time series data, under homogeneous condition are circular and the streamlines of the natural groundwater flow are found to be straight lines. Each streamline, in this case, is tangent to the corresponding well capture zone at the IC. Figure 4.16 shows the superimposition of the well capture zone and the streamlines. Thus, for a circular capture zone where the radial flow is dominant, the streamtube areas can be calculated using the rectangular equivalent discussed in the preceding section (see Equation 4.14 and Equation 4.15).

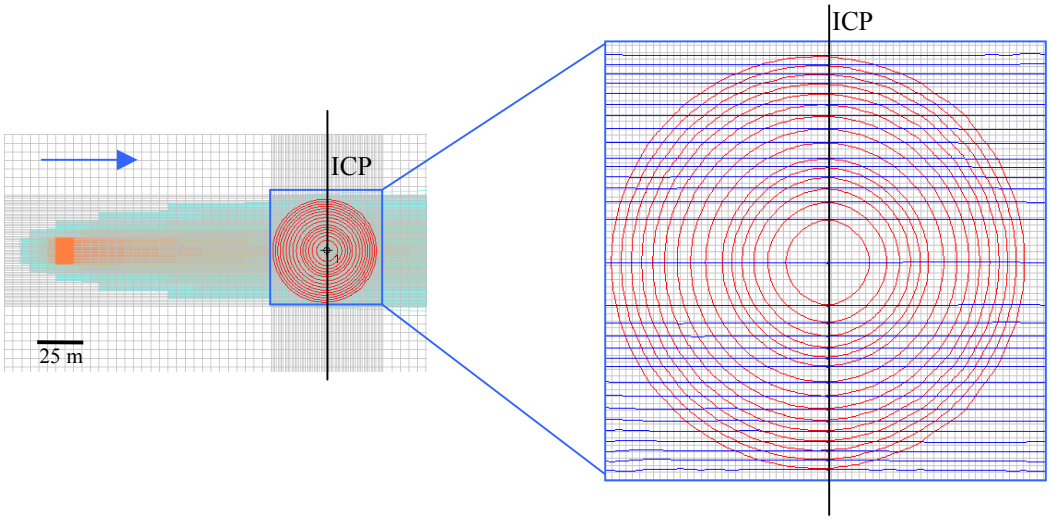

Figure 4.16 Superimposition of well capture zones and streamlines from numerical simulation under homogeneous condition.

Figure 4.17 shows the inverted concentration distribution with VINMOD compared with the concentration distributions from the analytical inversion and the "real" concentration distribution. It can be noticed that the trend of the inverted concentration distribution with VINMOD shows a similar trend as that of the analytically inverted concentration using PINwin and the "real" concentration distribution.

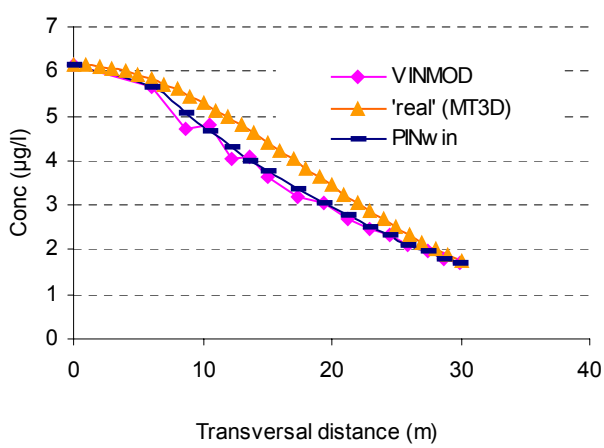

Figure 4.17 Comparison of inverted and "real" concentration distributions.

Due to the presence of dispersion, the inverted concentration distribution passes slightly below the "real" concentration distribution trend as discussed in the preceding chapter (Chapter 3). However, the general trend of the inverted concentration distribution with VINMOD indicates that the model works well and confirms its validity for the inversion of pumped concentration with a similar degree of certainty as the analytical inverse model for a radially dominated flow field. In addition, because of the flexibility for handling irregular well capture zones, VINMOD can further be applied for use under heterogeneous conditions and for homogeneous conditions where uniform flow is no longer negligible.

4.4.2 Model verification under heterogeneous scenario

For using VINMOD under heterogeneous condition, the hydraulic conductivity around the pumping well of the numerical model used for validation test under homogeneous scenario is modified as shown in Figure 4.18 while keeping all other parameters as in Table 4.1.

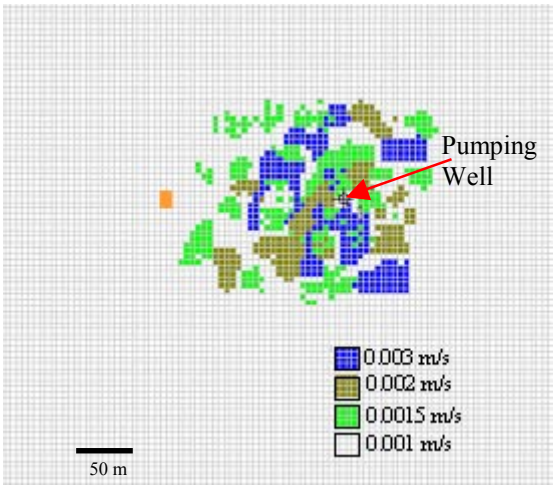

Figure 4.18 Randomly assigned local heterogeneity with highly permeable field in the vicinity of the pumping well

Figure 4.19 shows the concentration-time series data obtained from the MT3D simulation. The values of the pumped concentration in the heterogeneous case are slightly lower than that of homogeneous case shown in the preceding section. This can be due to

the modified permeability around the pumping well. In this case, the relatively higher groundwater velocity involved in the modified high permeability zones could cause more dilution effect.

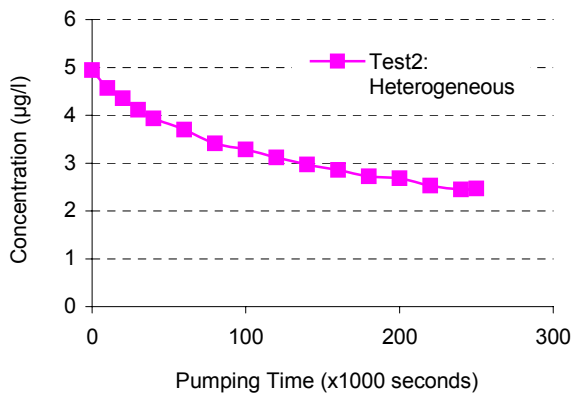

Figure 4.19 Concentration-time series data from MT3D simulation output.

As it can be seen in Figure 4.20, the resulting well capture zone is no longer circular and, after superimposition with the corresponding streamlines, the streamtube areas for the mirror image streamtube indices are not necessarily equal.

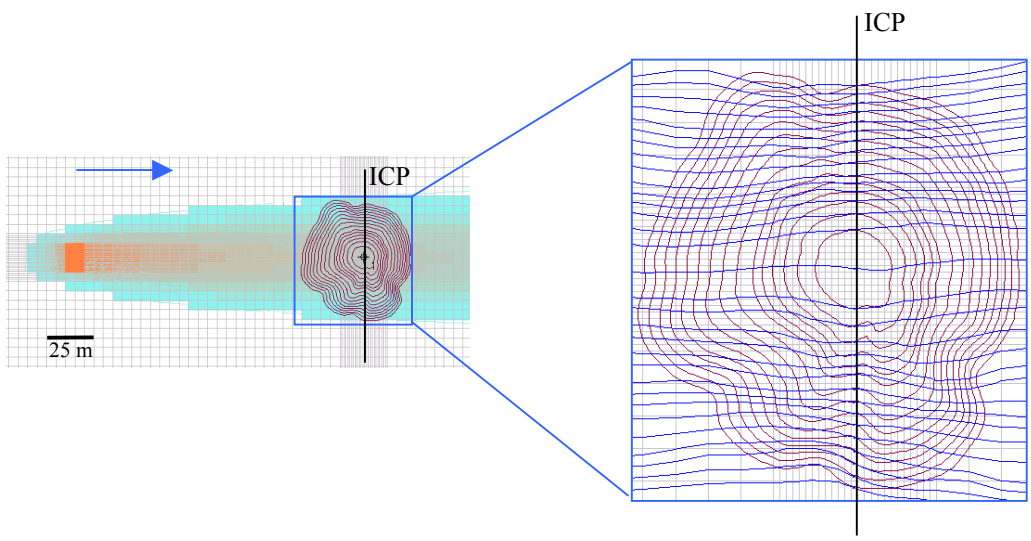

Figure 4.20 Superimposed well capture zones and streamlines with randomly distributed hydraulic conductivity values.

In this case, the streamtube areas cannot be handled by the rectangular equivalent area method that is applied in the preceding section for circular capture zone. Therefore, the OS Digitizer is used to digitize and calculate the resulting streamtube areas.

Figure 4.21 compares the resulting inverted concentration distribution obtained with VINMOD to the "real" concentration distribution for the heterogeneous case under consideration. It can be noticed that the inverted concentration distribution shows some oscillation effect compared to the "real" concentration distribution (Figure 21a). Since the inversion of pumped concentration with VINMOD depends on the volume of the capture zone and the inversion method is recursive, any irregularities on the shape of the capture zone causes oscillation.

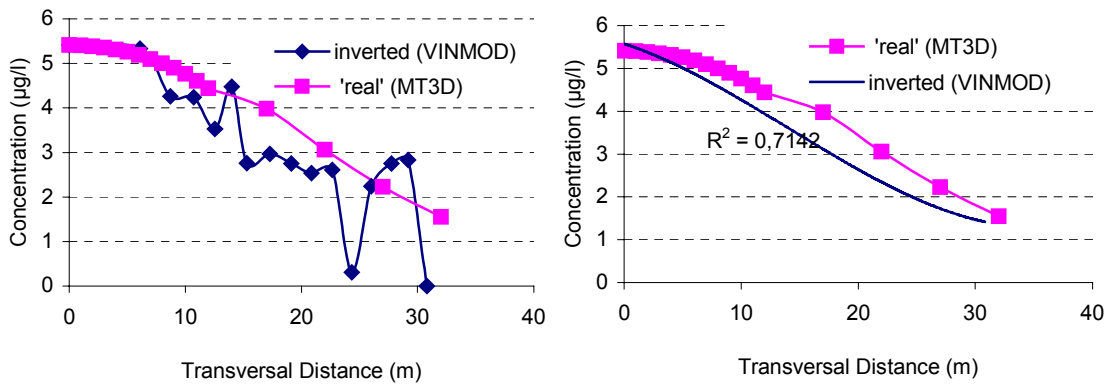

Figure 4.21 Inverted concentration distribution compared with the "real" concentration distribution at the predefined ICP: a) inverted concentration distribution before filtering, b) inverted concentration distribution after filtering.

However, as can also be seen from the filtered values of the inverted concentration distribution, the general trend of the inverted concentration distribution follows the trend of the "real" concentration distribution. In this case, taking the area under the two distribution curves, the values of the inverted concentration distributions are less than that of the "real" concentration distributions by about 11 %. Though this margin of error cannot be taken as conclusive, as results from a single simulation may not be adequate,

the inversion of pumped concentration with VINMOD in the heterogeneous case can provide a reasonably acceptable results.

In the case when the permeability distribution around the pumping well is unknown, one may estimate the inverted concentration distribution from the equivalent homogeneous media. The resulting error depends on several factors such as the differences in parameter values, the geometry of the well capture zone, etc. The change of the geometry of the well capture zone, as a result of local heterogeneity, resulted a slight increase of about 4 % on the inverted concentration distribution (Figure 4.22). It is also noticed that, the values of the inverted concentration distribution from a reference homogeneous model are inferior to that of the "real" concentration distribution by about 15 %. In this case, the streamtube areas are determined from the rectangular equivalent streamtube area (RESA). It should be noted here that the concentration-time series used here for evaluating the error is the same concentration-time series data obtained from the MT3D simulation under heterogeneous condition, while keeping all other parameters equal to those of the homogeneous model presented in Table 4.1.

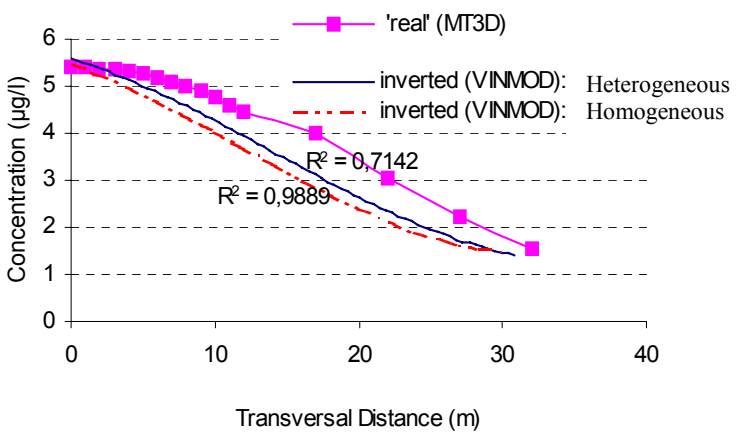

Figure 4.22 Comparison of inverted concentration distributions from both the heterogeneous and simplified heterogeneous case with the "real" concentration distribution under heterogeneous case.

Figure 4.23 shows the calculated total mass flow rate is increased by about 43 % relative to the mass flow rate that can be obtained in the homogeneous case. It should be noted

that, if lower permeabilities are used in the modified zones around the pumping well, the total mass flow rate at the ICP can be lower than the one demonstrated here.

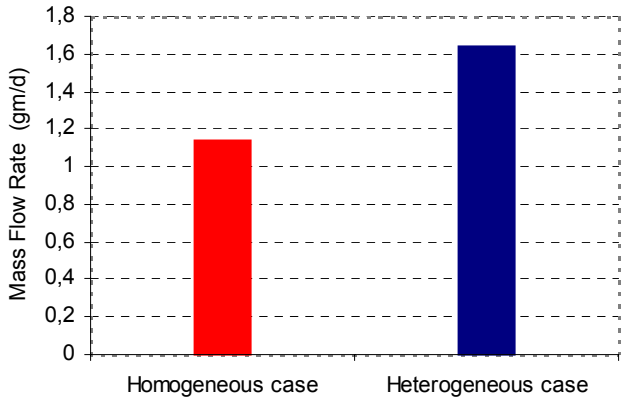

Figure 4.23 Total mass flow rate calculated at the ICP with the presence of local heterogeneity relative to the reference homogeneous model set up.

In this particular example, it is noticed that the groundwater flow velocity profile at the ICP has influenced significantly the total mass flow rate. The inverted concentration distribution as a result of the deformed capture zone, caused by the presence of local heterogeneity, contributed about a 7 % increase on the total mass flow rate. Whereas about 35 % of the increase on the total mass flow rate is attributed to the groundwater flow velocity profile at the ICP. Figure 4.24 shows the groundwater flow velocity profile at the ICP for the modified heterogeneous field relative to that of the reference homogeneous case. The drop in the values of the velocity profile below the reference velocity under the homogeneous case around the streamtube indices on the Cartesian co-ordinate is due to the effect of the neighboring high permeability zones at local scale that could cause preferential flow paths.

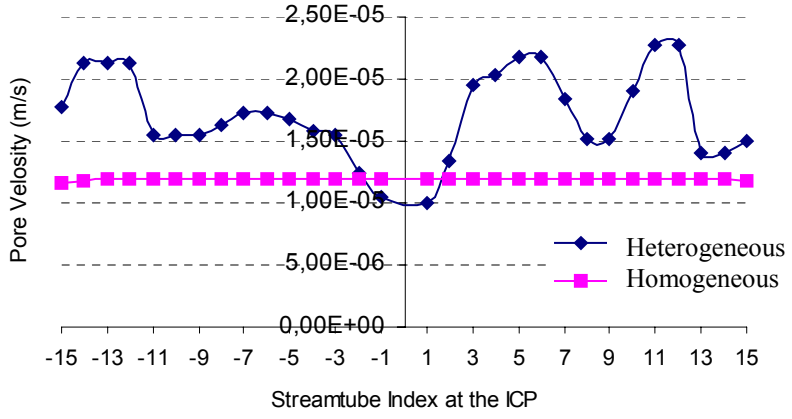

Figure 4.24 Groundwater flow velocity profile at the predefined ICP.

Thus, the velocity profile at the ICP, depending on the distribution of the permeability, can have a significant effect, i.e. the way that the calculated total mass flow rate varies significantly with respect to a reference homogeneous aquifer model. In addition, the pattern of the permeability distribution around the pumping well that determines the geometry of the well capture zones slightly affects the value of the inverted concentration distribution. Therefore, the change of both the velocity profile as well as the well capture zone, caused by the presence of local heterogeneity around the pumping well can significantly alter the magnitude of the total mass flow rate at the ICP.

4.5 Summary

With a small number of monitoring wells, the inversion of pumped concentration can be used as an alternative method to other conventional methods such as point measurements, interpolation, and geophysical methods, for determining the state of groundwater pollution.

In the case of homogeneous-isotropic media where radial flow is dominant and the effect of the natural flow is negligible, the method of inversion of pumped concentration can be performed analytically. However, in many cases, the real geo-hydrological systems are complex and, therefore, the aquifer must be considered as by heterogeneous. In this case,

the method of inversion of pumped concentration can be approached numerically. A **v**olume based **in**verse **mod**el (VINMOD) is developed and used for the numerical inversion of pumped concentration by taking into account heterogeneity within the entire well capture zone. VINMOD calculates the mean concentration, the concentration distribution and the corresponding mass flow rate of the "undisturbed" plume for groundwater pollution quantification taking a predefined imaginary control section (ICP) as a reference.

It has been noticed that, in the heterogeneous case, VINMOD is very sensitive to the groundwater flow velocity variations within the stream-tubes. The groundwater velocity profile at the ICP can strongly influence the total mass flow rate that can be calculated. In addition, the geometry of the well capture zone showed slight change on the value of the mean of the inverted concentration distribution relative to that the reference homogeneous model. The presence of local heterogeneity can significantly affect the inversion of pumped concentration for the determination of the mean concentration and the corresponding total mass flow rate at a predefined ICP and, therefore, numerical inversion of pumped concentration can be appropriate.

It should be noted here that, while employing numerical inversion of pumped concentration with VINMOD, any deviation of the values of the streamtube areas from the theoretical values can cause oscillations of the concentration distribution. In addition, the accuracy of the streamtube areas can be affected by errors associated with digitization and the grid resolution of the numerical model itself. Digitization errors by using OS Digitizer are in general less significant and are, on the average, in the range of 2 - 3 %. However, errors associated with the grid resolution of the numerical model affects the size of the well capture zone which in turn results in faulty values on the streamtube area that can be calculated. The higher the resolution of the model grid, such as 1 m by 1 m, the more accurate the streamtube area obtained.

Chapter 5

Application at the industrial site in the city of Strasbourg

5. Application at the industrial site in the city of Strasbourg

This chapter addresses the application of the inversion of pumped concentration at the industrial site Plaine des Bouchers in Strasbourg where significant PCE contamination has been detected. The effect of the concentration gradient and the presence of local heterogeneity discussed in the preceding chapters are taken into consideration. The calibrated numerical flow model is used for the numerical inversion of pumped concentration. The concentration-time series data obtained from two pumping wells (PW1 and PW2) are used for the inversion of pumped concentration. The imaginary control plane (ICP) is defined through the separation distance of about 300 meters between PW1 and PW2. For the homogeneous scenario, the total mass flow rate and the corresponding mean concentration is determined by taking into account the concentration gradient in the PCE plume. However, since significantly higher PCE contamination is observed in PW2, more focus for further evaluation of the effect of local heterogeneity is made using the integral test parameters of PW2. Due to the absence of detailed knowledge about the local heterogeneity in the vicinity of the pumping wells, only a conceptual model for high permeability zones are used for demonstration purpose. The resulting mass flow rate relative to the mass flow rate that can be obtained from the reference homogeneous model setup is used to demonstrate the effect of heterogeneity on the quantification of groundwater pollution with the inversion of pumped concentration.

5.1 Introduction

Strasbourg is one of the two big economic centers of the region of Alsace (France). It covers about a quarter of the industrial sector of the region. In the Alsace plain, the population density is known to be high, i.e., about 200 inhabitants per square kilometer, dense. The region Alsace has immense groundwater reserves of about 300 billion cubic meters (IFARE/DFIU, 1998) with annual production of about 500 million cubic meters (Delporte and Talbot, 1994). However, with the expansion of industrialization and the

ever increasing human activities, concerns on possible pollution threats on these immense water reserves are becoming real. This is due to the fact that the risk of groundwater contamination is significant, owing to uncontrolled or deliberate discharge of industrial contaminants, accidental spills and leaks of petrochemical products, which in turn could cause substantial health and environmental problems.

Recently studies on the level and extent of groundwater contamination at the site *Plaine des Bouchers*, one of the industrial sites in Strasbourg, have been carried out under the framework of the European funded R&D project INCORE (integrated concept for groundwater remediation) with a new approach involving the inversion of pumped concentration (see section 2.2.4). However, elements such as the effect of concentration gradient and local heterogeneity were not considered. Moreover, due to the lack of complete information on the details of the heterogeneity around the pumping wells, the inversion of pumped concentration was performed without taking into account the effect of local heterogeneity.

Therefore, this chapter demonstrates the application of the inversion of pumped concentration by taking into account the concentration gradient as well as local heterogeneity as described in detail in the preceding chapters (chapter 3 and chapter 4).

5.2 Study site Plaine des Bouchers

5.2.1 Site description

The site *Plaine des Bouchers* is located at about 3 km to the south of the center of Strasbourg. The site has a size of 1 kilometer by 2 kilometers. Figure 5.1a shows the map of the site *Plaine des Bouchers* near Strasbourg. It is an industrial site with a long history of industrialization. It has been used for many industrial activities, storage facilities, commercial activities related to garages, used car lots, etc, since before the second world war (Schäfer et al., 2004). Figure 5.1b shows the inventory map of the various landuse types at the site *Plaine des Bouchers*.

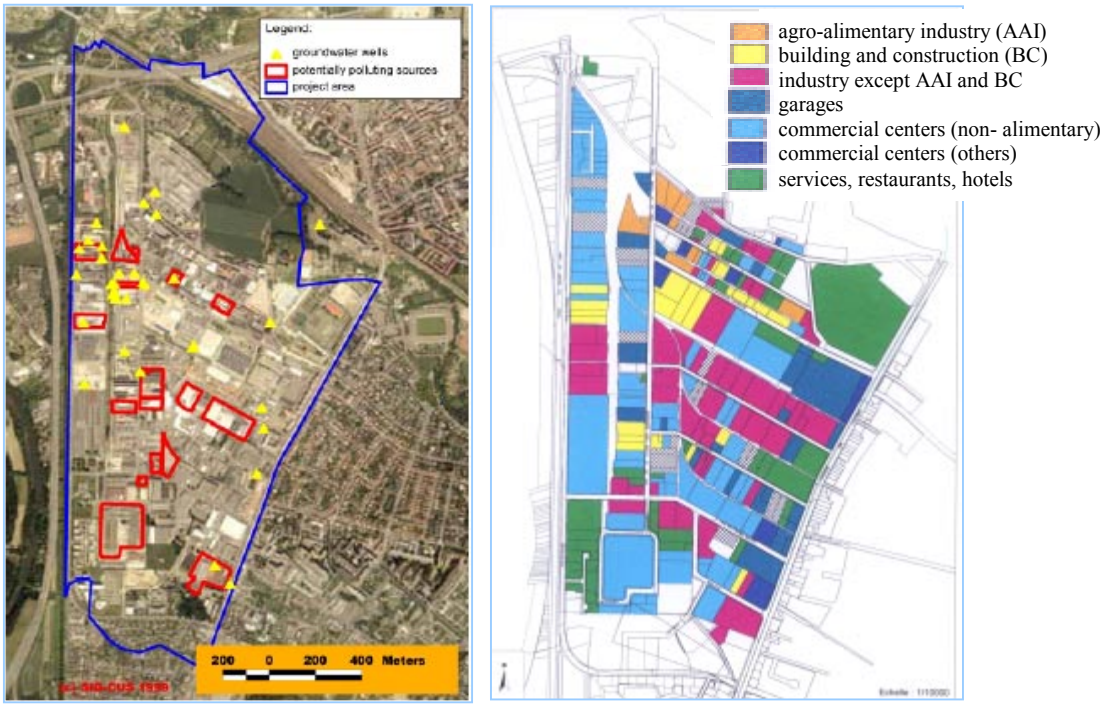

(a) (b)

Figure 5.1 Site *Plaine des Bouchers* in Strasbourg: a) map of *Plaine des Bouchers* with potential pollution sources (Spausta and Prokop, 2003), b) inventory map of the site *Plaine des Bouchers* on the various types of landuses as of the year 2000 (after Hoang, 2000).

5.2.2 Hydrogeology

The underlying geological formation of the site is characterized by highly permeable alluvial deposits with a thickness of about 80 meters (Schäfer et al., 2004). Since the site *Plaine des Bouchers* is located in the Rhine basin, it is assumed that the underlying geological formation could have highly permeable zone similar to the formation of the Rhine River system which consists of a system of braided channels. Figure 5.2 shows an example of braided channels and the kind of materials of the underlying geological formation. Braided channels consist of alternating layers of sandy gravel and gravel materials without matrix having a spoon-like shape. The pattern of the channels follow the main flow direction of the groundwater.

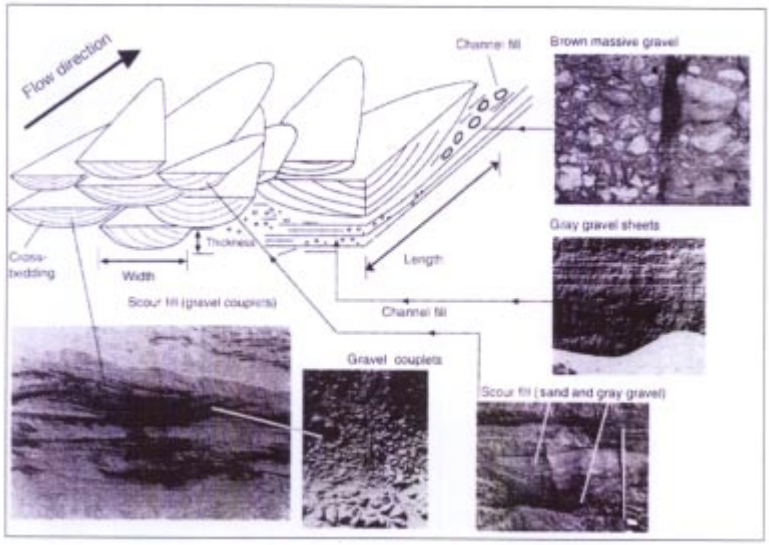

Figure 5.2 General model of architectural elements in glaciofluvial environments of, for instance, the former Rhine River system in which the size of the elements is a function of dynamics of fluvial system (*source*: Beres et al., 1999)

According to the measured groundwater head distributions from 22 monitoring wells, the average depth of the water table ranges from 2.5 meters to 3.5 meters with respect to the ground surface, with the groundwater head between 136.8 meters and 137.3 meters at the study site (Schäfer et al., 2004). The mean groundwater flow direction is from southwest to northeast and the average hydraulic gradient is about 7×10^{-4}.

5.2.3 Groundwater pollution

From the long history of industrialization at the site, the underlying groundwater quality can well be threatened as a result of contamination related to industrial waste disposals, waste damps, spills of cleaning agents, as well as chemical storage. According to the site screening criteria proposed by the French Environmental Ministry (DPPR/SEI/BPSE of April 1996), the site *Plaine des Bouchers* is known to be one of the thirty old industrial sites which have been classified as potentially contaminated sites related to groundwater quality (Hoang, 2000).

The main groundwater contaminants observed recently at the site are chlorinated solvents such as PCE and TCE. A significant quantity of PCE contamination with concentrations

of 10 µg/l for the outer isoline to values greater than 100 µg/l has been detected. Figure 5.3 depicts an overview of the PCE and TCE concentrations interpolated from measured concentrations (Appendix B1). The point kriging method is used for the interpolation. Figure 5.4 shows measurement points for the PCE concentrations and the kriging variogram. The oscillation of the variogram is due to the inadequate data. The coefficient of variance in this case is about 1.55, indicating that the interpolated isolines are not very good but can still be useful.

The detected PCE plume reaches a length of several kilometers and a width of about 200 meters (Schäfer et al., 2004). It is assumed that the groundwater pollution by PCE and TCE is due to a nearby chemical storage and manufacturing site. The detection of such contaminants has prompted the municipal authorities and environmental institutions towards the site investigation to evaluate the state of groundwater contamination.

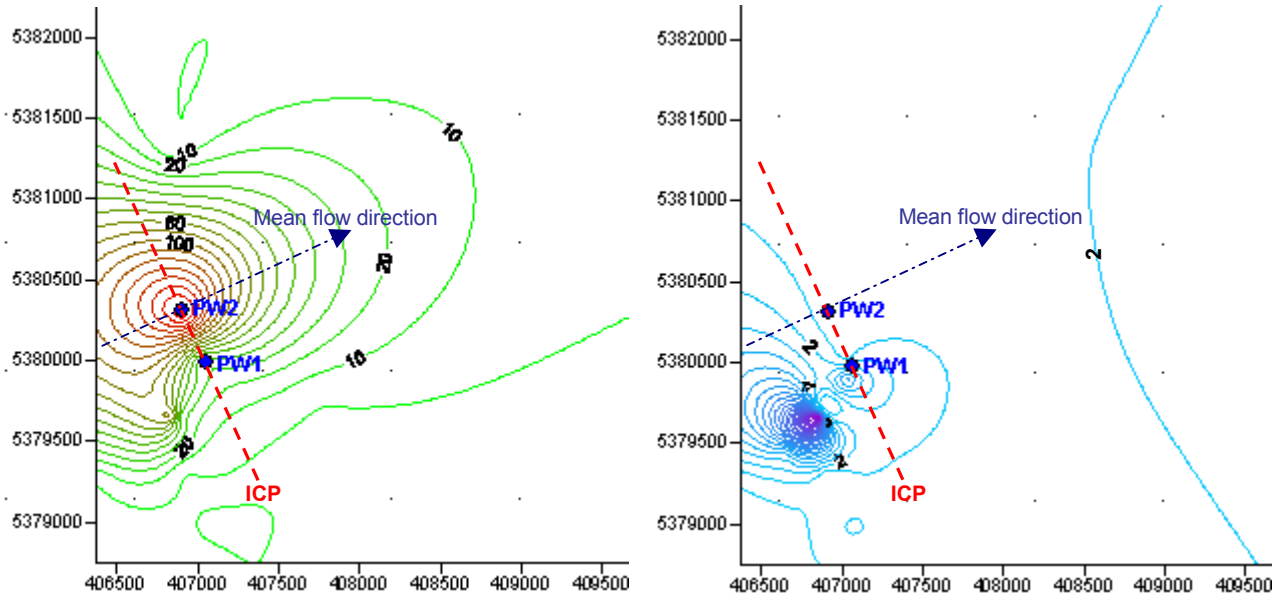

Figure 5.3 Isolines of measured PCE and TCE concentrations at the site *Plaine des Bouchers* as of year 2000 measurement data (Appendix B1.1), axes in real world coordinates: a) isoline of PCE with a maximum value of 180 µg/l at PW2, b) isoline of TCE.

Although the nearby chemical storage and manufacturing plants should be the possible source of the detected PCE plume, the source parameters are not known exactly. Figure 5.5 shows the inventory map of the industrial site *Plaine des Bouchers* on the classification of potential risks, indicating significant groundwater risks at several sub-zones of the site.

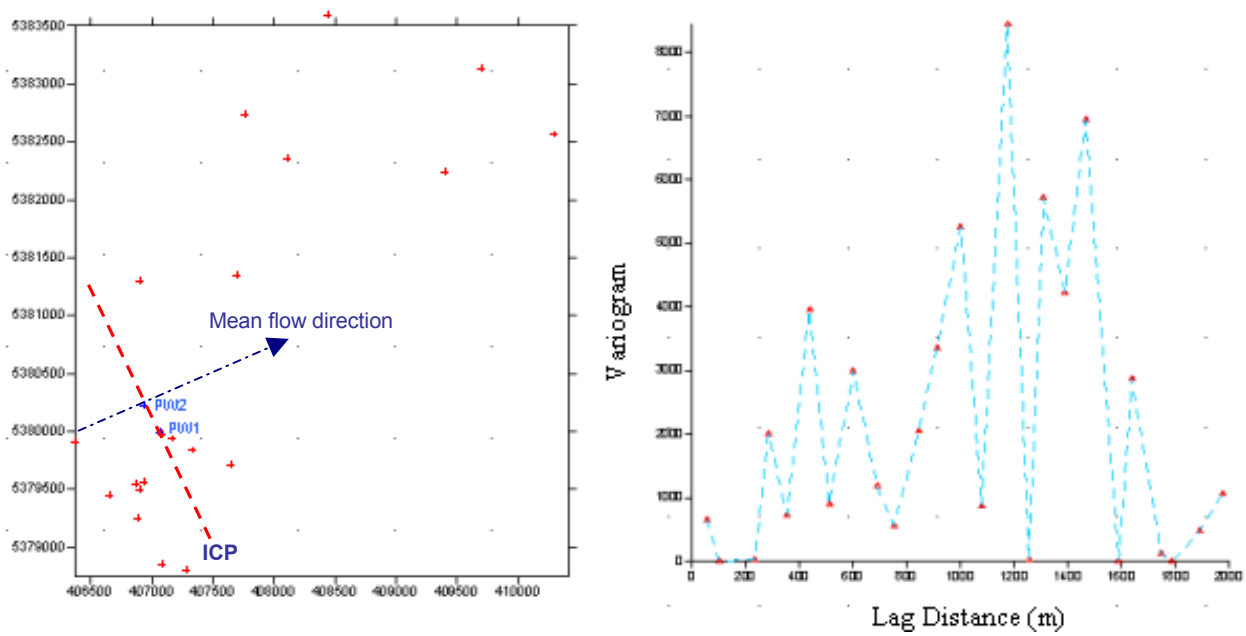

(a) (b)

Figure 5.4 Measurement points of PCE at the site *Plaine des Bouchers* as of year 2000 (Appendix B1.1): a) measurement points, b) kriging variogram.

Due to the limited number of monitoring wells available in the study area, the effort to quantify the state of groundwater pollution by the dissolved PCE plume from the available few point is not adequate. The method of the inversion of pumped concentration has thus been employed for determining the total mass flow rate of the detected PCE and the corresponding mean concentration.

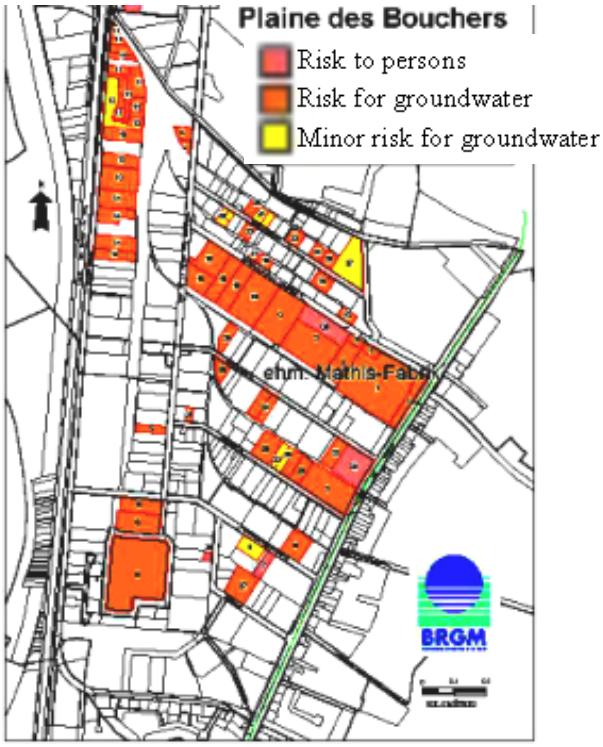

Figure 5.5 Inventory map for classification of potential risks at the industrial *site Plaine des Bouchers* (Ménillet, 1997; Widory and Elsass, 2003)

5.3 Integral pumping test

Integral pumping test refers the simultaneous measurement of the concentration of dissolved compounds during the pumping test operation. In order to carryout the inversion of pumped concentration for quantifying the state of groundwater pollution by the detected PCE, the concentration-time series data has been taken from two pumping wells PW1 (well Nr. 933) and PW2 (well Nr. 1120) which are separated by a distance of 300 meters.

Figure 5.6 shows the location of PW1 and PW2 and the nearby monitoring wells used for calibration studies for the groundwater flow model. An imaginary control plane (ICP),

passing through the two pumping wells PW1 and PW2, is defined. The predefined ICP is nearly perpendicular to the mean groundwater flow direction.

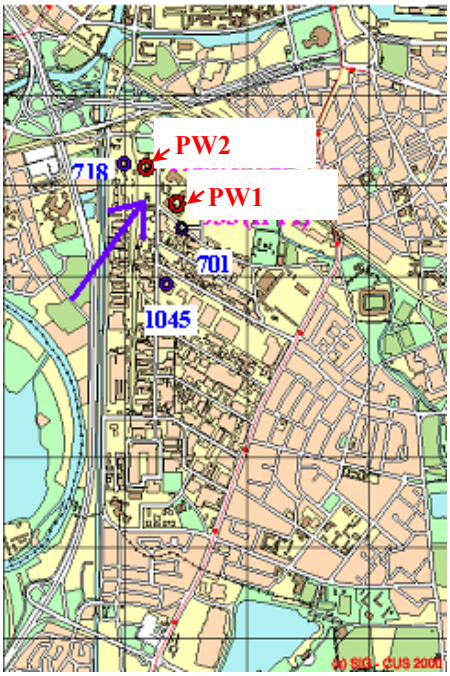

Figure 5.6 Location of the selected pumping wells and monitoring wells (Schäfer et al., 2004)

The measurement of the concentration-time series data were carried out during November/December 2000. Table 5.1 shows the pumping tests set up, the size of the concentration-time series data points as well as relevant aquifer related parameters assuming that the aquifer materials in a given layer are homogeneous. The concentration-time series data with 24 measurement samples from PW1 at the 1st layer and 14 calculated and measured samples were from PW2 at the 2nd and 3rd layers respectively. Figure 5.7 and Figure 5.8 show the concentration-time series of each layer.

Table 5.1 Pumping test setups and aquifer parameters

	Layer1	Layer2	Layer 3
Pumping Well (PW) #	1	2	2
Pumping Period [hours]	72	72	72
PCE sample numbers [-]	24	14	14
Pumping Rate [m^3/s]	0.055	0.0542	0.0233
Layer Thickness [m]	9.7	9.7	40
Hydraulic Gradient [-]	0.0007	0.0007	0.0007
Porosity [-]	0.15	0.15	0.15
Hydraulic Conductivity [m/s]	0.033	0.0198	0.019985
Groundwater Flow [m^3/s]	0.0246	0.0149	0.0200

The first pumping test is made at the first layer using PW1 whereas PW2 is used for the second and third layers. The oscillations in pumped concentrations at PW1 during the first 40 hours are supposed to be due to the fluctuations of the well discharge that may be caused by water-air mixture (Schäfer et al., 2004).

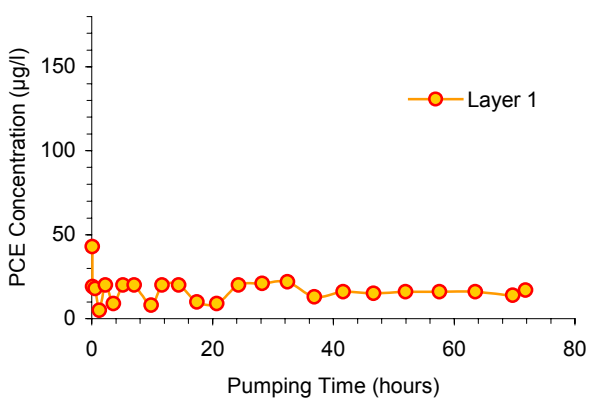

Figure 5.7 PCE concentration from PW1

Since the second pumping well at PW2 is screened in the second and third layer, the concentration-time series obtained from PW2 represents the global concentration of the second and third layer. However, simultaneous point measurements were also taken at the third layer using a peristaltic pump (Schäfer et al., 2004). Thus, the concentration-time series data that can be attributed to the second layer is determined from the proportion of

the transmissivities of the second and the third layers. As can be seen form the concentration-time series data, the level of PCE concentration in the first and third layer is significantly smaller than that of the second layer. It can be deduced from here that the major parts the PCE plume which passes through PW2 could be located in the second layer.

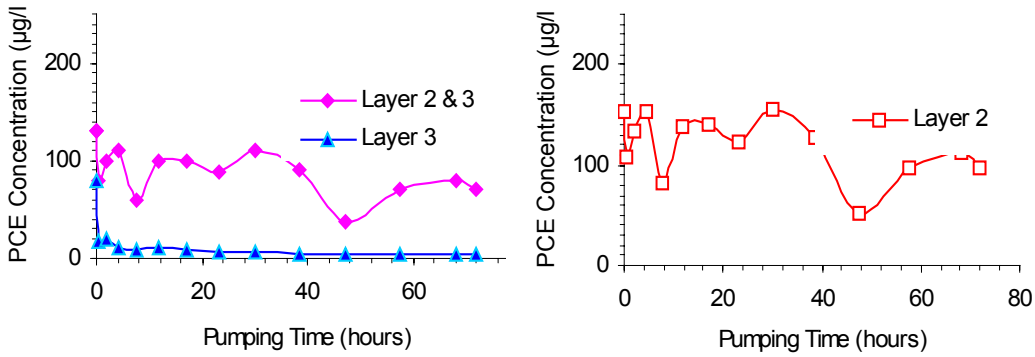

(a) (b)

Figure 5.8 PCE concentration-time series data for the second and third layer: a) for the second and third layer using PW2 and measured concentrations for the layer, b) calculated concentration-time series data for the second layer (Schäfer et al., 2004).

In addition, the measured concentration of dissolved oxygen ranges from 2.2 µg/l to 4 µg/l during the period of the pumping test operations. This indicates that biodegradation process by anaerobic microorganisms is not present in the detected PCE plume.

5.4 Numerical groundwater flow model

The existing and calibrated numerical groundwater flow model for the site *Plaine de Bouchers* is used in for the inversion of pumped concentration. A more detailed description and the calibration procedures are presented in Schäfer et al. (2004). The numerical finite difference groundwater flow model for the site *Plaine des Bouchers* in a local model is extracted from the regional multilayer model (Strasbourg-Offenburg)

developed in the LIFE-project for steady state flow conditions of the mean groundwater level of October 1986. Figure 5.9 shows the finite difference numerical model domains of the local and regional model.

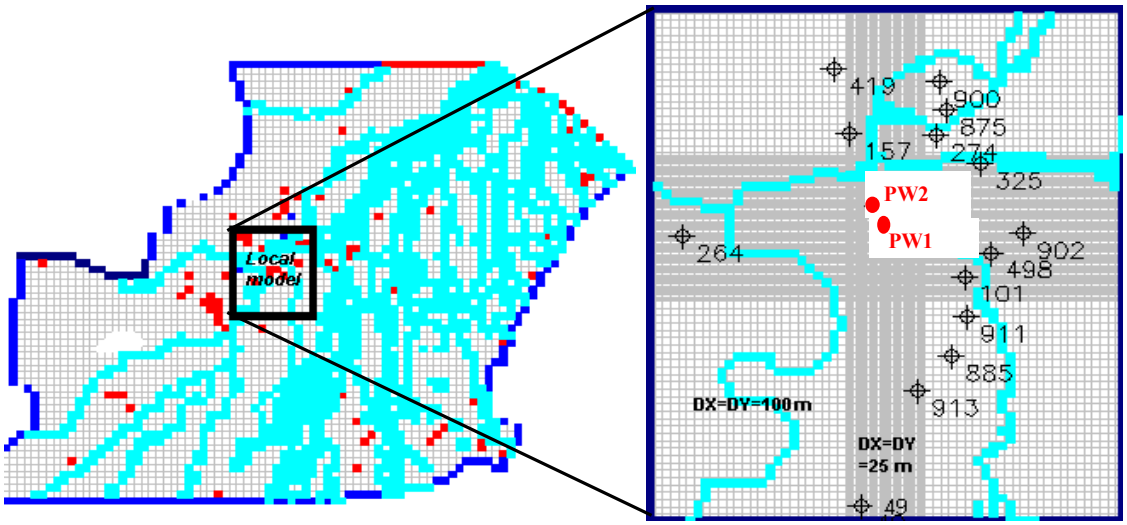

Figure 5.9 Schematic representation of the extracted local model, location of the pumping wells PW1 and PW2 used for the integral pumping tests, and selected monitoring wells (source : Schäfer et al., 2004).

The local domain has an area of 6 kilometers by 7 kilometers and is discretized with finite difference grid cells of 25 m × 25 within the study area and 100 m × 100 m outside the study area. The numerical groundwater flow model Processing Modflow (Chiang and Kinzelbach, 1998) interfaced with the 3D numerical code MODFLOW (McDonald and Harbaugh, 1988) is used to simulate the groundwater flow of the site *Plaine des Bouchers*. The groundwater model for the site Plaine des Bouchers is bounded by two rivers, the river *Ill* to the west and the river *Rhin Tortu* to the east. The alluvial unconfined porous aquifer of the study site comprises 4 layers with average thicknesses of 10 m, 10 m, 40 m and 15 m for the first, second, third and fourth layers respectively. The corresponding hydraulic conductivity values for the respective layers vary from 1.7×10^{-3} m/s to 1.2×10^{-2} m/s, 3×10^{-3} m/s to 1.2×10^{-2} m/s, 2×10^{-3} m/s to 1.2×10^{-2} m/s and 2×10^{-4} m/s to 4×10^{-3} m/s.

The calculated heads of the regional model of the LIFE project are used to specify the boundary conditions of the local model. Figure 5.10a shows the groundwater head distribution of the calibrated local model. As can be seen, the groundwater heads decrease globally from about 140 m to the southwest to about 135 m to the northeast. The simulated drawdowns at PW1 and PW2 after calibration of the local model show relatively good agreement with the measured drawdowns in the respective pumping wells. Figure 5.10b shows simulated drawdowns for the calibrated local groundwater flow model and the measured drawdowns at PW1 and PW2.

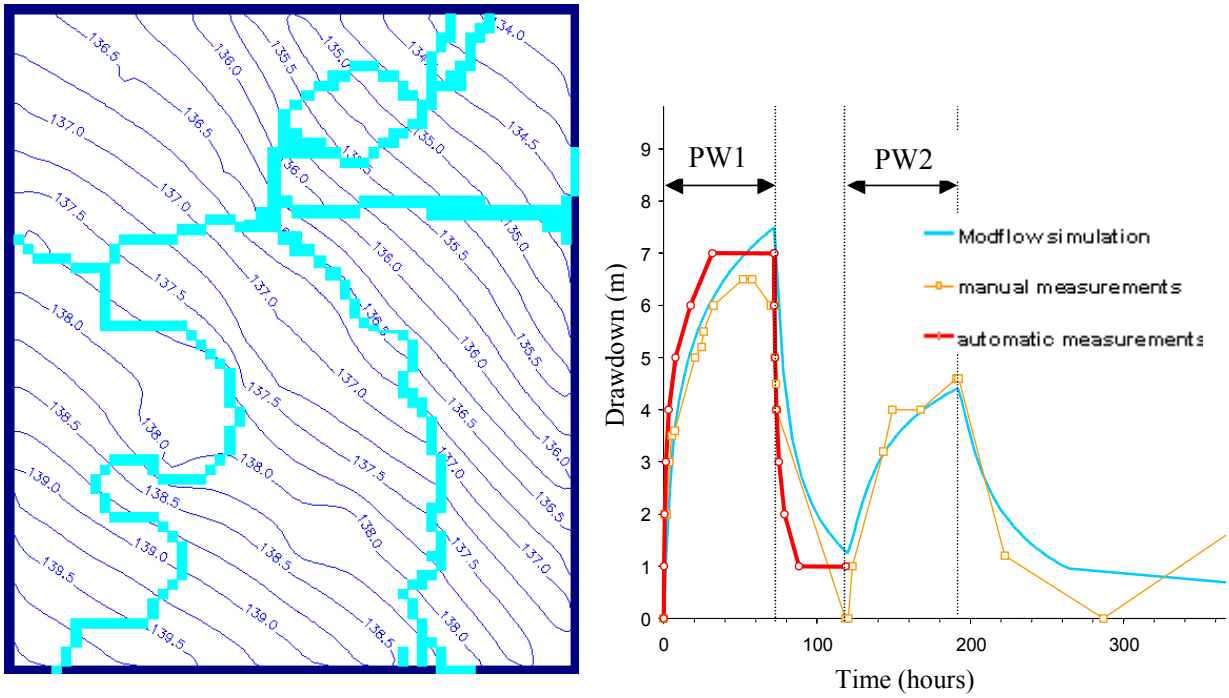

(a) (b)

Figure 5.10 Calibrated flow model for the local groundwater flow model: a) calculated groundwater head distribution (m), b) comparison of simulated drawdown and measured drawdown at monitoring well 701 (Source: Schäfer et al., 2004).

Therefore, the calibrated numerical flow model of the site Plaine des Bouchers is assumed to well represent the flow system of the study area.

5.5 Inversion of pumped concentration

5.5.1 Homogeneous case

In addition to the integral pumping test parameters presented previously in Table 5.1, the mean gradient ratio (MGR) for the contaminated site with PCE is also determined from the concentrations measured at the site *Plaine des Bouchers* during November/December 2000. The measured concentration values with the corresponding location of the monitoring wells in the national grid system is given in Appendix B1. The MGR is calculated as demonstrated earlier (see Chapter 3) using the directional averaged mean gradient ratio and taking PW2 position as a reference.

The longitudinal dispersivity of 10 meters with a dispersivity ratio of 0.1 is used to determine gradient adjusted mean concentration and mass flow rate. As both layers under consideration have the same hydraulic gradient and pumping tests were performed in the same period as that of the on-site concentration measurements, it is assumed that the MGR estimated around PW2 can similarly be used for the other layers. Thus, a MGR value of 0.85 was estimated and used for both layers where the concentration-time series data for the PCE was taken. In addition, for better evaluation of the well capture zone at the two pumping wells, the numerical model grid closer to the pumping wells is further refined to 1 m $\times$ 1m.

The well capture zone obtained after three days of pumping, using the numerical simulation of the transient flow field, shows nearly radial flow and the streamlines of the steady-state flow are straight (Figure 5.11). Thus, in the case when the capture zones are quasi circular in a radially dominated flow under homogeneous conditions and when streamlines are straight, the inversion can be made analytically or numerically. Previous studies suggest that the use of the analytical inversion at the study site can equally be applicable as the numerical inversion under homogeneous case with radially dominated flow field. In this case both the analytical inverse solution and VINMOD can be used.

Interfacing the analytical inverse solution (see Section 2.3.2, Chapter 2) and integrating the mean concentration gradient ratio (MGR) term discussed in Chapter 3, the analytical inversion code PINwin (Appendix A1) is used here to evaluate the effect of concentration gradient (Zeru and Schäfer, 2003b) at the site *Plaine des Bouchers* under homogeneous scenario with radially dominant flow. It should be noted here that the effect of the existing pumping well at PW2 is not taken into account while superimposing the streamlines with the well capture zones. The effect of the existing pumping well and the treatment of the streamtubes near the pumping well for use in the inversion of pumped concentration is described in the next section (Section 5.5.2).

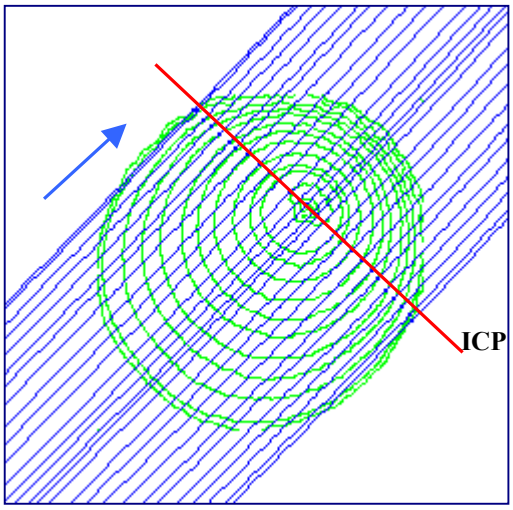

Figure 5.11 Superimposed well capture zones and streamlines for the homogeneous scenario (Example of the capture zones from PW2).

Figure 5.12 shows the inverted concentration distribution at the three layers under homogeneous scenario around the pumping wells PW1 and PW2. The concentration distribution from PW2 at the second layer is highly elevated compared to the other layers, which is in fact proportional to the input concentration-time series data used for the inversion. The oscillation of the inverted concentration distribution could be due to the non-linearity of the concentration time series data, the limits and the recursive nature of the inverse model itself.

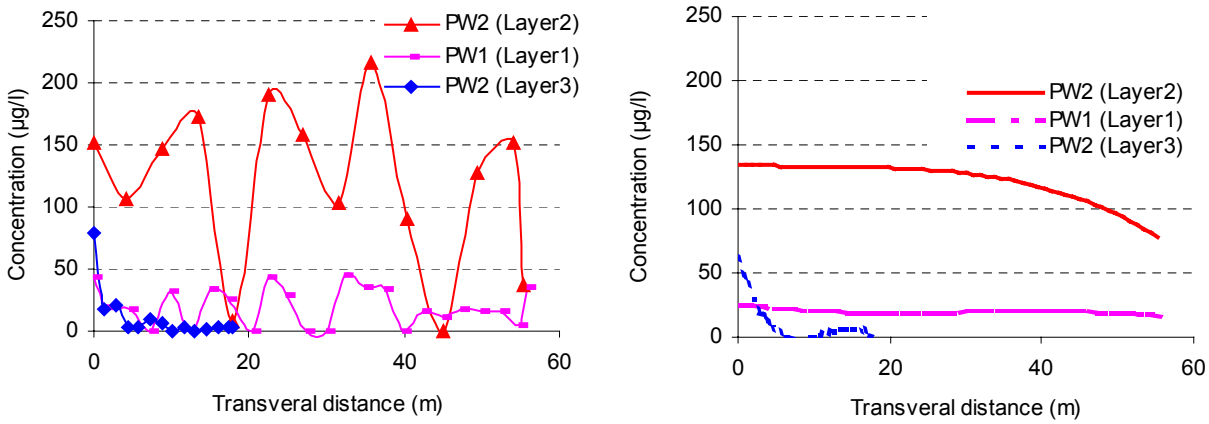

(a) (b)

Figure 5.12 Inverted concentration distributions: a) inverted concentration distributions, b) trend lines for the inverted concentration distributions.

Since the concentration-time series data obtained from the integral pumping shows fluctuation of the measured concentrations in the pumped water, it could then contribute to the oscillation of the inverted concentration distribution. In addition, since the inverse model requires the inverted concentration(s) of the preceding time(s) in order to calculate the concentration at the time under consideration, any deviations of the value(s) of the preceding concentration(s) can cause a sag or a peak in the inverted concentration distribution curve.

The calculated mean concentration and the corresponding mass flow rates at the predefined ICP for the three layers under consideration are presented in Figure 5.13. The estimated gradient ratio GR value is smaller than 1 and, therefore, the effect of concentration gradient on the calculated mass flow rate is less significant. For instance, the predicted total mass flow rate without the concentration gradient is about 203 grams per day whereas that of the gradient adjusted total mass flow rate is decreased only by about 5 per cent to 191 grams per day. This indicates that the ICP position used for the pumping tests is acceptable.

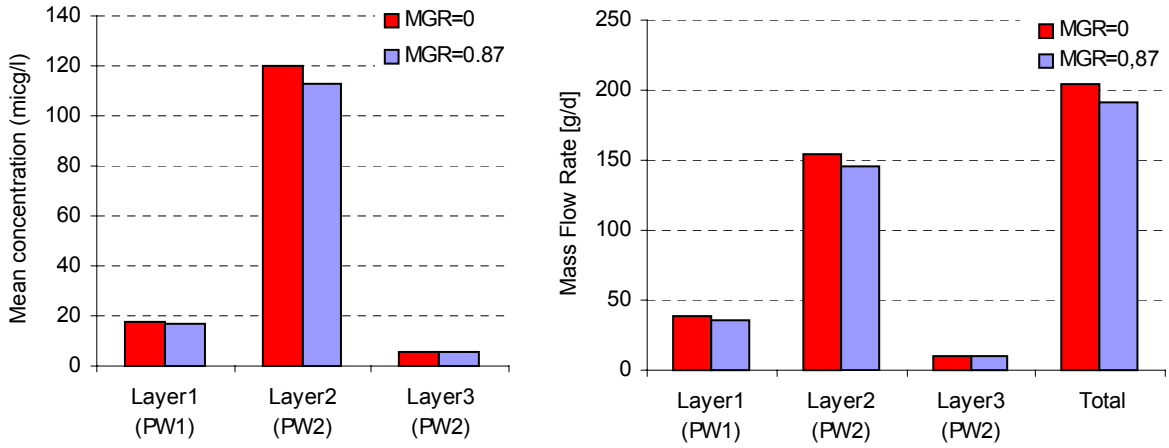

Figure 5.13 Mean concentration and corresponding mass flow rate in the respective layers.

However, it must be noted here that the real total mass flow rate which can be expected from the detected PCE plume can even be greater than the estimated value presented here. This is due to the fact that the two pumping test positions did not have capture zones covering the entire width of the ICP. The maximum capture width at the ICP for PW1 and PW2 is about 222 meters, leaving a gap of about 200 meters between the capture zones of the respective pumping wells.

5.5.2 Heterogeneous case

The permeability of the site at local scale, particularly in the vicinity of the pumping wells considered in this study, is not known. However, it is believed that highly permeable materials may exist around the study area and, therefore, it could be a source of uncertainty for the inversion of pumped concentration. Thus, in order to test the effect of local heterogeneity on the inverted concentration, the hydraulic conductivity around PW2 is modified based on the conceptual model proposed by the BRGM at Strasbourg (Personal Communication, Ph. Elsass) following a pattern of highly permeable blocks (Figure 5.14a) similar to the gravel pits with highly permeable layers observed at Hirtzfelden in Southern Alsace (Figure 5.14b).

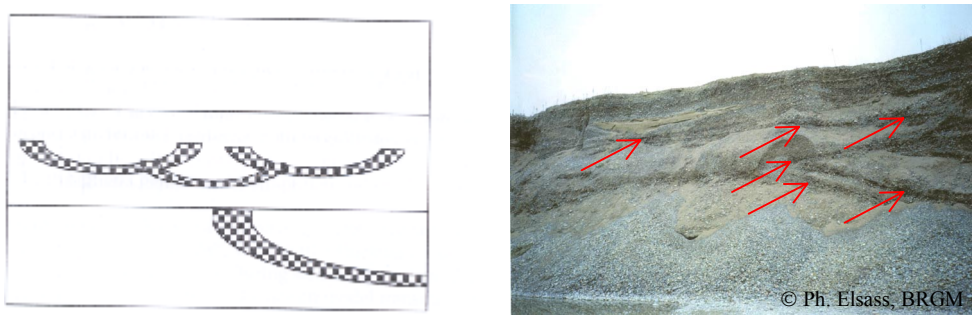

(a) (b)

Figure 5.14 Braided channel system representation: a) schematic representation of alternating channels, b) a gravel pit with highly permeable channels observed at *Hirtzfelden (source: Meijer, 2002)*

Beres and Huggenberger (1999) provided a generalized estimate on the relative dimensions such as on length-width and width-thickness proportion of braided channels as well as the spacing between them. Thus, using a length-width ratio of 2, different patterns of highly permeable blocks have been tested on the existing local groundwater flow model described in the preceding section. Figure 5.15 shows two conceptual models with highly permeable blocks around PW2 at the second layer of the finite difference numerical flow model.

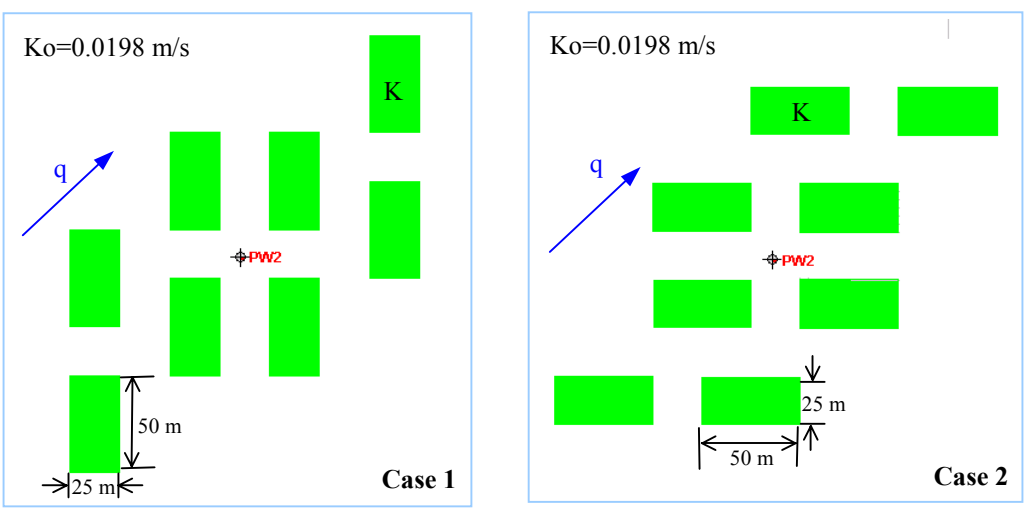

Figure 5.15 Conceptual model for highly permeable blocks used in the finite difference numerical flow model around the PW2 (case1: conceptual model 1; case 2: conceptual model 2).

The highly permeable blocks are set following the mean flow direction of the groundwater at the study site. The two orientations of the highly permeable blocks shown in the two conceptual models are used just to test the stability of the flow field after the modification of the permeability zone. The original mean hydraulic conductivity values of about 0.0198 m/s in each block is modified into a new hydraulic conductivity value K by a factor of 5, 10 and 20.

The drawdown values observed for the various permeability values of the two conceptual models (Figure 5.16) show that the simulated drawdown values after the introduction of the highly permeable blocks are almost the same as the measured drawdown value of about 7 cm that is shown in the numerical model calibration (see Section 5.4). In this case, the nearby monitoring well (N° 718) is used to observe the simulated drawdown.

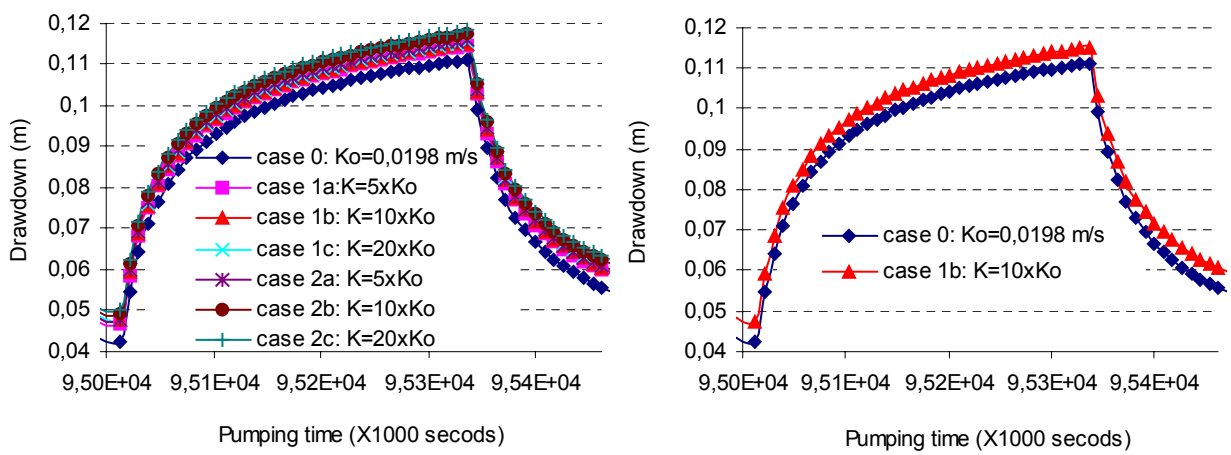

Figure 5.16 Comparison of simulated drawdown with measured drawdown: a) two conceptual models with six cases, b) one conceptual model with the selected case

The drawdown representing the original calibrated model is considered here as the original case (case 0). The other cases and corresponding indices refer to the conceptual model of the high permeability blocks and introduced hydraulic conductivity factors in each high permeability block. Therefore, for the demonstration purpose, the conceptual model with blocks oriented relatively towards the mean flow direction of the groundwater

(case 1) is considered and a hydraulic conductivity factor of 10 is used in the highly permeable block.

As shown in Figure 5.17, the resulting well capture zone and the streamlines are highly affected by the high permeability blocks introduced around PW2 in the local numerical flow model. As it can be seen in Figure 5.17a, the particles in the middle streamlines are captured by the existing pumping well at the site which has always been in operation, before and during the integral pumping test operation, at the rate of about 18 cubic meters per second. In the case when there are discontinuities of the streamtubes, as a result of the discontinuous middle streamlines caused by the abstraction of existing wells, it becomes inconvenient to implement the method of inversion of pumped concentration with the current models presented in this study. Thus, in order to get continuous streamtubes, the middle streamlines are removed in the way that a streamtube common to the replaced streamtubes can be obtained (Figure 5.17b).

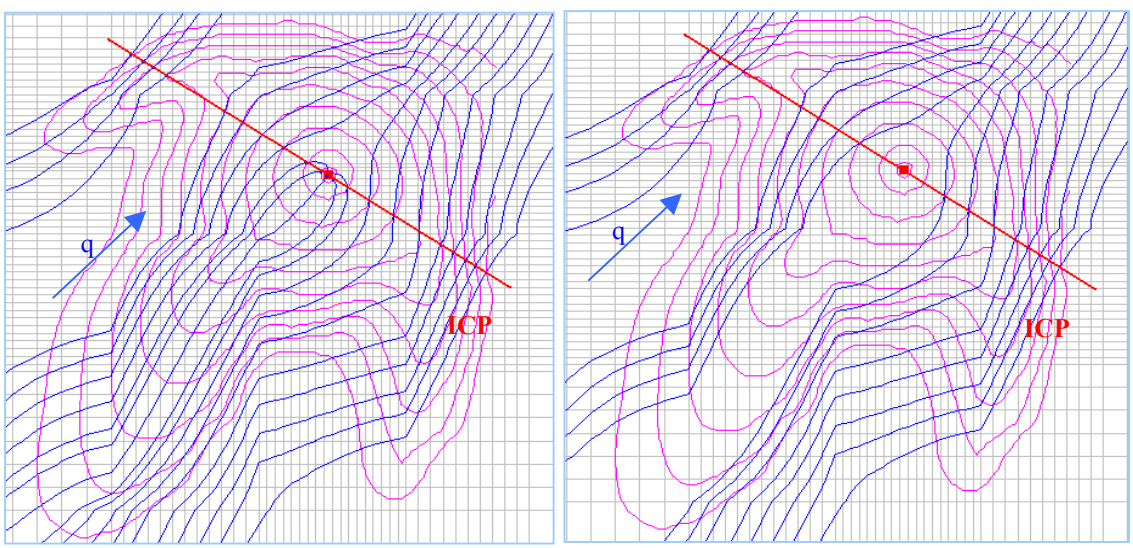

(a) (b)

Figure 5.17 The capture zones of the pumping well PW2 at the second layer in the presence of high permeability blocks: a) with middle streamlines, b) after the middle streamlines are removed.

However, while removing the middle streamtubes, it should be noted that the concentration values and the corresponding pore velocities for each isochrone within the modified streamtube need to be updated. In this particular study, a distance weighted

method is employed to get the mean concentration and pore velocity values for the modified middle streamtube. The areas of the streamtubes in the capture zone needed for VINMOD are digitized and calculated using OS Digitizer. Since overlapping of streamtube areas are observed, inclusions and exclusions are employed as described in Chapter 4 (see Section 4.3.3).

The concentration-time series data provided in the preceding section for PW2 (see Section 5.3) is used for the numerical inversion of pumped concentration with VINMOD in heterogeneous conditions. Figure 5.18 shows the concentration-time series data and the inverted concentration distribution. Due to the very narrow interval in the concentration-time series data for the last few isochrones, only the first 10 data points (Figure 5.17a) are used for the numerical inversion with VINMOD. Since the pumped concentrations of the inner isochrones, where the middle streamtubes are removed, are interpolated into one mean value, the inverted concentration distribution curve closer to the pumping well shows a relatively flat value.

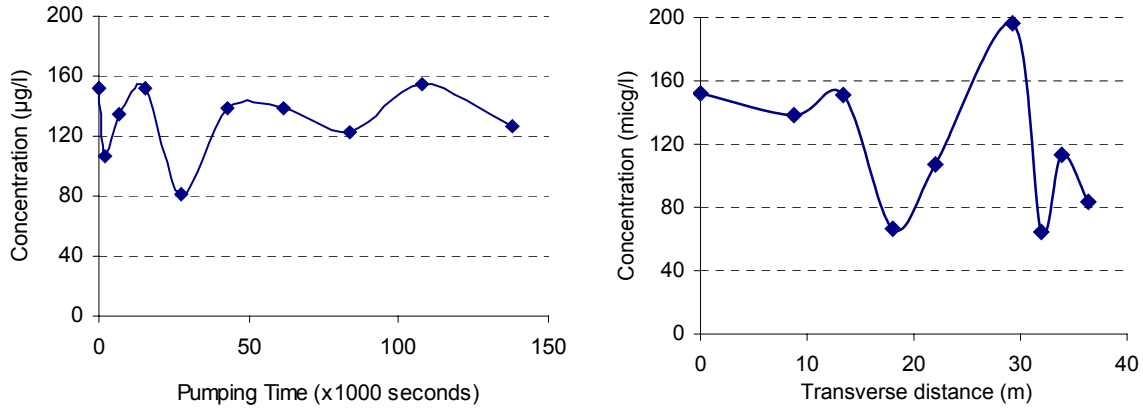

Figure 5.18 a) Concentration-time series data from PW2, b) numerically inverted concentration distribution with VINMOD

The inverted concentration distribution under heterogeneous condition shows logical trend with respect to the input concentration-time series data. However, a comparison test with a homogeneous equivalent capture zone, assuming radially circular well capture

zones, shows that the inverted concentration distribution for the homogeneous case oscillates by large compared with the heterogeneous case (Figure 5.19). Such high oscillation could be induced by the mass loss or gain due to the non-linearity of the concentration-time series data while, at the same time, the capture zone in the homogeneous case is simplified by circular isochrones. For the capture zone in heterogeneous media, the contaminant masses in the concentration-time series data could be adjusted by the corresponding capture volumes that may vary depending on the state of the permeability. As a result, the inverted concentration distribution under heterogeneous condition oscillates less than that of the homogeneous case.

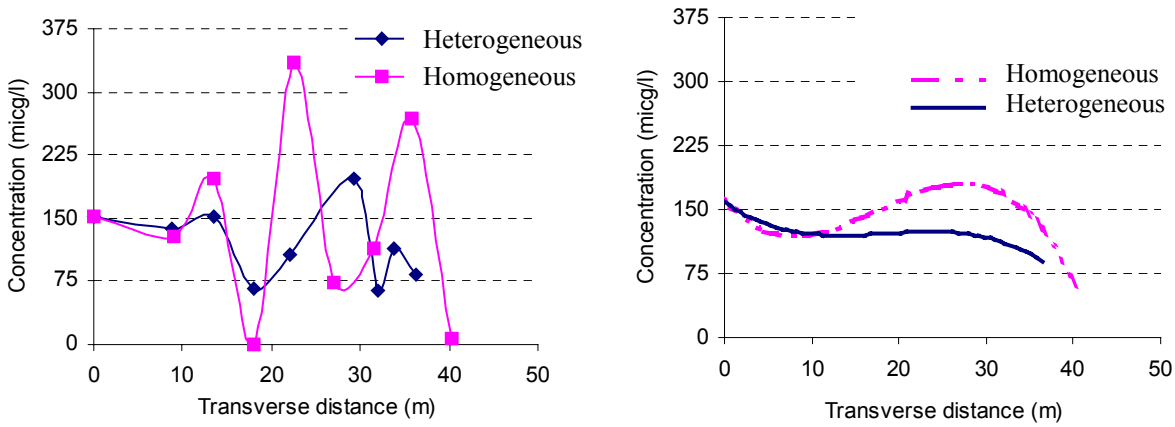

(a) (b)

Figure 5.19 Comparison of the inverted concentration distribution with VINMOD for the heterogeneous case under consideration and the homogeneous case with simplified circular capture zone: a) inverted concentration distribution curves, b) trend lines of the inverted concentration distributions.

If the non-linearity of the concentration-time series data is related to the heterogeneous concentration distribution in the contaminant plume, it can be inferred from here that the choice for using VINMOD, whether to use an irregular capture zone as a result of local heterogeneity or a simplified homogeneous equivalent circular capture zone, can be made by evaluating the linearity of the concentration time series data profile (see Figure 4.14).

Figure 5.20 shows the effect of the introduced high permeability blocks on the calculated mean concentration and the total mass flow rate. For instance, the irregular well capture zones used in the numerical inversion results in a reduction of the mean concentration by about 18 % relative to the equivalent homogeneous case with circular capture zone. On the other hand, a high rise in the total mass flow rate is observed. As can be seen, the mass flow rate after the introduction of the high permeability blocks in the vicinity of the pumping well PW2 induced an increase of the total mass flow rate by about two times the value that could otherwise be calculated from the reference homogeneous case with radially circular capture zone assumption.

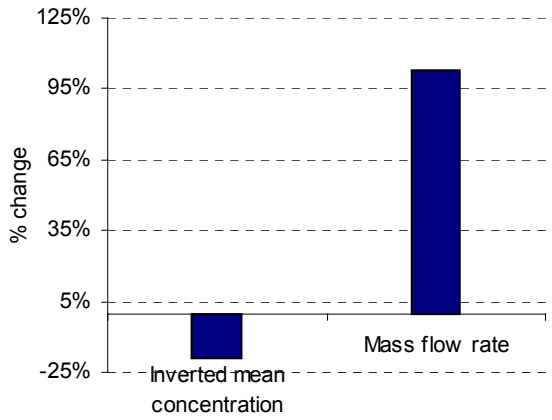

Figure 5.20 An example demonstrating the effect of local heterogeneity on the inverted concentration and the mass flow rate relative to a reference homogeneous case with circular capture zone.

As it was noticed in the preceding chapter (Chapter 4), the significant increase of the total mass flow rate is influenced by the groundwater flow velocity profile at the ICP. Figure 5.21 shows that the groundwater flow velocity profile at the ICP, after the introduction of the high permeability blocks around the pumping well PW2, is significantly higher than that of the reference homogeneous case. Thus, the groundwater flow velocity profile at the ICP is an important parameter which can significantly influence the total mass flow rate that can be calculated at the same ICP.

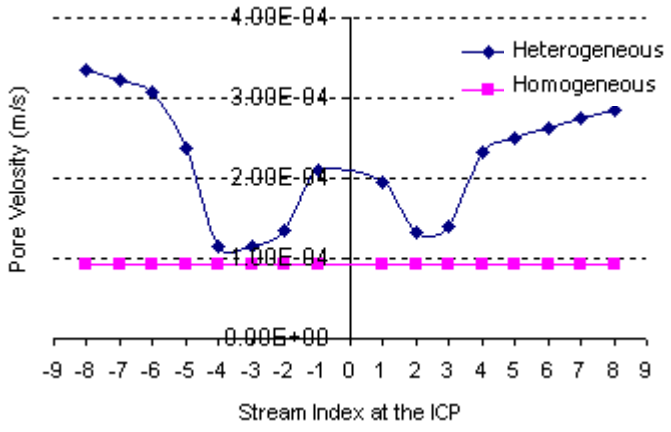

Figure 5.21 Comparison of groundwater flow velocity profile at the ICP for the heterogeneous case under consideration and the equivalent homogenous case.

Due to the lack of detailed information about the presence of local heterogeneity at the study site under consideration, the result of this study related to the heterogeneity should not be attributed to the real situations of the site. However, this test study demonstrates that the effect of local heterogeneity is significantly important on the determination of the state of groundwater pollution with the inversion of pumped concentration.

Therefore, whenever detailed information on the local heterogeneity pattern is known at the study site under consideration, the state of groundwater pollution at the site could be varied from the interpretations that can be made from the homogeneous assumption. If high permeability zone exists around the detected PCE plume, it can be inferred that the real mass flow rate at the study site could be greater than the one calculated with the homogeneous case.

5.6 Summary

The inversion of pumped concentration is applied at the industrial site *Plaine des Bouchers* by taking into account the effect of the concentration gradient in the PCE

plume and the presence of local heterogeneities. The field data obtained during the integral pumping test at the study site is used for this application study.

The effect of a concentration gradient in the plume is tested in a homogeneous aquifer scenario using two pumping well settings PW1 and PW2. The calibrated numerical flow model of the study site is used to support the inversion of pumped concentration both in the homogeneous and heterogeneous assumptions. For the homogeneous scenario, the calculated total mass flow rate from the pumping test settings using two pumping wells (PW1 and PW2) at three aquifer layers, is about 203 grams per day. The inverted concentration from the concentration-time series calculated for PW2 at the second layer shows the highest proportion of the calculated mass flow rate with a value of about 155 grams per day. In both cases, an estimated mean gradient ratio (MGR) of 0.85 shows the presence of a weak concentration gradient and contributes only little reduction of the calculated mass flow rate by about 5 %.

Further evaluation on the effect of local heterogeneity is demonstrated on the PW2 field data by introducing high permeability blocks based on the chosen conceptual model imitating the highly permeable braided channels around the study area. With the introduction of the high permeability field, the geometry of the well capture zones contributed a reduction in the mean concentration by about 18 % relative to the equivalent homogeneous case with radially circular capture zone. However, the total mass flow rate calculated at the chosen ICP is increased by one fold. The higher increase of the total mass flow rate is attributed to the magnitude of the groundwater flow velocity profile at the ICP. Due to the lack of precise information on the local heterogeneity, the conceptual model used for the chosen pattern of hydraulic conductivity blocks around the pumping well is used for demonstration purpose only.

However, this study demonstrates that whenever detailed information on the local heterogeneity pattern is known at the study site under consideration, the state of groundwater pollution at the site could vary from the interpretations that can be made from the homogeneous case assumptions. If high permeability zones exist around the

detected PCE plume, it can be inferred that the real mass flow rate at the study site could be greater than the one calculated previously with the homogeneous aquifer assumption.

Conclusions and Perspectives

Conclusions and Perspectives

Conclusions:

The ever growing and increasing diversities of industrial activities have been a threat to the underlying groundwater reserves in many industrial areas. Industrial waste discharges, accidental spills, and leaks of petroleum products are some of the many sources of industrial zone groundwater contamination. Among others, chlorinated solvents are toxic chemicals that are known to be the most common groundwater contaminants of industrial origin found. Exposure to these chemicals may cause serious health problems to humans and the natural environment.

In the case when groundwater contamination is detected, it becomes essential to determine the extent, level and source of contamination. The inversion of pumped concentration, a novel approach involving the inversion of the pumped groundwater quality data, in this case the concentration-time series data, can be used as an alternative and/or complementary method for groundwater pollution evaluation. This approach is particularly important when there are no enough point measurements and can be applied to both cases of known and unknown sources of contamination.

The method of the inversion of pumped concentration was initially applied at the industrial site *Plaine de Bouchers* in Strasbourg in order to quantify the mean concentration and the mass flow rate of PCE in the groundwater, assuming that the concentration gradient in the longitudinal axis of the plume is constant and the aquifer at the real site is a homogeneous and isotropic porous medium. Therefore, this study has focused on some of the elements such as the concentration gradient and local heterogeneity that were not considered previously and could be sources of uncertainties while applying the method of inversion of pumped concentration.

Inversion of pumped concentration with presence of concentration gradient in the plume:

The experience of this study shows that if concentration-time series measurements are taken around the very tail of the plume, the effect of a longitudinal gradient relative to the transverse gradient, expressed in terms of a mean gradient ratio (MGR), on the inverted concentration distribution is very significant and the associated error is proportionally high. This results in an overestimation of the real concentration distribution and of the corresponding mass flow rate at the predefined imaginary control plane (ICP). For instance, in this particular study, a mean gradient ratio (MGR) of 3 or more can induce an error of more than 50 %, leading to an overestimation of the real concentration distribution and of the corresponding mass flow rate by more than 50 %. A MGR of less than or equal to 1 causes only about 5 % error, which provides an acceptable range for determining the inverted concentration distribution and the total mass flow rate even though the error that might be encountered depends also on the dispersivity values.

In the case of a contaminant plume under higher dispersivity condition, the method of the inversion of pumped concentration can result in an underestimation of the real concentration distribution. For instance, assuming a dispersivity ratio of 10 %, the inversion of pumped concentration from aquifer materials with dispersivity values greater than 15 meters can result in underestimated values relative to the real concentration distribution and the corresponding mass flow rate. Underestimation of the actual concentration implies higher risk from the environmental and health issues context and, therefore, special care should be taken while making a decision from using the method of the inversion of pumped concentration in highly dispersive aquifer materials.

It should be noted, however, that the adjusted mass flow rate does not necessarily represent the "actual" mass flow from the detected plume. The relatively maximum value for the total mass flow rate depends on the ICP-Pump position which in turn determines the magnitude of the mean gradient ratio as well as the dispersivity values. Relatively minimum mean gradient ratio (MGR), closer to zero, can be obtained for an ICP that is

positioned towards the suspected source of contamination. For a contaminant plume with unknown source and without additional point measurements in the longitudinal and transverse direction, locating an ICP-Pump position by trial and error where a gradient ratio is closer to zero may be practically difficult. Nevertheless, results can be improved or errors can be minimized by considering the relatively closest ICP-Pump position from the suspected source.

The overall experience with regard to the effect of concentration show that the method of inversion of pumped concentration for groundwater pollution analysis can provide reasonable estimates in the case when the mean gradient ratio is correspondingly low (MGR < 1) and the dispersivity values are relatively low such as for longitudinal dispersivity values of less than 15 meters.

Inversion of pumped concentration with the presence of local heterogeneities:

In many cases the real geo-hydrological systems are complex and, therefore, the aquifer can be considered as heterogeneous. In this case, the method of inversion of pumped concentration can be approached numerically. A **v**olume based **in**verse **mod**el (VINMOD) is developed and used for the numerical inversion of pumped concentration by taking into account heterogeneity within the entire well capture zone.

It has been noticed that, due to the presence of heterogeneity, VINMOD is very sensitive to the groundwater flow velocity variations within the streamtubes of a plume under consideration. The geometry of the well capture zone with local heterogeneity showed slight change on the value of the mean of the inverted concentration distribution relative to that of the circular capture zone with homogeneous model set up. However, the groundwater velocity profile at the ICP can strongly influence the corresponding total mass flow rate that can be calculated at the same ICP. Thus, with the presence of local heterogeneity, numerical inversion of pumped concentration can be appropriate.

It should be noted here that, while employing numerical inversion of pumped concentration with VINMOD, any deviation of the values of the streamtube areas from the theoretical values, added to the recursive nature of the inverse solution, can cause oscillation of the concentration distribution. In addition, the accuracy of the streamtube areas can be affected by errors associated with digitization and the grid resolution of the numerical model itself. Digitization errors by using OS Digitizer are in general less significant and are, on the average, in the range of 2 - 3 %. However, errors associated with the grid resolution of the numerical model affect the size of the well capture zone which in turn results in faulty values on the streamtube area that can be calculated. The higher the resolution of the model grid, for instance 1 m by 1 m, the better the streamtube area that can be obtained.

Application at the industrial site Plaine des Bouchers:

By taking into account the concentration gradient in the PCE plume and local heterogeneities, the inversion of pumped concentration is applied at the industrial site Plaine des Bouchers where significant PCE contamination has been detected. In this case, the effect of concentration gradient in the plume is tested under homogeneous aquifer scenario using two pumping well settings PW1 and PW2. The calculated total mass flow rate from the pumping test settings using two pumping wells (PW1 and PW2) at three aquifer layers is about 203 grams per day. The inverted concentration from the concentration-time series calculated for PW2 at the second layer shows higher proportion of the calculated mass flow rate with a value of about 155 grams per day. In both cases, an estimated mean gradient ratio (MGR) of 0.85 shows the presence of weak concentration gradient and contributes only little reduction of the calculated mass flow rate by about 5 %.

Further evaluation of the effect of local heterogeneity is demonstrated on the PW2 field data by introducing high permeability blocks based on the chosen conceptual model that represents schematically highly permeable braided channels around the study area. With

the introduction of the high permeability field, the geometry of the well capture zones contributed a reduction of the mean concentration by about 18 % relative to the equivalent homogeneous case with radially circular capture zone. However, the total mass flow rate calculated at the chosen ICP is increased by about one fold. The higher increase of the total mass flow rate is attributed to the magnitude of the groundwater flow velocity profile at the ICP. Due to the lack of precise information on the local heterogeneity, the conceptual model used for the chosen pattern of hydraulic conductivity blocks around the pumping well is used for demonstration purpose only.

This study demonstrates that whenever detailed information on the local heterogeneity pattern is known at the study site under consideration, the total mass flow rate for determining the state of groundwater pollution at the site could vary from the one that was calculated under homogeneous assumptions. If high permeability zones exist around the detected PCE plume, it can be inferred that the previously calculated total mass flow rate at the site could be underestimated, assuming that the flow velocity of the groundwater influences more the total mass flow rate that can be calculated.

Though this study has focussed on single well systems with symmetrical plume relative to the pumping well position, both the effect of the concentration gradient as well as the presence of local heterogeneities on the inversion of pumped concentration described above can be extended to multiple pumping well systems as well. Some of the technical considerations of the inversion of pumped concentration for field applications are:

- The inversion of pumped concentration from an asymmetrical plume may require a new solution through, for instance, coupling of the inverse solution provided for a single well.
- In the case when multiple wells are to be applied under field conditions, simultaneous pumping can be advisable so as to minimize possible displacement of the contaminant plume.

- In the case of heterogeneous media, the settings of the pumping wells may need to be designed in a way that the respective capture zones are closer or overlapping to each other for better quantification of the underlying groundwater contaminant.
- In the case of shallow aquifers with very low hydraulic conductivity, for instance with a hydraulic conductivity value less than 10^{-5} m/s, the use of the inversion of pumped concentration can be less feasible. For very low permeable aquifers, the pumping well needs to be designed in a way that drying up of the well should be avoided. In this case, a very small well discharge may be required, which can in fact make the method of inversion of pumped concentration time consuming and costly.
- In the case of contaminant plumes with a vertical concentration gradient, concentration measurements down the vertical are preferable so that relatively representative depth averaged concentration values can be used in the concentration-time series data. For instance, the vertical concentration distribution can be estimated with multilevel sampling. As such, estimated concentration distribution values can then be used for statistical treatment in the event of averaging or extracting a representative concentration of a given grid cell.

Perspectives:

For broader use and application of the inversion of pumped concentration, some other elements such as the effect of source stratification, biodegradation of dissolved contaminant, the geometry of the imaginary control plane (ICP) relative to the presence of local heterogeneity can be possible research segments in the future. In addition, the method of source localization such as with backtracking that can either be integrated or inherent to the method of inversion of pumped concentration can provide a relatively complete tool for groundwater pollution analysis.

Apart this, an integral pumping test in the industrial sector of Dreieckland, a transborder region between France, Germany and Switzerland, is proposed to be applied under a R&D project with the partnership of AERM, BRGM, IMFS-IFARE, and ADEME.

Appendices

Appendix A1: PINwin v1.2.4 - Applications, features, and short guide

PINwin: Pump and Inverse for windows
Version : 1.2.4, December 2002
Platform/operating system : Windows 95/98 or NT/2000/XP
Program language: Salford Fortran 95 (GUI with Clearwin 6)
Developer : Allelign Zeru
Availability : PINwin can be available up on request
Contact (Email) : zeru@imfs.u-strasbg.fr or azeru@yahoo.com

Applications/Features:

PINwin is used as a tool for groundwater pollution analysis based on a concept involving the inversion of the concentration-time series data that can be obtained during conventional pumping tests. It can be used in case of known or unknown sources of contamination. It is based on the analytical inversion solution (see Section 2.2.4) that can only be applicable for homogeneous aquifer with radially circular well capture zones. Figure A1.1 shows a screen shot summary of the graphical interface of PINwin.

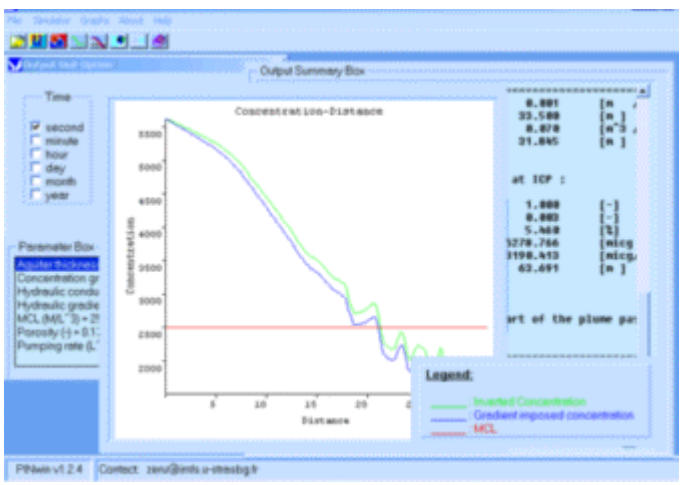

Figure A1.1 Screen shot summary of PINwin graphical interface

PINwin simulates the contaminant concentration distribution and the corresponding total mass flow rate at a predefined control plane (ICP), imaginary plane located perpendicular to the main groundwater flow direction, based on concentration-time series data measurements from a real site. From a site specific gradient ratio value, the mean concentration and the total mass flow rate can be recalculated by taking into account the concentration gradient in the plume. PINwin has graphical interface for parameter inputs, output display, output curves, output unit conversion, online and interactive help, internet

and email features for update news and technical support. The parameter input and output display units are structured in the way that any sensitivity studies on the input parameters can easily be evaluated with PINwin.

A brief guide for using PINwin with practical implementation of the integral pumping test is provided below, as extracted and updated from Zeru and Schäfer (2003b).

Quick guide:

For the inversion of pumped concentration with PINwin, a pumping well with appropriate ICP position needs to be defined in the way that it is perpendicular to the mean groundwater flow direction. If horizontal position of a plume is not known, one should carryout multiple pumping tests at the point where contamination is detected.

Step1: Implementation of Integral Pumping Test:

1. Take initial concentration samples at any detected points, particularly in the pumping well(s) where future integral pumping test can be made.

   Check whether there is the possibility to measure any variation of concentration along the vertical profile, such as availability of measuring devices. If yes, see step **1a**. if no, see step **1b** :

   Step **1a**.

   Apply multilevel sampling and analyze concentration data structure along the vertical depth. In this case, if there is high variability on the data structure, one needs to take samples at a depth where such higher concentration value is measured. Thus, integral pumping test with simultaneous sampling, at the depth where higher concentration is observed, can be performed.

   If no significant variability on the data structure, consider step **1b**

   Step **1b**.

   Use traditional integral pumping test, i.e. without multilevel sampling. In this case, concentration measurements will be made from the water samples taken during the integral pumping test. Therefore, the assumption here is the concentration along the vertical depth is somehow constant and uniformly mixed with the sampled water.

Step 2: Preparing input data for PINwin:

2. In the case of **1a** or **1b**, whichever comes out, prepare concentration-time series data for the analytical inversion. The general format of the concentration data series for use in PINwin is a "*.txt" or "*.dat" file format with two column each for the time and measured concentration. The concentration-time series data can be prepared in any one of the formats shown below, for instance Format 1 or Format 2. The first format shows the concentration-time series data extracted from a long-time series data where as the second format shows the concentration-time series data record from the initial time t=0. For a wrong formatted file or empty file, the user will be prompted with the associated error messages.

Format 1

9.467E+07	5527.829
9.468E+07	5048.227
9.469E+07	4808.672
9.47E+07	4593.449
9.471E+07	4444.405
9.472E+07	4198.981
9.473E+07	4142.262
9.474E+07	3946.144
9.475E+07	3886.625
9.476E+07	3781.639
9.477E+07	3756.523
9.478E+07	3587.013
9.479E+07	3483.876
9.48E+07	3413.413
9.481E+07	3375.348
9.482E+07	3258.085
9.483E+07	3185.904
9.484E+07	3227.039

Format 2

0	5645.446
1.000E+04	5138.428
2.000E+04	4873.165
3.000E+04	4676.777
4.000E+04	4538.396
5.000E+04	4370.923
6.000E+04	4248.175
7.000E+04	4167.732
8.000E+04	4007.584
9.000E+04	3859.224
1.000E+05	3790.325
1.100E+05	3715.289
1.200E+05	3641.353
1.300E+05	3496.736
1.400E+05	3530.966
1.500E+05	3361.739
1.600E+05	3355.933
1.700E+05	3302.118

Step 3: Prepare other input parameters

3. Prepare the input parameters such as the hydraulic conductivity, hydraulic gradient, porosity, pumping rate, aquifer thickness, and site specific mean gradient ratio (MGR).

   If there is measured concentration data in the flow (x) and transverse (y) direction near the pumping well, then follow steps **3a** & **3b** or steps **3a** & **3c**:

   Step **3a** : calculate the mean concentration gradient ratio (MGR), the ratio of the longitudinal concentration gradient to the transverse concentration gradient:

$$MGR = \frac{\partial c / \partial x}{\partial c / \partial y} \tag{A1.1}$$

Step **3b**

Based on the calculated GR, possible errors can be estimated by PINwin based on the experimental graph presented in Figure 3.20a (see Section 3.3.4, Chapter 3). More errors can be expected if the ICP-Pump is positioned somewhere at the tail of a plume. Therefore, if there is an optional pumping well located upstream on the same flow axis, it is advisable to use the closest pumping well to the suspected source.

Step **3c**

If step **3b** is not considered, given estimated values of the mean gradient ratio in the parameter input field of PINwin, the corresponding errors that can be encountered due to the presence of concentration gradient can be calculated with PINwin based on the on Equation 3.15 (see Section 3.3.4, Chapter 3).

If there is no measured concentration data in the flow (x) and transverse (y) direction, i.e. if the mean gradient ratio can not be estimated, then to step **3d**:

Step **3d**

Accept the zero gradient (in the longitudinal direction for the inverted mean concentration distribution as a worst case scenario especially from the view point of possible remediation plan. In this case, the error is assumed to be zero.

Step 4: determine concentration distribution and mass flow rate

4. PINwin calculates the concentration distribution, mean concentration and the total mass flow rate at the predefined ICP based on Equation 2.5 (see Section 2.2.4, Chapter 2) and Equation 3.17 (see Section 3.3.4, Chapter 3) respectively. Figure A1.2 shows an example of the outputs for the inverted concentration distribution, mean concentration, total mass flow rate, etc (Figure A1.2a), and the graphical out put for the inverted concentration distribution curve (Figure A1.2b).

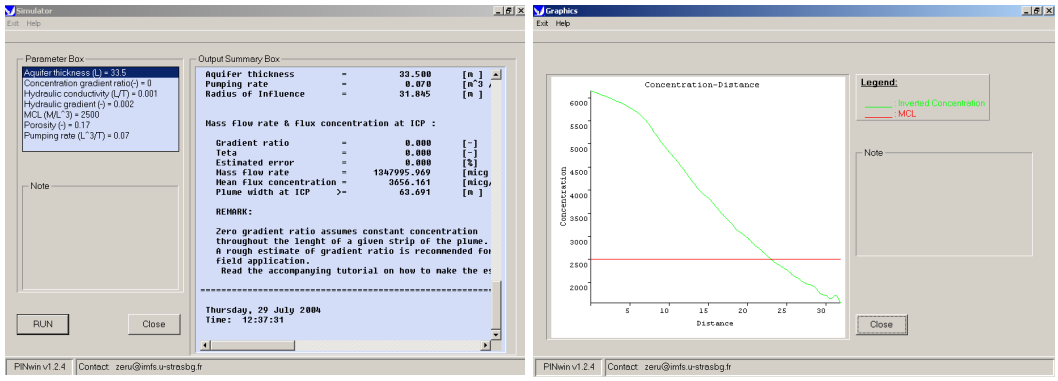

(a) (b)

Figure A1.2 Examples on the outputs from PINwin run: a) parameter input and simulation outputs, b) graphical output for the inverted concentration distribution.

Appendix A2: OS Digitizer v1.0 - Applications, features, and short guide

OS Digitizer: On-screen digitizer
Version 1.0; February 2004
Platform/operating system: Windows 95/98/NT/2000/XP
Program language: Visual Basic 6.0
Developer: Allelign Zeru
Availability: OS Digitizer can be available up on request
Contact (Email): zeru@imfs.u-strasbg.fr or azeru@yahoo.com

Applications/Features:

OS Digitizer (On-Screen Digitizer) is a tool for digitizing irregular surfaces and calculating corresponding areas. Figure A2.1 shows the graphical interface of OS Digitizer. OS Digitizer can also be used to load particles positions for well capture zone delineation based on the output of the particle tracking numerical code MODPATH. In this case, individual well capture zone can be loaded and corresponding capture area can also be calculated (Figure A2.2). It has features for loading maps, saving and loading areas and particle positions with the corresponding enclosed object geometry.

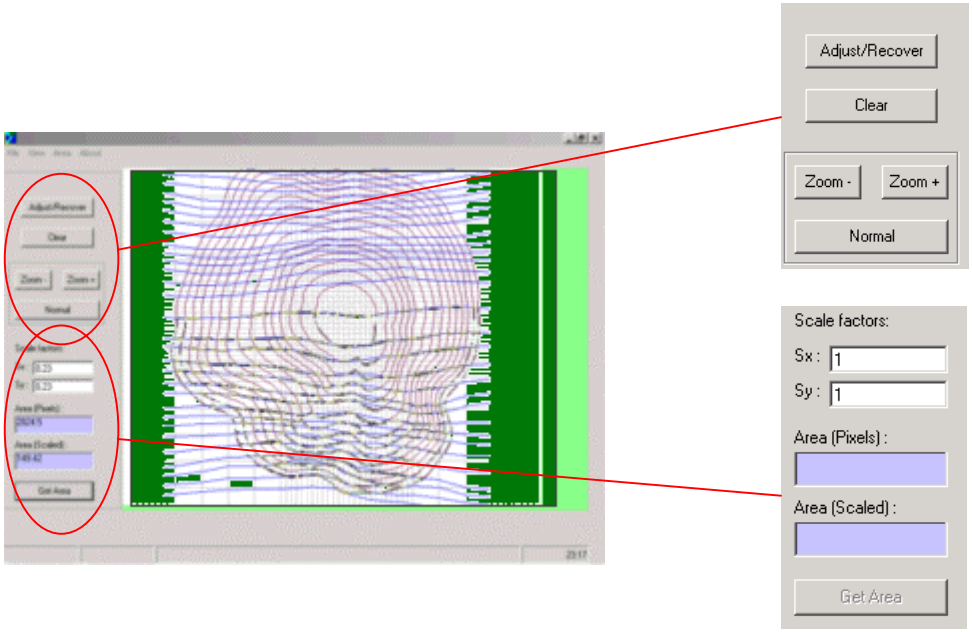

Figure A2.1 The OS Digitizer graphical interface

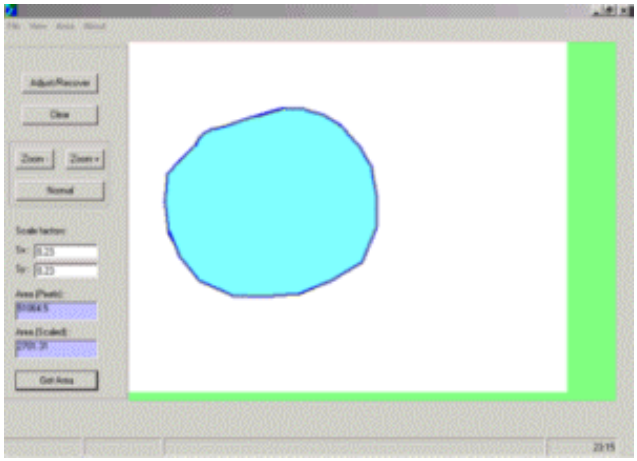

Figure A2.2 An example of a well capture zone loaded and delineated from backtracked particle positions with MODPATH

Method:

OS Digitizer calculates the area of a given closed, but non-crossing, surface based on the polygon method. Given a polygon with n sides, its area can be calculated based on the areas of the polygons surrounding the sides of the polygon under consideration. For instance, a polygon with n sides is surrounded by n polygons. The area A of the shaded polygon in Figure A2.2 is simply the sum of the areas of the polygons bordering the upper face of the shaded polygon minus the sum of the areas of the polygons bordering the lower face of the polygon.

$$\begin{aligned} &A(ABCDE) = \\ &\left[A(ABX_2X_1) + A(BCX_4X_2) + A(CDX_5X_3)\right] \\ &-\left[A(DX_5X_3E + A(EX_3X_1A)\right] \end{aligned} \tag{A2.1}$$

Given a polygon with *n* vertices (i.e. with *n* sides) in the Cartesian coordinate plane with X and Y axes, the generalized formulation for the area of an enclosed surface defined by a polygon is :

$$A = \frac{1}{2}\sum_{i=1}^{n}(X_i \times Y_{i+1} - X_{i+1}Y_i) \tag{A2.2}$$

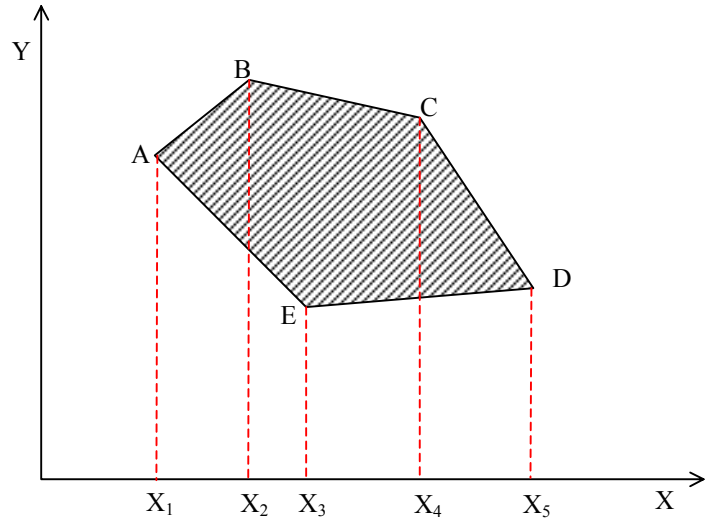

Figure A2.3 Demonstration of polygon method for calculating an enclosed surface.

Quick guide:

The OS Digitizer main menu is ready for digitization if one needs to digitize any kind of polygon or enclosed object as shown in Figure A2.4a. In this case, the vertices of the polygon can be saved or opened for latter use. If an object or a map is to be digitized, the image with bmp file format can be opened using the Load Image in the File menu (Figure A2.4b). OS Digitizer provides up to 18 levels for zoom in and zoom out features.

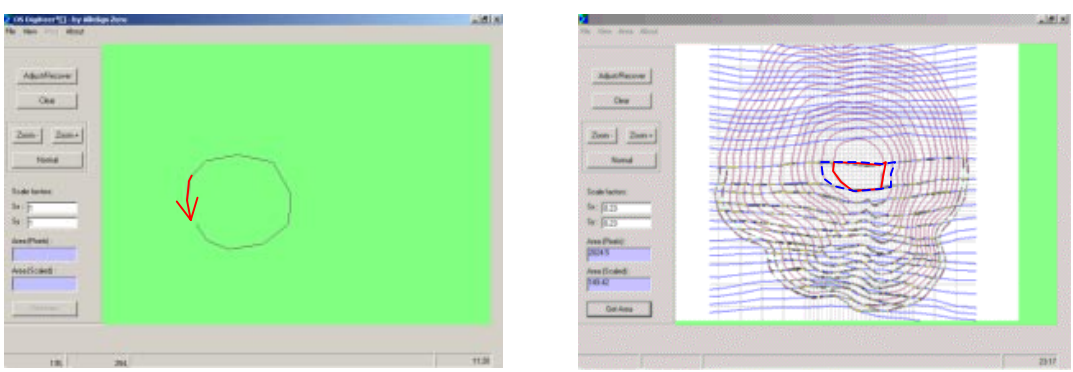

(a) (b)

Figure A2.4 Example of digitization with OS digitizer

The digitization can be performed my pressing the left mouse at the starting point, moving and single clicking until the final point. The active digitized line can be terminated by right clicking. Both clockwise or counter clockwise directions are possible directions of digitizing. Once the digitization is terminated, OS Digitizer calculates the area of the enclosed surface in terms of pixel areas. Thus, user defined scale factor s should be provided to calculate the real area.

$$S_x = \frac{MX_2 - MX_2}{PX_2 - PX_1} \tag{A2.3}$$

$$S_y = \frac{MY_2 - MY_2}{PY_2 - PY_1} \tag{A2.4}$$

Where s_x [-] and s_y [-] are scale factors in the x and y directions respectively , MX [L] and MY [L] are sample x and y distances on the map or image to be digitized in the respective directions, PX [L] and PY [L] are the equivalent distances on the screen as digitized from the opened image. Once the scale factors are given, the real area can be calculated by pressing the "Get Area" button (Figure A2.5). By default the respective scale factors are 1. In this case, the on-screen digitized area is equal to the scaled area.

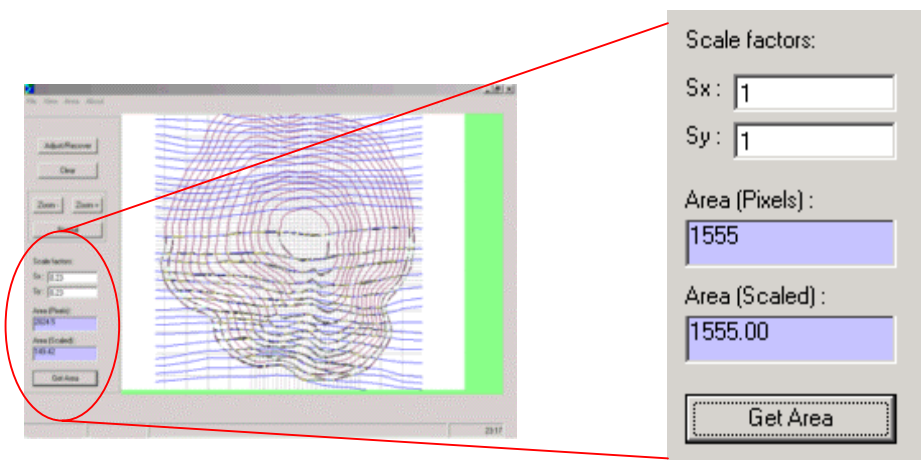

Figure A2.5 Demonstration of input and output fields

Digitized streamtube areas need to be arranged manually with the format that can be read by VINMOD. For instance, given 5 isochrones, the format of the file that needs to be prepared for VINMOD is shown bellow. Where **AL** and **AR** columns are for the

streamtube areas on the left and right sides of the pumping well respectively; **SI** and **TI** represents the streamtube index and the time index respectively.

AL [L^2]	**AR [L^2]**	**SI [-]**	**TI [-]**
115.755	115.755	1	1
199.77	199.77	1	2
87.2	78.42	2	2
227	227	1	3
137	143.55	2	3
95.68	76.36	3	3
365.5	365.5	1	4
179.65	187.25	2	4
146.25	133.6	3	4
106.04	86.07	4	4
443.32	443.32	1	5
218.55	238.88	2	5
189.04	195.9	3	5
153.33	124.99	4	5
115.84	116.21	5	5

Appendix B1: Measured Concentrations

Table B1.1 Concentration data from several measurement points in the study site *Plaine des Bouchers*

Index	**Coordinate**				**Pollutants**	
	X	***Y***	***X (m)***	***Y (m)***	***TCE (µg/l)***	***PCE (µg/l)***
			(UTM - GWS84)	***(UTM - GWS84)***	*MCL=0,3*	*MCL=0,2*
02722**X**0050	997,86	109,673	406367.268	5379273.019	<0,2	0,7
02723**X**0564	998,631	109,771	407143.662	5379302.723	1	<0,2
02723**X**0701	998,461	110,354	407025.708	5379898.245	6,9	35,3
02723**X**0703	999,42	112,97	408211.037	5382418.832	0,3 / *0,6*	4,5 / *8,9*
02722**X**0706	998,138	109,873	406661.711	5379447.703	4,1	43,5
02723**X**0708	999,17	111,94	407871.387	5381415.164	0,8 / *0,7*	14,4 / *17,5*
02723**X**0758	1000,9	113,76	409754.401	5383075.189	1,1 / *0,7*	10,2 / *6,9*
02723**X**0781	1000,68	112,975	409462.211	5382313.207	1,5 / *1,8*	9,6 / *12,4*
02723**X**0870	998,155	111,749	406843.823	5381314.340	<0,2 / *<0,2*	0,2 / *0,3*
02723**X**0904	999,048	113,295	407869.216	5382775.228	< 0,2	2,8
02723**X**0908	999,527	114,074	408414.808	5383508.783	0,5 / *0,6*	10,3 / *13,1*
02723**X**0933	998,449	110,454	407022.563	5379998.882	0,8 / *0,5*	32,1 / *18,2*
02723**X**0357	999,166	110,305	407723.436	5379787.375	0,9	2
02723**X**0400	998,396	109,756	406908.327	5379308.477	<0,2	0,3
02723**X**0437	998,914	109,507	407402.229	5379014.913	0,7	0,9
02723**X**1120	998,314	110,729	406912.343	5380284.616	0,5 / *1,0*	181 / *291*
02723**X**1172	998,889	109,233	407353.209	5378744.264	< 0,2	< 0,2
02723**X**1186	998,296	110,152	406843.614	5379711.621	*1,9*	*72,6*
02723**X**1187	998,351	110,149	406898.119	5379703.791	*1,1*	*44,1*
02723**X**1190	998,568	109,448	407052.487	5378986.625	1,2	1,4
02723**X**1026	998,329	110,093	406871.281	5379649.963	6,6	43,2
02723**X**1027	998,301	110,098	406843.838	5379657.407	34,3	96,9
02723**X**1051	1001,6	113,405	410416.218	5382660.385	*3,9*	*7,9*

Source : CUS - CAC (2000)
Italics: for the sampling period between November and December 2000
Normal fonts: for the sampling period between July and September 2000

References

References

Bair, E. S.; R. A. Sheets; S. M. Eberts (1990). Particle-tracking analysis of flow paths and traveltimes from hypothetical spill sites within the capture area of a wellfield. Ground Water, 28 (6): 884-892.

Bair, E. S.; A. E. Springer; G. S. Roadcap (1991). Delineation of traveltime-related capture areas of wells using analytical flow models and particle-tracking analysis. Ground Water, 29(3): 387-397.

Bardos, P. (2001). REPORT OF THE NICOLE WORKSHOP: Information and Communication Technologies for Sustainable Land Management, and Monitored Natural Attenuation. 14-15 November, Port of Rotterdam, The Netherlands.

Basha, H. A.; F. S. El Habel (1993). "Analytical solution of the one-dimensional time-dependent transport equation." Water Resources Research, 29(9): 3209-3214.

Bennett, G. D; T.E. Reilly; M.C. Hill (1990). Technical Training Notes in Ground-Water Hydrology: Radial Flow to a Well. USGS Water Resources Investigation Report 89-4134.

Beres, M.; P. Huggenberger; A.G. Green; H. Horstmeyer (1999). Using two- and three-dimensional georadar methods to characterize glaciofluvial architecture. Sedimentary Geology, 129 (1-2) pp. 1-24

Beth, L. P.; J. A. Cherry (1999). Scale Considerations of Chlorinated Solvent Source Zones And Contaminant Fluxes: Insights From Detailed Field Studies. U.S. Geological Survey Toxic Substances Hydrology Program--Proceedings of the Technical Meeting Charleston South Carolina March 8-12, 1999--Volume 3 of 3--Subsurface Contamination From Point Sources, Water-Resources Investigations Report 99-4018C.

Bockelmann, A.; T. Ptak; G. Teusch (2001). An analytical quantification of mass fluxes and natural attenuation rate constants at a former gasworks site. Journal of Contaminant Hydrology 53, 429-453.

Bockelmann, A.; Z. Zamfirescu; T. Ptak; P. Grathwohl; G. Teusch (2003). Quantification of mass fluxes and natural attenuation rates at an industrial site with a limited monitoring network: a case study. Journal of Contaminant Hydrology 60, 97-121.

Brown, S. D.; S. Muralidhara; J. V. Bruckner; M. J. Bartlett (2003). Tracer level determination of trichloroethylene from liver, lung, and kidney by gas chromatography - magnetic sector mass spectrometry. Journal of chromatography B, 783, 319-325.

Cheremisinoff, P. N. (1990). Encyclopedia of Environmental Control Technology: Hazardous Waste Containment and Treatment. Houston, Texas: Gulf Publishing Co.

Chiang, W.-M.; W. Kinzelbach (1998). Processing Modflow: A simulation system for modeling groundwater flow and pollution, pp. 325.

CUS (2000). Observatoire de la nappe - Qualité des eaux souterraine en 2000. N° A23471/A. Communauté Urbaine de Strasbourg.

Cummings, J. (2002). Groundwater Remediation at DNAPL sites. RCRA National Meeting - January 2002.Technology Innovation Office, USEPA. (http://www.epa.gov/epaoswer/osw/meeting/pdf02/cummings.pdf)

Delporte, B; A. Talbot (1994). Mise en Place d'un observatoire des eaux souterraines sour le territoire de la Communauté Urbaine de Strasbourg. BRGM, N 0554, Ref. C 16211494.

Décret n°2001-1220 du 20 décembre 2001, Journal Officiel de la République Française, (http://www.admi.net/jo/2001/20389.html)

Dillon, P. J. (1989). "An Analytical Model of Contaminant Transport from Diffuse Sources in Saturated Porous Media." Water Resources Research, 25(6),1208-1218.

Domenico, P. A. (1987). An analytical model for multidimensional transport of a decaying contaminant species, Journal of Hydrology 91, 49-58.

Dou, C.; W. Woldt; I. Bogardi; M. Dahab (1997). Numerical solute transport simulation using fuzzy set approach. Journal of Contaminant Hydrology 27, 107-126.

ECSA (2000). Plain Facts about Chlorinated Solvents. http://www.eurochlor.org/chlorsolvents/issues/issues1_2_2.htm Last Update 20 June 2002.

Elder, C. R. (2002). Effect of heterogeneity on influent and effluent concentrations from horizontal permeable reactive barriers. Water Resources Research, 38(8):27, 1-19.

Fehr, R.; O. Mekel; M. Lacombe; U. Wolf (2003). Towards health impact assessment of drinking-water privatization - the example of waterborne carcinogens in North Rhine-Westphalia (Germany). Bulletin of the World Health Organization, 81 (6), 408-414.

Fisher, R.S., P. T. Goodmann (2002). Characterizing groundwater quality in Kentucky: from site selection to published information. Proceedings of the 2002 National Monitoring Conference, National Water Quality Monitoring Council, May 19-23, Madison, Wisconsin.

Fleming, S.W.; G.J. Ruskauff; A. Adams (2002). HJWFTAC: Software for Hantush_Jacob analysis of variable-rate, multiple-extraction well pumping tests. Computers & Geosciences 28, 669-677.

Franzetti, S. and A. Guadagnini (1996). Probabilistic estimation of well catchements in heterogeneous aquifers. Journal of Hydrology 174, 149-171.

Freissinet, C.; M. Vauclin; M. Erlich (1998). A fuzzy logic-based approach to assess imprecisions of soil water contamination modelling, Soil and Tillage Research, Volume 47, Issues 1-2, 2 June 1998, p. 11-17.

Frederick J. Spitz (2001). Method and computer programs to improve pathline resolution near weak sinks representing wells in MODFLOW and MODPATH ground-water-flow simulations. US. Geological Survey, Open-File Report 00-392.

GRC (2003). Pollution coverage rullings and maps. http://www.genre.com/sharedfile/pdf/PollutionMaps2003.pdf

Guillemin, C.; J.-C. Roux (1991). Pollution des eaux souterraines en France: Bilan des connaissances, Impacts, et moyens de prévention. Manuel et Méthodes No. 23. Editions du BRGM, pp. 262.

Harbaugh, A.W.; M.G. McDonald (1996). User's documentation for MODFLOW-96, an update to the U.S. Geological Survey modular finite-difference ground-water flow model: U.S. Geological Survey Open-File Report 96-485, pp. 56.

Hardisty, P. (2001). A methodology for assessing the full costs and benefits of groundwater remediation. Report of the NICOLE Workshop on Cost-effective clean-up technology: quality assurance and acceptance, 17-18 May 2001, Paris, France.

Hoang, M. (2000). Inventaire de la Plaine des Bouchers. Rapport de stage, Maîtrise de Sciences et Techniques "sols, pollution et réhabilitations", Université Louis Pasteur - Strasbourg.

Holder,Th; G. Teusch; T. Ptak; R. Schwarz (1998). A new approach for source zone characterization: the Neckar Valley study. In: Herbert, M. and K. Kovar (eds.). Groundwater Quality : Remediation and Protection. Proc. GO'98 Conference, Tübingen, Germany, September 1998. IAHS Publ. No. 250, pp. 49-55.

Holt, M.S. (2000). Sources of chemical contaminants and routes into the freshwater environment. *Food and Chemical toxicology 38, S21-S27.*

IFARE/DFIU (1998). La rechereche aujourd'hui pour mieux aqir demain: aquis scientifiques et résultats de travaux de recherche dans le domaine de l'environnement. Institut Franco-Allemend de Recherche sur l'Environnement, Edition 1998.

INCORE (2003). Integrated Concept for Groundwater remediation: Final Report. ISBN: 3-00-011706-7. (www.umweltwirtschaft-uw.de/incore/)

International Agency for Research on Cancer (IARC) (1995). Carcinogenic classification: Group 2A, Probably Carcinogenic to Humans, Vol 63, p.159. (http://www-cie.iarc.fr/) . Last Update : 05/20/97

Kamra, S.K.; L. Khajanchi; O.P. Singh; J. Boonstra (2002). Effect of pumping in temporal changes in groundwater quality. Agricultural Water Management 56, 169-178.

Kaleris, V.; C. Hadjitheodorou; A.C. Demetracopoulos (1995). Numerical simulation of field methods for estimating hydraulic conductivity and concentration profiles. Journal of Hydrology 171, 319-353.

Kerr, R.S. (1992). Estimating potential for occurrences of DNAPL at superfund sites. US EPA, Office of Emergency and Remedial Response, Hazardous Site Control Division (OS-220W), Quick Reference Fact Sheet Publication No. 9355.4-07FS.

Kinzelbach, W. (1987). Numeriche Methoden zur Modellierung de Transports von Schdstoffen im Grundwasser. R. Oldenbourg Verlag GmbH, München, pp. 317.

Kirchholtes, H. J; Ph. Elsass; C. Kolsar; C. Padovani; M. Schweiker (2003). INCORE: Cost effectiveness - costs and level of confidence. INCORE, Contract EVK1-CT-1999-00017, pp 22.

Lee, L. J.; C.-C. Chan; C.-W. Chung; Y.-C. Ma; G-S. Wang; J-D Wang (2002). Health Risk Assessment on Residents Exposed to Chlorinated Hydrocarbons Contaminated in Groundwater of a Hazardous Waste Site. Journal of Toxicology and Environmental Health, Part A, 65:219-235, 2002.

McDonald, M.G.; A. W. Harbaugh (1988). A modular three-dimensional finite-difference ground-water flow model: U.S. Geological Survey Techniques of Water-Resources Investigations, book 6, chap. A1, pp. 586.

Meijer, F. (2002). Highly permeable zones in the industrial area of the "Plaine des Bouchers". Rapport de Stage, Note: ALSNT02N21_PDB, BRGM.

Ménillet (1997) - Inventaire historique des anciens sites potentiellement à l'origine d'une pollution sur la zone de la Plaine des Bouchers Strasbourg (67). Rapport BRGM R 39363.

Mohamed, A. M. O.; K. Côté (1999). Decision analysis of polluted sites - a fuzzy set approach, Waste Management, 19(7-8): 519-533.

Morshed, J.; J. J. Kaluarachchi (1998). Application of artificial neural network and genetic algorithm in flow and transport simulations. *Advances in Water Resources, 22 (2): 145-158*.

NAVFAC (1999). Three-dimensional site characterisation technologies for DNAPL contamination sites. TechData Sheet, Naval facilities Engineering Command, Washington. NFESC TDS-2072-ENV.

Osienskya, J. L.; P. R. Donaldsonb (1995). Electrical flow through an aquifer for contaminant source leak detection and delineation of plume evolution, Journal of Hydrology, 169(1-4): 243-263

Olivar A. L. de Lima; H.K. Sato; M. J. Porsani (1995). Imaging industrial contaminant plumes with resistivity techniques, Journal of Applied Geophysics, 34(2): 93-108.

Pavard, L. (2001). Groundwater Pollution in France. Workshop on the protection of groundwater used as a source of drinking water supply, November 2001, Budapest.

Peng, H.-Y.; H.-D. Yeh; S.-Y. Yang (2002). Improved numerical evaluation of the radial groundwater flow equation. Advances in Water Resources 25, 663-675.

Prokop, G.; M. Schamann; I. Edelgaard (2000). Management of contaminated sites in Western Europe. Topic report No 13/1999. European Environment Agency.

Pollock, D. W. (1994). User's guide for MODPATH/MODPATH-PLOT, Version 3: A particle tracking post-processing package for MODFLOW, the U. S. Geological Survey finit-difference ground-water flow model. U. S. Geological Survey Open-file report 94-464.

Pollock, D. W. (1989). MODPATH (version 1.x)- Documentation of computer programs to compute and display pathlines using results from the U. S. Geological Survey modular three- dimensional finite-difference ground-water model. U. S. Geological Survey Open-file report 89- 381.

Puls, R.W.; C. J. Paul (1997). Multi-layer sampling in conventional monitoring wells for improved estimation of vertical contaminant distributions and mass. Journal of Contaminant Hydrology 25, 85-111.

Regional Analytics Inc. (2002). A Preliminary Investigation into the Economic Impact of Brownfield Redevelopment Activities in Canada. Final Report, November 15, 2002. Prepared for The National Round Table on the Environment and the Economy.

Riva, M; A. Guadagnini; F. Ballio (1999). Time-related capture zones for radial flow in two dimensional randomly heterogeneous media. Stochastic Environmental Research and Risk Assessment 13, 217-230. Springer-Verlag.

Rock, G.; H. Kupfersberger (2002). Numerical delineation of transient capture zones. Journal of Hydrology 269, 134-149.

Sampat, P. 2000. Deep trouble: The hidden threat of groundwater pollution. *Worldwatch Paper #154*. Worldwatch Institute, Washington, D.C. 55 pp.

Schäfer,G.; Ph. Elsass; S. Jellali; D. Nayagum; G. Rink (2001). The integral groundwater investigation method: 1st Field measurements in Strasbourg. 1st IMAGE-Train Cluster-Meeting, November 7-9, 2001, Karlsruhe, pp. 80-86.

Schäfer, G.; Ph. Elsass; S. Jellali; D. Nayagum; T. Ptak; G. Rinck; A. Zeru (2004). Application of the integral pumping test in Strasbourg. Special issue INCORE. In press, IGEA Journal.

Schwarz, R; T. Ptak; Th. Holder; G. Teusch (1998). Groundwater risk assessment at contaminated sites : a new investigation approach. In: Herbert, M. and K. Kovar (eds.). Groundwater Quality : Remediation and Protection. Proc. GO'98 Conference, Tübingen, Germany, September 1998. IAHS Publ.No. 250, pp. 68-71.

Spausta, G.; G. Prokop (2003). INCORE: Data inventory of the project areas. INCORE, Work-Package 1, Contract EVK1-CT-1999-00017, pp 25.

Tunks, J.; P. Guest; J. Santillan (2001). Diffusion Sampler Evaluation of Chlorinated VOCs in Groundwater, In: Vroblesky, D.A.(ed.), 2001, User's Guide for Polyethylene-Based Passive Diffusion Bag Samplers to Obtain Volatile Organic Compound Concentrations in Wells, Part 2: Field Tests, U.S. Geological Survey Water Resources Investigations Report 01-4061, pp. A-1 to A-8."

UNESCO (2002). Africa's hidden groundwater resources. UNESCOPRESS, Press Release No. 2000-35. *(*http://portal.unesco.org/en/ev.php@URL_ID=3026&URL_DO=DO_TOPIC&URL_SECTION=201.html), updated 14/11/2002.

US EPA (2002). National Primary Drinking Water Standards. Office of Water (4606), EPA 816-F-02-013 (www.epa.gov/safewater).

Wexler, Eliezer J. (1989). "Analytical Solutions for One-, Two-, and Three-Dimensional Solute Transport in Ground Water Systems with Uniform Flow." U.S. Geological Survey, Open-File Report, 89-56.

Widory, D.; Ph. Elsass (2003). INCORE: Fingerprinting at Plaine des Bouchers Strasbourg. Final Report of INCORE, Work-Package 4, Contract EVK1-CT-1999-00017, Strasbourg, pp 16.

Wilson, J.L.; P. J. Miller (1978). Two-dimensional plume in uniform ground-water flow. Journal of the Hydraulics Division, ASCE, (104) HY4, 503-512.

Zeru, A.; Schäfer, G (2004). Groundwater pollution analysis with the inversion of pumped groundwater quality data: focus on the effect of concentration gradient in the plume. Submitted to Journal of Contaminant Hydrology, February 2004, Ref.: CONHYD 1767.

Zeru, A; G. Schäfer (2003a). *Uncertainties in locating DNAPLs: combined numerical-analytical studies*. Proceedings, International Conference on Analytic Element Method (ICAEM), November 20-21, 2003, Saint-Etienne, France.

Zeru. A; G. Schäfer (2003b). INCORE: Practical guide for the analysis of concentration distribution. Final Report of IMFS/IFARE Research Activities for Work-Package 3 - INCORE, Contract EVK1-CT-1999-00017, IMFS/IFARE, Strasbourg, pp 11.

Zeru. A; G. Schäfer (2003c). INCORE: Uncertainty studies on the effect of concentration gradient in the plume for the IPT based groundwater risk assessment. Final Report of IMFS/IFARE Research Activities for Work-Package 3 - INCORE, Contract EVK1-CT-1999-00017, IMFS/IFARE, Strasbourg, pp 11.

Zeru, A.; G. Schäfer (2002). Uncertainties in locating chlorinated solvent plume using imission pumping tests : combined numerical-analytical studies. Abstract, European Conference on Natural Attenuation, October 15-17, 2002, Heidelberg, Germany.

Zheng, C. (1990). MT3D: A Modular Three-Dimensional Transport Model for Simulation of Advection, Dispersion and Chemical Reactions for Contaminates in Groundwater Systems. Prepared for USEPA, 163 p.

Zheng, C.; P. P. Wang (1999). *MT3DMS,* A modular three-dimensional multi-species transport model for simulation of advection, dispersion and chemical reactions of contaminants in groundwater systems; documentation and user's guide, U.S. Army Engineer Research and Development Center Contract Report SERDP-99-1, Vicksburg, MS, 202 p.

Zhou, Y. (1996). Sampling frequency for monitoring the actual state of groundwater systems. Journal of Hydrology 180, 301-318.